Initiation of Acute Graft-versus-Host Disease by Angiogenesis

Inaugural-Dissertation
to obtain the academic degree
Doctor rerum naturalium (Dr. rer. nat.)

Submitted to the Department of Biology, Chemistry and Pharmacy
of Freie Universität Berlin

by

Katarina Riesner

from Berlin

2017

The present thesis was prepared from December 2011 until April 2017 at the Medical Department of Hematology, Oncology and Tumor Immunology, Charité University Medicine under the supervision of PD Dr. Olaf Penack.

First Reviewer:	PD Dr. Olaf Penack
Second Reviewer:	Prof. Dr. Rupert Mutzel

Date of defense: 05.07.2017

Für meine über alles geliebte Familie

For my dearly beloved family

Danksagung

Hiermit möchte ich mich ganz herzlich bei allen bedanken, die mich während der gesamten Zeit meiner Doktorarbeit wissenschaftlich, organisatorisch sowie menschlich unterstützt haben und somit essentiell zum erfolgreichen Gelingen der vorliegenden Arbeit beigetragen haben.

Ein ganz besonderer Dank gilt meinem Doktorvater PD Dr. Olaf Penack für die Möglichkeit meine Doktorarbeit in seiner Arbeitsgruppe durchzuführen, für seine freundliche und hilfsbereite Betreuung und für die Einführung in das spannende Gebiet der translationalen hämatologischen Forschung. Ich bedanke mich für das entgegengebrachte Vertrauen meine wissenschaftlichen Arbeiten eigenständig bearbeiten zu können, für die wohlwollende Unterstützung meiner wissenschaftlichen Entwicklung, für die Herausforderungen, an denen ich wachsen konnte und für die von ihm eröffneten wissenschaftlichen sowie persönlichen Möglichkeiten.

Prof. Dr. Rupert Mutzel danke ich ganz herzlich für das Interesse an meiner wissenschaftlichen Arbeit und für die Übernahme des Zweitgutachtens.

Ein weiterer sehr besonderer Dank gilt meinen aktuellen und ehemaligen Kollegen aus der Arbeitsgruppe, ohne die diese Arbeit so nicht möglich gewesen wäre: Martina, Sarah, Steffen, Yu, Aleix, Jörg, Tharsana. Besonders Sarah und Steffen, vielen Dank für eure unermüdliche Unterstützung, eure Kompetenz, euren Teamgeist, eure stetige Hilfsbereitschaft, fürs gemeinsame „Lachen und Weinen“ und für eure Freundschaft. Und insbesondere meiner Martina, für dein bedingungsloses „Immerbereitsein“, für deine allgegenwärtige Unterstützung, für deinen Fleiß und deine hervorragende Arbeit; aber besonders für die vielen Stunden, die uns zusammengeschweißt haben, sodass ich deine Freundschaft nicht mehr missen möchte („Denn was die Wissenschaft zusammenführt, das soll der Mensch nicht trennen“).

Ebenfalls gilt mein herzlicher Dank den Kooperationspartnern, die mit ihrer experimentellen sowie persönlichen Hilfe essentiell zum Gelingen dieser Arbeit beigetragen haben. Um einige wenige zu nennen: Angela Jacobi und Martin Kräter für die außergewöhnliche persönliche und wissenschaftliche Unterstützung, Jens-Florian Schrezenmeier für die langen, aber amüsanten und fröhlichen Stunden am FACS, Sabine Schmidt und Giannino Patone für ihre beharrliche Hilfe bei den Microarrays, Gunnar Dittmar und Daniel Perez-Hernandez für die Durchführung der Proteomanalysen, Sefer Elezkurtaj für das genaue Hingucken unter dem Mikroskop und besonders Prof. Lena Claesson-Welsh für die zweimonatige Aufnahme in ihrem Labor und für die Möglichkeit mich persönlich und wissenschaftlich weiterzuentwickeln. Chiara Testini möchte ich ganz besonders danken für die hervorragende Betreuung und Hilfe während dieser Zeit als auch danach und für die daraus hervorgegangene Freundschaft.

Außerhalb der Arbeitsgruppe bedanke ich mich bei den vielen anderen Doktoranden, Postdoktoranden und Technischen Assistenten, die mit ihrer experimentellen Hilfe als auch dem wissenschaftlichen und persönlichen Austausch, meine Doktorarbeitszeit sowohl erfolgreich als auch besonders gemacht haben, um nur einige zu nennen: die Leute aus Würzburg, Freiburg und Frankfurt, Marie, Jacky, Rainer, Katharina und viele andere, die sich bitte, wenn auch nicht explizit erwähnt, angesprochen fühlen.

Zu guter Letzt möchte ich meiner Familie danken, die mit ihrer bedingungslosen Liebe und Unterstützung jeglichen Weg, den ich einschlage, mit Freuden mit mir geht. Meinem Mann Kevin, der mir mit seiner Liebe immer zur Seite steht, meine „Hochs und Tiefs“ fürsorglich begleitet, mich immer unterstützt und mir emotionalen und ja auch fachlichen Rückhalt gibt. Meinem Sohn Oliver, der zwar nicht aktiv zum Gelingen dieser Arbeit beigetragen hat (außer ein paar Buchstaben zur späteren Verwendung im Manuskript zu hinterlassen), dessen Geburt aber immer untrennbar mit meiner Doktorarbeitszeit verbunden sein wird und durch sein sonniges und liebevolles Gemüt jeden Tag zu etwas Besonderem macht. Meinem Bruder Robert, der spontan und nicht spontan immer seine zuverlässige Hilfe bereitstellt. Und meinen wunderbaren Eltern, die in mir das tiefe Selbstvertrauen verwurzelt haben, dass erstmal alles möglich ist. Ihr seid mit eurer bedingungslosen Liebe und unendlichen Unterstützung immer bei mir, die mich sehr glücklich macht und vieles ermöglicht, was nicht selbstverständlich ist. Danke, dass wir immer für einander da sind. Für meine über alles geliebte Familie.

Berlin, Mai 2017

1. Table of contents

2. List of abbrevations

2PG	2-phosphoglycerate
6PGL	6-phosphonoglucono-delta-lactone
3PO	3-(3-pyridinyl)-1-(4-pyridinyl)-2-propen-1-one
Acss2	acyl-coenzyme A synthetase short-chain family member 2
Aldob	fructose-bisphosphate aldolase B
allo-HSCT	allogeneic hematopoietic stem cell transplantation
APCs	antigen-presenting cells
ATG	anti-thymocyte globulins
ATP	adenosine triphosphate
BM	bone marrow
Cas9	CRISPR associated protein 9
CAT	carnitine translocase
Ca^{2+}	calcium
CCL	CC-chemokine ligand
CLL	chronic lymphocytic leukemia
CMV	cytomegalovirus
CoA	Coenzyme A
COX	cyclooxygenase
CPT	carnitine palmitoyltransferase
CRISPR	Clustered Regularly Interspaced Short Palindromic Repeats
CSA	cyclosporin A
CXCL	CXC-chemokine ligand
DAMPs	damage-associated molecular pattern
DLI	donor lymphocyte infusions
DLL4	delta-like 4
DNA	deoxyribonucleic acid
dNTPs	deoxynucleotide triphosphates
EBMT	European Society for Blood and Marrow Transplantation
ECs	endothelial cells
EGFR	epidermal growth factor receptor
Eno3	enolase 3
EPCs	endothelial precursor cells
ERK	extracellular-signal regulated kinase
ETC	electron transport chain
F1,6BP	fructose 1,6-bisphosphate
F2,6BP	fructose-2,6-bisphosphate
F6P	fructose-6-phosphate
Fabp	fatty-acid-binding protein
FACS	fluorescence-activated cell sorting
FADH2	flavin adenine dinucleotide
FAO	fatty acid β-oxidation
FGF	fibroblast growth factor
FGFR	fibroblast growth factor receptor
Fuca1	lysosomal enzyme α-L-fucosidase

G3P	glyceraldehyde 3-phosphate
G6P	Glucose-6-phosphate
G6PDX	glucose-6-phosphate dehydrogenase
G-CSF/GM-CSF	granulocyte or granulocyte-macrophage colony stimulating factor
GI	gastrointestinal
GlcA6P	glucosamine-6-phosphate
GlcNAc1P	N-acetyl-D-glucosamine-1-phosphate
GlcNAc6P	N-acetyl-D-glucosamine-6-phosphate
GPCR	G-protein-coupled receptors
GSH	glutathione
GTP	guanosine triphosphate
GVHD	graft-versus-host disease
GVT	graft-versus-tumor
Gy	Gray
H-2	histocompatibility 2
HBP	hexosamine biosynthesis pathway
HIF	hypoxia-inducible factor
HLA	human leukocyte antigen
HMGB-1	high-mobility-group-protein B1
HSC	hematopoietic stem cell
HSPGs	heparan-sulphate proteoglycans
ICAM-1	intercellular adhesion molecule 1
Ig	immunoglobulin
IFN-γ	interferon γ
iNOS	inducible nitric oxide synthase
IκBα	NFκB inhibitor alpha
IL	Interleukin
IL-1Ra	human IL-1 receptor antagonist
IRAK	IL-1R-associated kinase
JAK	janus kinase
kD	kilo Dalton
KGF	keratinocyte growth factor
LPS	lipopolysaccharides
MAPK	mitogen-activated protein kinase
MHC	major histocompatibility complex
miHAs	minor histocompatibility antigens
MIP-1α	macrophage inflammatory protein 1α
MLC	myosin light chain
MMF	mycophenolate mofetil
MMPs	matrix metalloproteases
MS	mass spectrometry
mTOR/ mTORC	mechanistic Target of Rapamycin (complex)
MTX	methotrexate
MyD88	myeloid differentiation primary-response gene 88
NADH	nicotinamide adenine dinucleotide
NADPH	nicotinamide adenine dinucleotide phosphate

NAGK	N-acetylglucosamine kinase
NFAT	nuclear factor of activated T-cells
NFκB	nuclear factor 'kappa-light-chain-enhancer' of activated B-cells
NGS	next-generation sequencing
NO	nitric oxide
NOD	nucleotide-binding oligomerization domain
PAF	platelet activating factor
PAMPs	pathogen-associated molecular patterns
PBSC	peripheral blood stem cells (progenitor) cells
PCR	polymerase chain reaction
PDGF	platelet-derived growth factor
PEP	phosphoenolpyruvate
PFK-1	6-phosphofructokinase-1
PFKFB3	6-Phosphofructo-2-Kinase/Fructose-2,6-Biphosphatase
PGI_2	prostaglandin I_2
PHD	oxygen-sensing prolyl hydroxylase
PI3K	phosphoinositide 3-kinase
PLC	phospholipase C
PPP	pentose phosphate pathway
R5P	ribose-5-phosphate
Rac1	Ras-related C3 botulinum toxin substrate 1
Ras	rat sarcoma
RHO	Ras homologue
RNA	ribonucleic acid
SCID	severe combined immunodeficiency
SOS	sinusoidal obstruction syndrome
SPF	specific pathogen-free
ST2	suppression of tumorigenicity 2
STAT	signal transducer and activator of
TBI	total body irradiation
TCA	tricarboxylic acid
TCR	T cell receptor
TKT	transketolase
TNF	tumor necrosis factor
TRADD	TNFR-associated via death domain protein
UDP-GlcNAc	uridine diphosphate N-acetylglucosamine
VCAM-1	vascular cell adhesion protein 1
VE-cadherin	vascular endothelial cadherin
VEGF	vascular endothelial growth factors
VEGFR	vascular endothelial growth factor receptor
ZO-1	Zonula occludens-1

3. Abstract

For a variety of malignant diseases of the hematopoietic system, the allogeneic hematopoietic stem cell transplantation (allo-HSCT) is the only curative treatment option. Accordingly, the number of allo-HSCTs performed worldwide has increased greatly in the past decades. However, the mortality after allo-HSCT is high: more than half of the patients die within the first two years because of graft-versus-host disease (GVHD) or GVHD-associated complications as tumor relapse or fatal infections. Acute GVHD is a systemic inflammatory disease caused by alloreactive T cells primarily affecting liver, skin and intestines; so that current therapeutic approaches aim at supressing these effector T cells. This has the significant disadvantage of creating a secondary immune deficiency with increased risk for the above named complications; and most GVHD-related deaths are due to treatment failure or significant toxicities of the used immunosuppressive agents. Therefore, there is an urgent medical need for alternative therapies, which do not attenuate the immune system.

Recent work identified such a novel approach: the inhibition of pathologic angiogenesis, which is involved in GVHD as well as in tumor growth after allo-HSCT. The crosstalk between angiogenesis and inflammation is well-established and used in anti-angiogenic treatment strategies. However, it is still not clear if angiogenesis is a consequence or the cause of inflammation. This obstacle and missing suitable targets that are differentially regulated during pathologic and physiologic angiogenesis limit the efficacy of current anti-angiogenic therapies and hinder the development of novel therapeutic approaches.

This cumulative thesis consists of two publications, aiming to understand GVHD-initiating mechanisms related to angiogenesis and to provide potential new therapeutic targets being involved in early GVHD while aiming at the endothelium.

For a better translation of experimental results into the human setting of allo-HSCT, I first established a clinical relevant, acute GVHD mouse model; as the most commonly used ones exhibit significant clinical limitations. The features of our novel chemotherapy-based, major histocompatibility complex (MHC)-matched GVHD model included profound engraftment, typical clinical features of GVHD, and systemic and target organ-specific inflammation. The clinical pattern and timing of GVHD closely resembled the clinical situation of human leukocyte antigen (HLA)-matched allo-HSCT with GVHD prophylaxis, providing a suitable tool to better understand pathogenic mechanisms in GVHD as well as to develop and translate new treatment approaches.

Second, I provided novel evidence on a primary involvement of angiogenesis in the initiation of tissue inflammation in GVHD and found that during initial angiogenesis classical inflammation-associated endothelial activation signs were absent, but metabolic and cytoskeletal alterations occurred, resulting in enhanced migratory and proliferative potential of endothelial cells. I identified potential novel targets for pursuing mechanistic studies and the development of anti-inflammatory therapies aiming at angiogenesis.

This study helps to amend the knowledge on the interplay between the vasculature and inflammation and opens a new window to develop novel therapeutic strategies targeting the endothelium after allo-HSCT.

3.1 Zusammenfassung

Für verschiedene maligne Erkrankungen des hämatopoetischen Systems stellt die allogene hämatopoetische Stammzelltransplantation (allo-HSZT) die einzige kurative Therapieoption dar, sodass die Anzahl der weltweit durchgeführten allo-HSZTs in den letzten Jahrzehnten deutlich angestiegen ist. Allerdings ist die Mortalität nach allo-HSZT sehr hoch. Mehr als die Hälfte der Patienten versterben in den ersten zwei Jahren an der graft-versus-host Krankheit (GVHD) oder an GVHD-assoziierten Komplikationen wie Tumorrezidive oder tödlich verlaufende Infektionen. Die akute GVHD ist eine systemische Entzündungskrankheit bei der alloreaktive T-Zellen in die Leber, Haut und den Gastrointestinaltrakt einwandern und diese Organe schädigen. Die aktuellen GVHD Therapien sind daher auf eine Unterdrückung dieser T-Zellfunktionen ausgerichtet, wodurch sich allerdings häufig kritische sekundäre Immundefizienzen entwickeln, die mit einem erhöhten Risiko eine der oben genannten Komplikationen zu entwickeln, einhergehen. Fast alle GVHD Todesfälle lassen sich auf ein Therapieversagen oder auf erhebliche Nebenwirkungen der eingesetzten Immunsuppressiva zurückführen, was einen dringenden medizinischen Bedarf an alternativen therapeutischen Ansätzen, die nicht das Immunsystem schwächen, aufzeigt.
Vorarbeiten konnten solch einen innovativen therapeutischen Ansatz identifizieren: die Hemmung der pathologischen Gefäßneubildung (Angiogenese), die sowohl bei Tumorwachstum als auch während der GVHD nach allo-HSZT involviert ist. Antiangiogene Therapiestrategien bauen auf der weithin etablierten Beobachtung auf, dass Angiogenese und Entzündung zwei eng miteinander verknüpfte Prozesse sind. Allerdings ist nicht geklärt, ob die Angiogenese ein initiales oder sekundäres Ereignis gegenüber der Entzündung darstellt. Dies und das bisherige Fehlen von therapeutischen Zielstrukturen, die bei pathologischer und physiologischer Angiogenese unterschiedlich reguliert werden, behindern zurzeit die effektive therapeutische Nutzung der Hemmung des Blutgefäßwachstums.

In der vorliegenden Arbeit wurde untersucht, ob die Angiogenese einen initialen Mechanismus bei der Entstehung der GVHD darstellt. Zusätzlich sollten neue potentielle therapeutische Ansatzpunkte am Endothel identifiziert werden, die in der frühen Entstehungsphase der GVHD eine Rolle spielen. Dieser kumulativen Arbeit liegen zwei eigene Publikationen zugrunde.

Für eine bessere translationale Übertragung der experimentell gewonnenen Daten, wurde zunächst ein neues Mausmodell der akuten GVHD entwickelt, welches im Gegensatz zu den zurzeit am häufigsten genutzten Mausmodellen, die klinische Situation der allo-HSZT besser abbildet. Dieses neue Chemotherapie-basierte, Haupthistokompatibilitätskomplex (MHC)-kompatible GVHD Modell ist charakterisiert durch ein stabiles Anwachsen der Knochenmarksstammzellen, einen klinisch-vergleichbaren GVHD-Phänotyp sowie durch eine systemische als auch Zielorgan-spezifische Entzündungsreaktion. Die GVHD-Pathogenese im Mausmodell ist eng vergleichbar mit dem klinischen GVHD-Verlauf nach einer humanen Leukozyten-Antigen (HLA)-kompatiblen allo-HSZT mit GVHD-Prophylaxe. Daher stellt dieses Modell ein geeignetes Werkzeug dar, um pathogene Mechanismen der GVHD und translationale Therapieansätze zu untersuchen.

In diesem Mausmodell konnte erstmalig gezeigt werden, dass die Angiogenese ein initiales Ereignis während der GVHD-Pathogenese darstellt und der charakteristischen Entzündungsreaktion vorausgeht. Während dieser initialen Angiogenese zeigte sich keine entzündungs-assoziierte Endothelzellaktivierung. Stattdessen traten signifikante metabolische und zytoskeletale Veränderungen in den Endothelzellen auf, die zu einem erhöhten Migrations- und Proliferationspotenial führten. Neue Kandidatengene und Proteine wurden identifiziert, die in Endothelzellen während der pathologischen Angiogenese nach allo-HSZT unterschiedlich reguliert waren. Diese sollen in weiterführenden mechanistischen Studien untersucht werden.

Insgesamt konnte die Arbeit neue Erkenntnisse zur Entstehung der pathologischen Angiogenese bei entzündlichen Erkrankungen wie der GVHD liefern und sie leistet einen substantiellen Beitrag für die translationale Entwicklung der therapeutischen Hemmung der pathologischen Angiogenese nach allo-HSZT.

4. Introduction

4.1 Allogeneic hematopoietic stem cell transplantation

Allogeneic hematopoietic stem cell transplantation (allo-HSCT) refers to any procedure where haematopoietic stem cells and the immunological repertoire from a donor are given to a recipient with the intention to repopulate and replace the hematopoietic system.[1,2] Originally developed to treat 1) patients with inherited anemias or immune deficiencies by replacing the abnormal hematopoietic system and 2) patients with cancer by delivering myeloablative doses of irradiation and/or chemotherapy; it represents nowadays the only curative treatment option for a multitude of malignant and non-malignant hematologic diseases, autoimmune disorders, amyloidosis and inherited genetic hematological disorders.[3] It also represents an interface between three emerging fields of current clinical research: stem cell therapies, immune-modulating therapies and individualization of cancer therapeutics.[3] Accordingly, the number of allo-HSCTs performed worldwide has increased greatly in the past decades (**Figure 1**) and over the last 50 years more than one million HSCTs have been performed.[4,5]

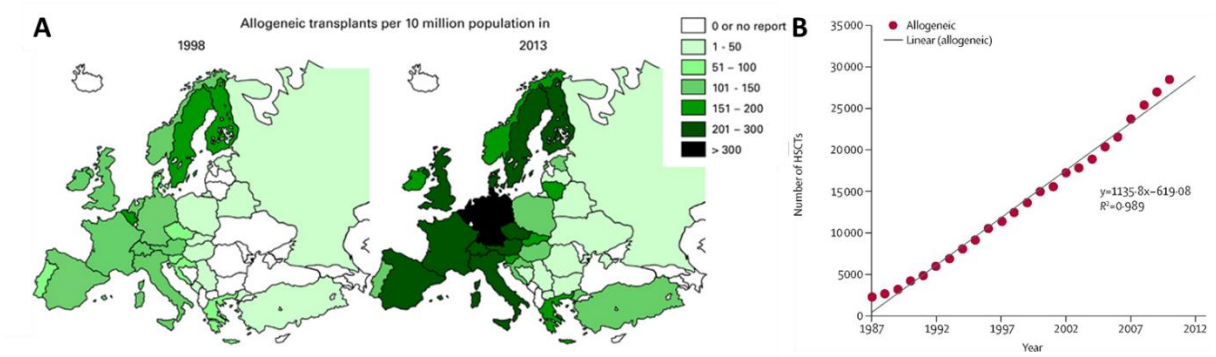

Figure 1: Number of performed allo-HSCTs increased in the last years. (**A**) Allogeneic transplant rates in Europe per 10 million population in 1998–2013 (modified according to Passweg et al. 2015).[4] (**B**) Global development of performed allo-HSCTs from 1987 to 2010 based on retrospective and validated data (from Gratwohl et al. 2015).[5]

The therapeutic success of allo-HSCT derives both from the possibility to treat patients with higher doses of radiation or chemotherapy; and from the potent graft-versus-tumor (GVT) effect where the donor immunity can also target malignant cells of the recipient.[2] However, this principle bears significant complications; more than half of the patients die within the first two years because of graft-versus-host disease (GVHD), a progressive inflammatory disease, or due to GVHD-associated complications as tumor relapse or fatal infections.[3]

4.1.1 Initial evolution and milestones of allo-HSCT

Due to immense preclinical and clinical research over the last 60 years, allo-HSCT has evolved from a highly experimental and high-risk technique to a standard treatment option.[2] Detailed studies about the biology of hematopoiesis and the application of HSCT to treat bone marrow injuries began after the detonation of nuclear weapons in Nagasaki and Hiroshima in the

Second World War.[2] In the 1950´s, animal studies revealed the first elementary key observations: spleen shielding in mice preserved hematopoiesis after lethal irradiation,[6] bone marrow infusions protected mice from lethal irradiation,[7] murine leukemia was successfully treated with irradiation and bone marrow infusions,[8] and the bone marrow is the source of “cellular elements” important for hematopoietic recovery.[9]

The research of Thomas and colleagues enabled the application of the first successful HSCT in 1959 by treating a patient with advanced leukemia with supralethal irradiation and syngeneic bone marrow transfusion.[10] For their contributions to the preclinical and clinical development of allo-HSCT as a therapy modality in the following years, E. Donnall Thomas and Joseph E. Murray received the Nobel Prize in Medicine in 1990.[11] However, the first performed HSCTs in the 1950´s and early 1960´s were characterized by a high relapse rate of the disease, failed engraftment and significant immunological reactions in the recipient.[12]

Only additional key observations in animal models and the development of initial techniques to perform human leukocyte antigen (HLA) typing[13] led to the successful development of HSCT for the clinical use: Billingham et al. described in 1959 an immune reaction after HSCT in mice as “Runt disease” characterized by rash and diarrhea,[14] later known as GVHD when van Bekkum and Vries identified it as a donor-versus-host reaction in 1967.[15] Methotrexate was used to prevent GVHD in mice.[16] Storb et al. used chemotherapy conditioning with cyclophosphamide in addition to irradiation.[17] Snell et al. identified histocompatibility antigens influencing graft tolerance in mice.[18] Epstein et al. identified a leukocyte antigen system in dogs (DLA) and showed its importance for the determination of graft failure and occurrence of GVHD after HSCT as DLA typing led to reduced mortality after HSCT.[19]

In 1968, Gatti and colleagues reported the first successful allo-HSCT in an infant with congenital immune-deficiency using bone marrow from an HLA-matched sibling donor.[20] In 1969, Thomas performed the first allo-HSCT with HLA-matched sibling donor transplants in humans with hematologic malignancies.[21] Although the next several years, allo-HSCT was mainly used for the treatment of congenital and acquired bone marrow failures, immune deficiencies and advanced refractory leukemia; further research and milestones (**Figure 2**) increased areas of application, application outcome and safety as well as fundamental understanding of biological processes behind allo-HSCT.[2]

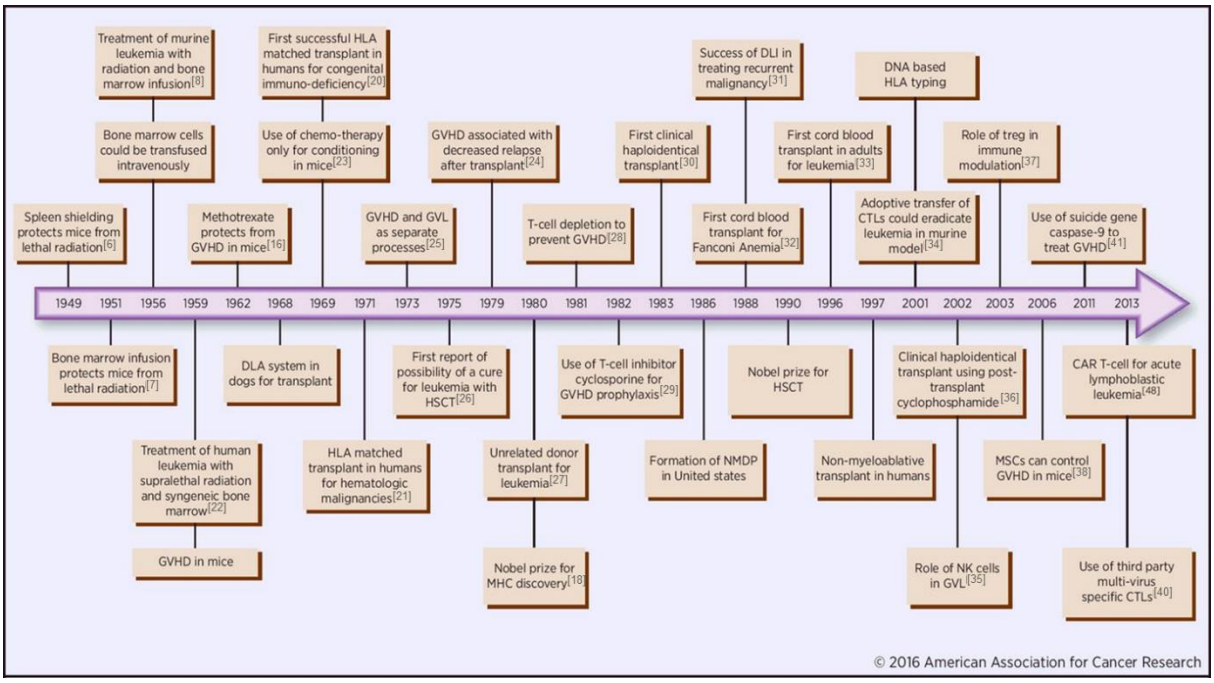

Figure 2: Milestones in allo-HSCT. GVHD, graft-versus-host disease. DLA, dog leukocyte antigen. HLA, human leukocyte antigen. GVL, graft-versus-leukemia. HSCT, hematopoietic stem cell transplantation. MHC, major histocompatibility complex. NMDP, National Marrow Donor Program. DLI, donor lymphocyte infusions. DNA, deoxyribonucleic acid. CTL, cytotoxic T lymphocytes. NK cells, natural killer cells. treg, regulatory T cells. MSCs, mesenchymal stromal cells. CAR, chimeric antigen receptor. Milestones are referenced in parentheses.[6-8,16,20,21,22-41] (modified according to Singh et al. 2016).[2]

4.1.2 Indications of allo-HSCT

The European Society for Blood and Marrow Transplantation (EBMT) regularly publishes and updates the current practice and indications for allo-HSCT in Europe. Allo-HSCT represents a major curative treatment option for multiple malignant and non-malignant diseases shown in **Table 1** (according to EBMT special report 2015).[1]

Table 1: Indications for allo-HSCT. (according to Sureda et al. 2015 and Kröger/ Zander 2011).[1,42]

Malignant diseases		Non-malignant diseases
Leukemias	Solid tumors	Aplastic anemia
Acute myeloid leukemia (AML) Acute lymphoblastic leukemia (ALL) Chronic myeloid leukemia (CML) Myelofibrosis Myelodysplastic syndrome (MDS) Myeloproliferative neoplasms Chronic lymphocytic leukemia (CLL)	Breast cancer Germ cell tumors Ovarian cancer Small cell lung cancer Renal cell cancer Ewing´s sarcoma Pancreatic cancer Colorectal cancer	Thalassemia Sickle cell anemia Inherited anemias Auto immune diseases (AID) Inherited diseases of metabolism (IDM) Primary immune diseases (PID) Severe combined immunodeficiency (SCID)
Lymphoid malignancies		
Diffuse large B cell lymphoma Waldenstrom macroglobulinemia T cell lymphoma Multiple Myeloma	Mantel cell lymphoma Follicular lymphoma Hodgkin lymphoma Amyloidosis	

Hematologic malignancies still represent the main indication for allo-HSCT, especially leukemia (particular acute myeloid leukemia with 36 % of performed allo-HSCTs in Europe) and lymphomas (**Figure 3**). Compared to this, solid tumors, e.g. renal cell cancer and breast cancer, or non-malignant diseases still account for a minor part of performed allo-HSCTs.[43]

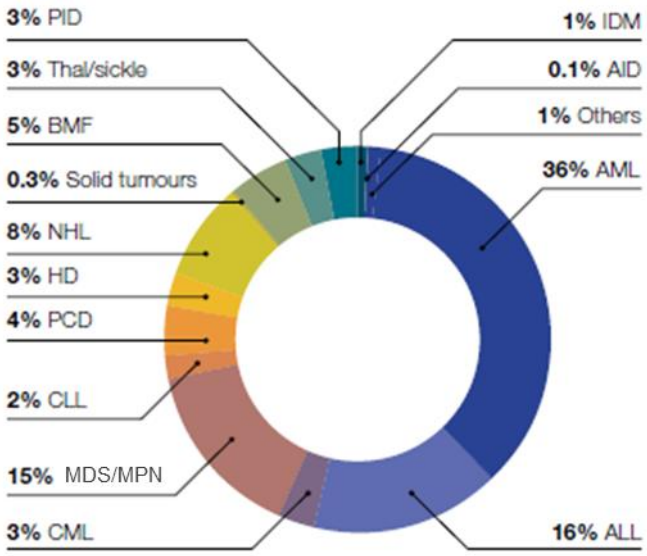

Figure 3: Main indications for allo-HSCT. Shown are percentage of transplants in 2014 (modified according to EBMT Annual Report 2015).[43] AML: acute myeloid leukemia, ALL: acute lymphoblastic leukemia, CML: chronic myeloid leukemia, MDS: myelodysplastic syndrome, MPN: myelo-proliferative neoplasm, CLL: chronic lymphocytic leukemia, PCD: plasma cell disorders, HD: Hodgkin's disease, NHL: Non-Hodgkin's lymphoma; BMF: bone marrow failure, Thal/sickle; thalassemia/sickle cell disease, PID: primary immune diseases, IDM: inherited diseases of metabolism, AID: auto immune diseases.

4.1.3 Immunological basis of allo-HSCT: the HLA system

The major histocompatibility complex (MHC) is the most-gene dense loci in the human genome and encodes for highly polymorphic cell surface molecules, which have central importance for the regulation of the immune response and for the outcome of transplantation between donor and recipient.[44] Historically, the MHC locus was first discovered on chromosome 17 in mice being responsible for rapid rejection of skin grafts between inbred mice strains. Mouse MHC molecules were entitled as H-2 for histocompatibility 2, whereas human MHC molecules (encoded by human MHC loci on chromosome 6) are known as HLA for human leukocyte antigens, as these antigens were first identified and studied using alloantibodies against leukocytes.[45]

The human MHC is composed of three regions: MHC class I and II genes, which encode the antigen-presenting MHC molecules; and class III region which encodes for various genes with immune function (e.g. complement components as C2, C4, Factor B; 21-hydoxylase or tumor necrosis factors (TNFs)) or others with no known immune function (**Figure 4**).[44,46] The MHC class I region contains the classical HLA-A, HLA-B and HLA-C genes that encode the heavy chains α (light chain β_2-microglobulin is encoded outside the MHC locus on chromosome 15) of MHC class I molecules being responsible for antigen presentation. The non-classical MHC I genes HLA-E, HLA-G, HLA-F, HFE, MICB and MICA encode for numerous and diverse molecules, e.g. some being important for activating distinct T cell subsets. The class II region consists of the classical DR, DP and DQ families each containing A and B genes encoding the

α and β chains of the MHC II molecules being responsible for antigen presentation. The DR family consists of a single DRA gene and up to nine DRB genes; the DP and DQ families have one single DPA/DQA gene and one single DPB/DQB gene. The non-classical MHC II genes DN, DM and DO encode for molecules which regulate peptide loading onto classical MHC II molecules.[44,45,47]

The organization of the mouse MHC is very similar (MHC class I, II and III) and is also divided into classical and non-classical MHC molecules (**Figure 4**): the classical MHC class I genes H-2D, H-2K and H2-L, the non-classical MHC class I genes H-2Q, H2-M and H2-T as well as the classical MHC class II genes H-2A (I-A) and H-2E (I-E) and the non-classical MHC class II genes H-2M and H-2O.[44]

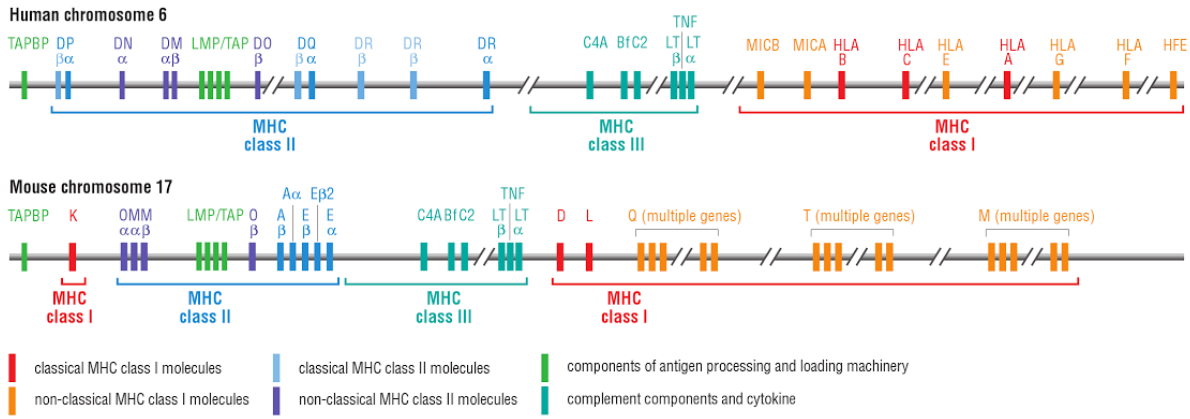

Figure 4: The human and mouse MHC. Simplified diagram of the human MHC on chromosome 6 and mouse MHC on chromosome 17. Organization of human and mouse MHC is very similar, except that mouse class I genes are separated at either end of the locus. Only class III genes with known function are shown (from DeFranco/ Locksley/ Robertson 2007).[44]

MHC molecules bind peptides on the cell surface, which are recognized by the T cell receptor of lymphocytes (called MHC restriction). MHC genes are highly polymorphic and polymorphisms are clustering in the antigen binding groove increasing the selection of peptides to be bound.[45] MHC class I and II genes encode two groups of structurally distinct but homologues proteins.[45]

MHC class I molecules are expressed on almost all nucleated cells and consist of a 44-47 kD highly glycosylated α heavy chain and noncovalent bound extracellular 12 kD β_2-microglobulin (β_2m) (**Figure 5A**). The heavy chain is composed of the three extracellular domains α1-3, an anchoring transmembrane region and an intracytoplasmic domain. α1 and α2 domains form a groove, which functions as the antigen binding site accommodating endogenous peptides with 8-10 amino acid residues. Polymorphic residues are located in the α1 and α2 domains determining the multiple antigenic specificities of the HLA class I molecules. The α3 and β_2m domains form non-polymorphic immunoglobulin (Ig)-like domains, which contain binding sites for the T cell molecule CD8. Therefore, CD8+ cytotoxic T cells recognize endogenous antigens

synthesized within the target cell (e.g. cellular, transformed or virus-induced proteins) and presented by the MHC class I molecules on the cell surface.[44,45,47]

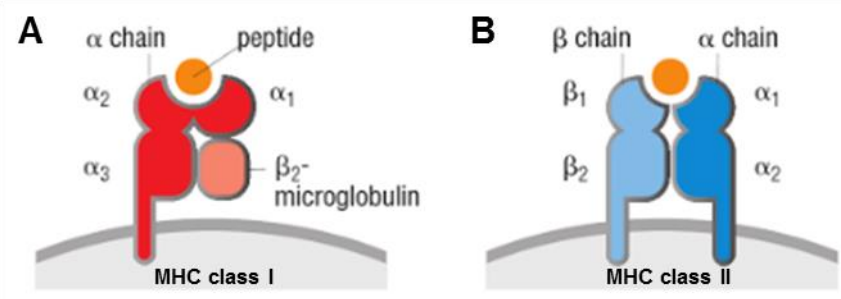

Figure 5: Structure of MHC class I (A) and II molecules (B). (modified from DeFranco/ Locksley/ Robertson 2007).[44]

MHC class II molecules are mainly expressed on antigen-presenting cells (B cells, monocytes/macrophages, dendritic cells, Langerhans cells) and are composed as heterodimers of two noncovalent bound glycosylated 32-34 kD α and 29-32 kD β polypeptide chains (**Figure 5B**). They share the same structure, with two extracellular domains each (α1 and 2, β1 and 2), an anchoring transmembrane region and an intracytoplasmic domain. The α1 and β1 domains contain the polymorphic residues and form the antigen binding site accommodating exogenous peptides with 10-30 (or more) amino acid residues. The β2 region forms the Ig-like domains containing the binding site for the T cell molecule CD4. CD4+ helper T cells recognize exogenous peptides which where endocytosed, degraded in the acidic endosomal compartment, bound to MHC class II molecules and transported back to the cell surface.[44,45,47]

MHC genes are closely linked and codominantly expressed as the entire MHC is inherited as a MHC (or HLA) haplotype in a Mendelian fashion from each parent, meaning that each individual expresses the MHC alleles from both parents on both chromosomes, respectively (**Figure 6**).[45,48] Therefore, the HLA haplotype means the set of MHC alleles present on each chromosome. As humans are heterozygous individuals, they exhibit two haplotypes and each HLA allele is given a numerical designation (e.g. HLA-A2, HLA-DR3). Inbred mice are homozygous and show a single haplotype with H-2 alleles designated with letters (e.g. H-2K^b, I-A^b).[45] In humans, the mendelian inheritance of HLA haplotypes lead to a 25 % chance that siblings are genotypically HLA-identical, a 50 % chance of sharing one haplotype (called haploidentical) and a 25 % chance of sharing no haplotypes.[47] The number of possible haplotypes is enormous due to the random combinations of antigens from different HLA loci, however some haplotypes are conserved in ethnic populations as they are found more

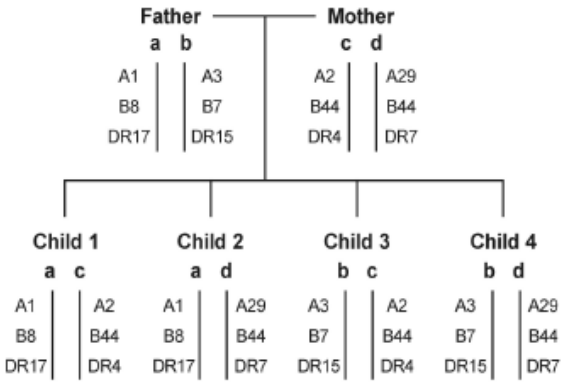

Figure 6: Mendelian inheritance of HLA haplotypes demonstrated in a model family study. (from Choo 2007).[47]

frequently as predicted by random assortment (e.g. most common haplotype among Caucasians with 5 % frequency is HLA-A1, B8, DR17), a phenomena called linkage disequilibrium.[45,47] This directly influences allo-HSCT: it is more likely to find a suitable donor with the same haplotype if a Caucasian patient exhibits a common haplotype compared to a rare haplotype (>90 % versus <10 % chance).[49]

HLA-A, HLA-B, HLA-C, HLA-DR and to lesser extent HLA-DQ are considered as the major transplantation antigens[1] and the corresponding genes show a high number of currently identified alleles (**Table 2**).[47] To find a suitable donor, the above named loci are typed. As every individual contain two alleles, 8 or 10 (if HLA-DQ is included) loci are tested.[1] HLA typing can be performed serologically with a complement-mediated microlymphocytotoxicity technique or by molecular typing with polymerase chain reaction (PCR) or next-generation sequencing (NGS)-based methods. The molecular typing is the gold standard as it is more sensitive and can distinguish more variants and subtypes.[47]

Table 2: Number of recognized alleles for HLA-loci in humans. (from Choo 2007).[47]

Locus	Alleles
HLA-A	303
HLA-B	559
HLA-C	150
HLA-DRB1	362
Total	**1,374**

4.1.4 Requirements for allo-HSCT

The performance of allo-HSCT is defined by the selection of the conditioning, the donor category and the stem cell source.[1]

Prior to allo-HSCT, the conditioning of the recipient by total body irradiation (TBI) or chemotherapy is performed to: 1) eliminate cancer cells, 2) suppress the recipient´s immune system to prevent graft rejection, and 3) create a “space” in the bone marrow for donor stem cell engraftment.[42] Current conditioning protocols mainly use a chemotherapy alone with busulfan and cyclophosphamide as well as other cytotoxic agents or a combination of TBI and chemotherapy (**Table 3**).[42] However, the high toxicity of these myeloablative regimens increases the treatment-associated mortality especially in elderly patients (>50 years). These observations and the growing understanding that the GVT effect sufficiently eradicate malignant cells and increases relapse-free long-term survival, led to the development of reduced-intensity conditioning.[3] Although this non-myeloablative conditioning results in less tumor killing, it still provides a sufficient GVT effect and

Table 3: Most common chemotherapy regimens before allo-HSCT. Gy, Gray. (from Kröger/ Zander 2011).[42]

TBI plus chemotherapy
TBI with 8-14 Gy + cyclophosphamide (120-200 mg/kg body weight)
Chemotherapy alone
Busulfan (14-16 mg/kg body weight) + cyclophosphamide (120-200 mg/kg body weight)
Other chemotherapies or combinations
Melphalan (140-200 mg/m^2)
Thiotepa (500-800 mg/kg body weight)
Etoposide (30-60 mg/kg body weight)
Treosulfan (30-42 g/kg body weight)

allows successful engraftment, allowing older patients, heavily pre-treated patients or patients with co-morbidities to benefit from allo-HSCT.[3]

The selection of the donor type is based on the HLA system and categorized as HLA-identical sibling donor, other family donor or unrelated donor. A well-matched unrelated donor is defined as a 10/10 or 8/8 identical donor based on HLA typing for class I (HLA-A,-B,-C) and II (HLA-DRB1,-DQB1). A mismatched unrelated donor is mismatched in at least one antigen or allele at HLA-A, -B, C or –DR.[1] A HLA-identical sibling donor remains the gold standard;[50] however unrelated transplantations increased due to the growing availability of bone marrow donor registries.[51] Clinical studies showed no differences in overall survival after allo-HSCT with HLA-identical sibling donor, HLA-matched family or HLA-matched unrelated donor.[50] Haploidentical donors are an alternative source for patients who do not have a HLA-identical sibling or unrelated donor from the registry, however incidence of graft failure and GVHD is higher.[52,53]

The regenerative potential of the hematopoietic stem cell (HSC) is the basis for allo-HSCT. After intravenous infusion, the HSC has the ability to reach the bone marrow, engraft and give rise to all the various cells of the hematopoietic lineage.[42] The HSC used for allo-HSCT is characterized by the expression of the cell surface protein CD34, the absence of the glycoprotein CD38 and absence of known myeloid and lymphatic markers (Lineage-negative).[42] The three commonly used sources for HSCs are the bone marrow, cytokine-mobilized (mainly granulocyte or granulocyte-macrophage colony stimulating factor (G-CSF, GM-CSF)) peripheral blood progenitor cells (PBSC) and cord blood cells.[1,42] PBSC as stem cell source are used in >70 % of adult allo-HSCTs,[54] while the bone marrow still remains the common source for pediatric allo-HSCTs.[3]

4.1.5 Chimerism and immune reconstitution after allo-HSCT

During the first few days after allo-HSCT, the reinfused donor HSCs migrate to the bone marrow and begin to produce blood cells of donor origin, a process called engraftment. Allo-HSCT leads to a hematopoietic chimerism and central tolerance between the graft and the recipient because of the full establishment of the donor hematopoiesis.[42] To allow the engraftment of donor cells, the administration of immune suppressive agents is necessary at least in the first weeks to months after allo-HSCT. Generally, in the first six months after allo-HSCT a transient mixed chimerism is present (with 1-5 % of recipient cells) converting later to a full donor chimerism (100 % of donor cells).[42] Especially after a non-myeloablative conditioning, also a stable mixed or progressive mixed chimerism is possible with the presence of both donor and recipient cells.[55] The loss of chimerism due to graft rejection (recipient hematopoiesis inhibits expansion of donor cells) is a dangerous complication after allo-HSCT, however due to improvements in immune suppression agents and HLA typing and -matching a rare circumstance.[42] The determination of the donor chimerism is used to control the

engraftment in the early weeks after allo-HSCT and in later phases to early detect a relapse as well as to predict overall survival and disease-free survival time.[56] To detect the percentage of donor cells, peripheral blood or bone marrow cells can be analyzed with a spectrum of methods (**Table 4**).[42]

Table 4: Methods for determining the chimerism in humans. FISH: fluorescence *in situ* hybridization, PCR; polymerase chain reaction, STR: short-tandem repeats, VNTR: variable number of tandem repeats, SNP: single nucleotide polymorphisms, Indel: insertions and deletions, FACS: fluorescence-activated cell sorting, MACS: magnetic-activated cell sorting (from Kröger/ Zander 2011).[42]

FISH analysis (XY-XX- chromosome) after sex-mismatched transplantation
RFLP (restriction fragment length polymorphism)
Analysis of polymorphic DNA sequences with PCR (STR and VNTR)
Analysis of SNPs and Indel-polymorphisms with quantitative real-time PCR
FACS and MACS to select immune cell populations

After conditioning and allo-HSCT, the transplantation-related immunodeficiency slowly recovers and hematological and immunological functions in the recipient are restored.[57] The success of allo-HSCT and long-term survival of the patient are therefore strongly connected with immunological reconstitution; especially in the context that significant bacterial, viral and mycotic infectious sequelae, particularly as a result of GVHD and its associated immunosuppressive prophylaxis, account for considerable transplantation-related mortality.[57] The reconstitution of innate immunity occurs rapidly within 20–30 days after allo-HSCT.[58] natural killer (NK) cells, monocytes, granulocytes, and dendritic cells are derived from myelomonocytic progenitor cells (**Figure 7**). Tissue macrophages show a donor origin within three months. The reconstitution of adaptive immunity is delayed following allo-HSCT and can require up to one year. B and T cells differentiate from lymphoid progenitor cells (**Figure 7**) and require specialized microenvironments in order to efficiently differentiate from primitive progenitors. They typically show delayed and incomplete recovery.[58] B cells recover within 12-24 months and cytotoxic CD8+T cells recover earlier than regulatory CD4+ T cells (6-10 versus 6-24 months).[42,58]

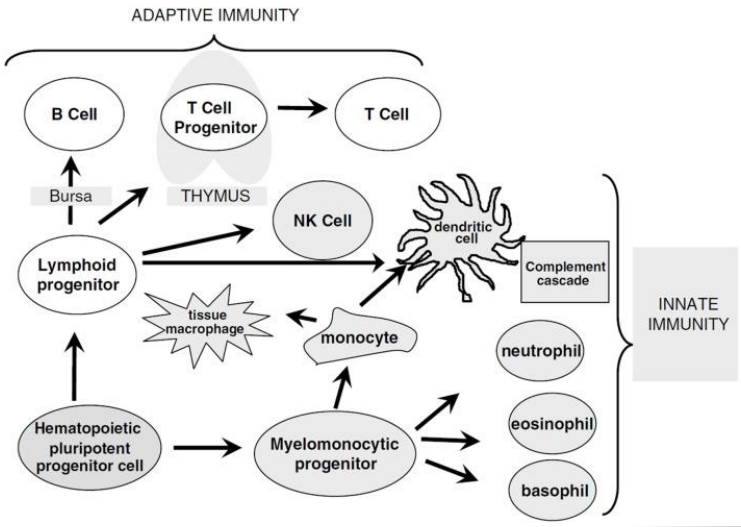

Figure 7: Overview of immune cell differentiation from HSC. The figure shows the different types of immune cells and their development from different precursors. The reconstitution of innate immunity occurs rapidly within 20–30 days after allo-HSCT while reconstitution of adaptive immunity is delayed following HSCT and can require up to one year (from Ogonek 2016).[58]

Immune reconstitution post-HSCT is influenced by several parameters (e.g. HLA-matching, stem cell source and quality or conditioning) and occurs in several phases (**Table 5**), which are connected to the occurrence of post-transplant complications.[42]

Table 5: Reconstitution phases before and after allo-HSCT. (from Kröger/Zander 2011).[42]

Pre-transplantation	During conditioning
Day of transplantation	Day 0
Pre-engraftment (aplastic phase)	Day 0-30
Engraftment	Granulocytes >1 x 10^9/l blood
Early reconstitution phase	Day 30-90
Intermediate reconstitution phase (post-engraftment)	Day 60-360
Late reconstitution phase	> 1 year post-HSCT

4.1.6 Complications after allo-HSCT

Despite therapy improvement and ongoing research, significant and fatal complications still occur after allo-HSCT.[3] GVHD is the major complication after allo-HSCT, leading to substantial morbidity and mortality. Despite prophylactic treatment, GVHD develops in 40-60 % of allo-HSCT recipients[59] and mortality can be as high as 50 %.[60] Due to its critical importance, it will be described in detail in chapter 4.2. Additional derogatory, GVHD prophylactic or therapeutic approaches, as T cell depletion[61] and immunosuppressive agents, create a secondary immune deficiency increasing the risk for tumor relapse[62] and fatal infections;[63,64] which account for significant post-transplant mortality. Graft rejection[65] and toxicities due to conditioning and other agents[66] are serious complications, however rather rare compared to GVHD occurrence.

Infectious complications are significantly GVHD-associated and occur i.a. due to the cell damage and immune deficiency caused by the conditioning and immunosuppressive agents.[67] It was shown that acute GVHD significantly increased the risk of developing life-threatening and fatal infections; and patients who developed acute GVHD experienced ~60 % more infections than patients who never develop acute GVHD.[63] During the aplastic phase (pre-engraftment) infections are mainly neutropenia-caused, so that bacterial sepsis, pneumonia or fungal infections represent the main cause of death.[42] With the beginning of the early reconstitution phase, the delayed reconstitution of adaptive immunity with insufficient T and B cell functions leads to viral and fungal infections; and viral reactivations, especially cytomegalovirus (CMV). In the post-engraftment phase, encapsulated bacterias (e.g. Streptococcus pneumoniae, Haemophilus influenzae) and respiratory viruses represent major risk factors (**Figure 8**).[42,58,68]

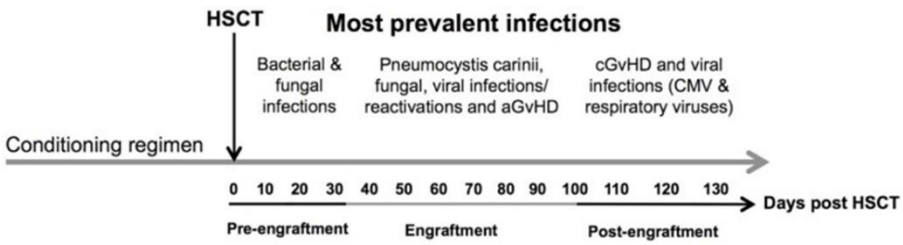

Figure 8: Time line of the most prevalent complications after allo-HSCT. According to the three phases of engraftment. CMV, cytomegalovirus. (from Ogonek 2016).[58]

Toxicities of conditioning regimens and other agents (e.g. for GVHD prophylaxis) can lead to i.a. oral and intestinal mucositis, renal and lung complications. A severe form of organ toxicity following high-dose therapy is the sinusoidal obstruction syndrome (SOS or hepatic veno-occlusive disease) in which detachment of damaged sinusoidal endothelial cells and impaired hepatic circulation occurs. It has variable incidence but is estimated at 10 % in allo-HSCT and SOS syndrome leads to a 90 % mortality rate.[69]

4.2 Graft-versus-Host Disease

GVHD is a systemic inflammatory disease caused by donor-derived, host-reactive T cells primarily attacking the epithelial cells of the GVHD target organs liver, skin and intestines; reflecting the major cause of morbidity and mortality in patients undergoing allo-HSCT.[70] Despite advances in prophylaxis and treatment, still 40-60 % of patients receiving transplants from HLA-identical sibling donors[3] and 60-80 % of patients receiving transplants from one antigen HLA-mismatched unrelated donors develop acute GVHD.[70,71] GVHD treatment mainly focus on the suppression of these host-reactive T cells,[59] however it favours the development of secondary immune deficiencies. Therefore, GVHD mortality is still high. More than half of allo-HSCT recipients die within the first two years[60] because of GVHD treatment failure or immunosuppressive treatment-associated complications as toxicities and increased risk for tumor relapse and fatal infections.[62,63]

That donor T cells are the main mediators of GVHD was elucidated in several animal, especially mouse, studies[2,70,72] and confirmed in humans e.g. when Horowitz showed that T cell depletion from the graft led to low levels of GVHD in humans, but was however associated with increased risk for relapse from distinct haematological malignancies and graft failure.[73] This phenomenon supports the evidence that donor T cells are also important for the immune-mediated GVT effect mediating effective elimination of malignant cells.[74-76] Other clinical studies support the central importance of donor T cells: 1) an increase in disease relapse is seen after allo-HSCT with HLA-identical twin, syngeneic or autologous transplants compared to HLA-matched transplants[73] and after *ex vivo* T cell depletion as GVHD prophylaxis;[62] 2) donor lymphocyte infusions (DLI) treat successfully recurrent leukemia after allo-HSCT;[31,77] and 3) withdrawal of immunosuppression induces remission in patients who relapsed after allo-

HSCT.[78] Therefore, immunosuppressive strategies completely abrogating host-reactive T cell impact are not favourable. Host-reactive T cell balancing strategies are needed, which maximize GVT effects, while minimizing GVHD.[2,79]

GVHD arises when donor T cells become alloreactive by the activation of their T cell receptor via MHC or minor antigens/peptides on host cells. The MHC encodes for HLA (class I and II), cell surface molecules that define histocompatibility and control T-cell recognition. Class I (HLA-A, B and C) are expressed on all nucleated cells; Class II (DR, DQ and DP) are mainly expressed on hematopoietic cells and abundantly in skin and intestines epithelium which may contribute to the specific target organ sites of acute GVHD.[70,80] Therefore, acute GVHD manifestations rely on the degree of donor/recipient HLA incompatibility; e.g. recipients from HLA-matched sibling donors develop less GVHD and show better engraftment compared to unmatched donors.[81,82] However, acute GVHD also develops in patients with HLA identity due to various genetic differences outside the MHC loci called minor histocompatibility antigens (miHAs). These peptides, derived from intracellular proteins, are presented by MHC molecules (in human mostly restricted to HLA class I) to donor T cells. miHAs show different expression, e.g. HA-Y and HA-3 are expressed on all tissues, HA-1 and HA-2 mainly on hematopoietic cells. miHA mismatches between recipient and donor create equal allo-activation, e.g. mismatches in HA-1, HA-2 and HA-5 were associated to increased risk for GVHD.[70,80]

Historically, GVHD was timely separated into acute GVHD (arising within 100 days after allo-HSCT) and chronic GVHD (developing thereafter), however this simple and convenient classification did not reflect the biology of the disease. Therefore acute and chronic GVHD are now classified as two separate diseases with distinct clinical and histopathological presentation and pathogenesis. While acute GVHD is characterized by an excessive inflammation and tissue damage, chronic GVHD resembles autoimmune disorders and represents the major cause of late non-relapse mortality after allo-HSCT.[83] The following chapters will focus on acute GVHD.

4.2.1 Pathogenesis of acute GVHD

Three mechanisms contribute to the development of acute GVHD: 1) Immunological competent donor lymphocytes in the graft react with recipient-specific tissue antigens. 2) Immunosuppression of the recipient hampers an effective response to eliminate transplanted donor cells. 3) Underlying disease, prior infections and conditioning regimens damage recipient tissues leading to the release of soluble mediators which further promote activation and proliferation of donor lymphocytes.[84] The pathophysiology of acute GVHD is a complex cascade of humoral and cellular interactions between donor and recipient cells and much of our current understanding derives from animal, especially mouse models.[59,70,85] Ferrara introduced a three sequential step model for the development of acute GVHD: 1) Immune

priming and activation of antigen-presenting cells (APCs); 2) donor T cell activation, proliferation and differentiation; and 3) effector cell response leading to target organ destruction (**Figure 9**).[70]

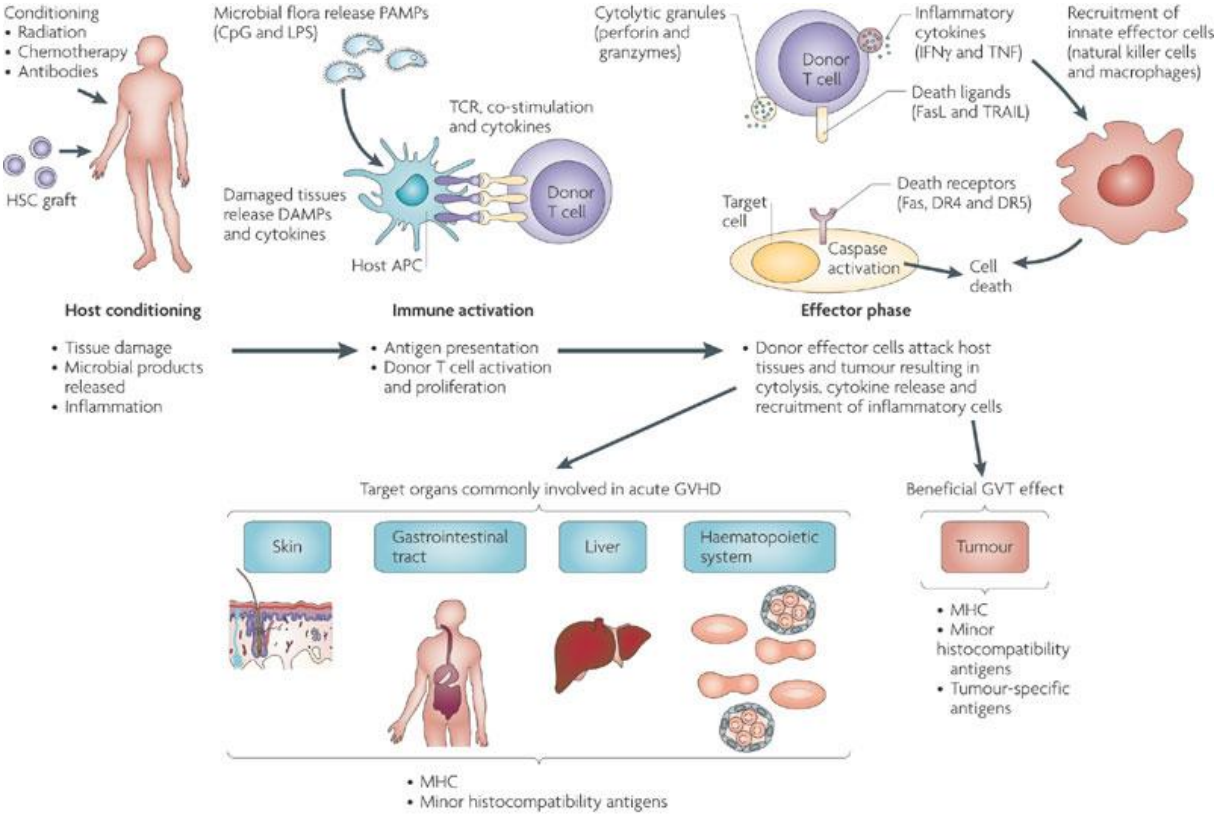

Figure 9: Pathophysiology of acute GVHD. HSC, hematopoietic stem cell. PAMPs, pathogen-associated molecular patterns. LPS, lipopolysaccharides. DAMPs, damage-associated molecular patterns. TCR, T cell receptor. APC, antigen-presenting cell. IFN-γ, interferon γ. TNF, tissue necrosis factor. TRAIL, TNF-related apoptosis-inducing ligand. DR, death receptor. GVHD, graft-versus-host-disease. GVT, graft-versus-tumor. MHC, major histocompatibility complex. (from Jenq and van den Brink 2010).[3]

In the first phase, the initial host conditioning leads to the damage and activation of the host tissue, especially the Gastrointestinal (GI) tract, and the establishment of a local inflammatory environment. Damaged tissue releases inflammatory mediators (cytokines as TNF-α, Interleukin 1 (IL-1), IL-6 and damage-associated molecular patterns (DAMPs) as Uric acid, extracellular adenosine triphosphate (ATP) or high-mobility-group-protein B1 (HMGB-1)). The microbial flora further enhances activation by the release of pathogen-associated molecular patterns (PAMPs) as lipopolysaccharides (LPS), CpG or Flaggelin. Pathogen recognition receptors as Toll-like or nucleotide-binding oligomerization domain (NOD)-like receptors on host innate immune cells recognize these “danger signals” leading to their activation characterized by increased expression of adhesion, antigen-presenting (MHC) and co-stimulatory molecules (**Figure 9**). These activated host cells (APCs) enhance the recognition of host antigens to mature donor cells, and the initial interaction site between host APCs and donor T cells is likely the secondary lymphoid tissue in the GI tract.[59,70,80,86]

In the second phase, donor CD4+ and CD8+ T cells proliferate and differentiate in response to T cell receptor (TCR) activation by minor and MHC antigens (CD4+ to MHC class I, CD8+ to MHC class II) presented by APCs (**Figure 9**).[70,80] In phase I activated host APCs further enhance activation by providing costimulatory signals. TCR stimulation without further costimulatory activation leads often to T cell anergy. There are several costimulatory interactions involved, leading to increased (CD86/CD80 on APCs and CD28 on T cells; CD40 on APCs and CD40L on T cells) or inhibitory pathways (CD80/CD86 on APCs and cytotoxic T-lymphocyte-associated protein 4 (CTLA-4) on T cells; programmed cell death 1 (PD1) and PD1L) (**Figure 10**). APCs provide a third proliferative signal to the donor T cells by releasing cytokines (e.g. IL-7, IL-15) and are involved in helper T polarization.[59,86]

TCR activation induces a complex intracellular signaling cascade including calcineurin activation and nuclear factor of activated T-cells (NFAT) dephosphorylation as well as nuclear factor 'kappa-light-chain-enhancer' of activated B-cells (NFκB) dissociation from NFκB inhibitor alpha (IκBα). Translocation of NFAT and NFκB to the nucleus finally leads to transcription of cytokines (predominantly IL-2, the key cytokine for T cell proliferation, differentiation and survival), IL-2 receptor and costimulatory molecules. IL-2 receptor stimulation on T cells activate i.a. mechanistic Target of Rapamycin (mTOR) and janus kinase (JAK)/ signal transducer and activator of transcription (STAT) pathways regulating cell cycle and therefore determining T cell proliferation and differentiation (**Figure 10**).[59,86]

Naive donor T cells differentiate into different lineages in the presence of distinct cytokines, which can show preferentially sensitivity to the GVHD target organs: type I T cells involved in GI tract, type 2 T cells in cutaneous and hepatic, and type 17 T cells in cutaneous and pulmonary acute GVHD.[59]

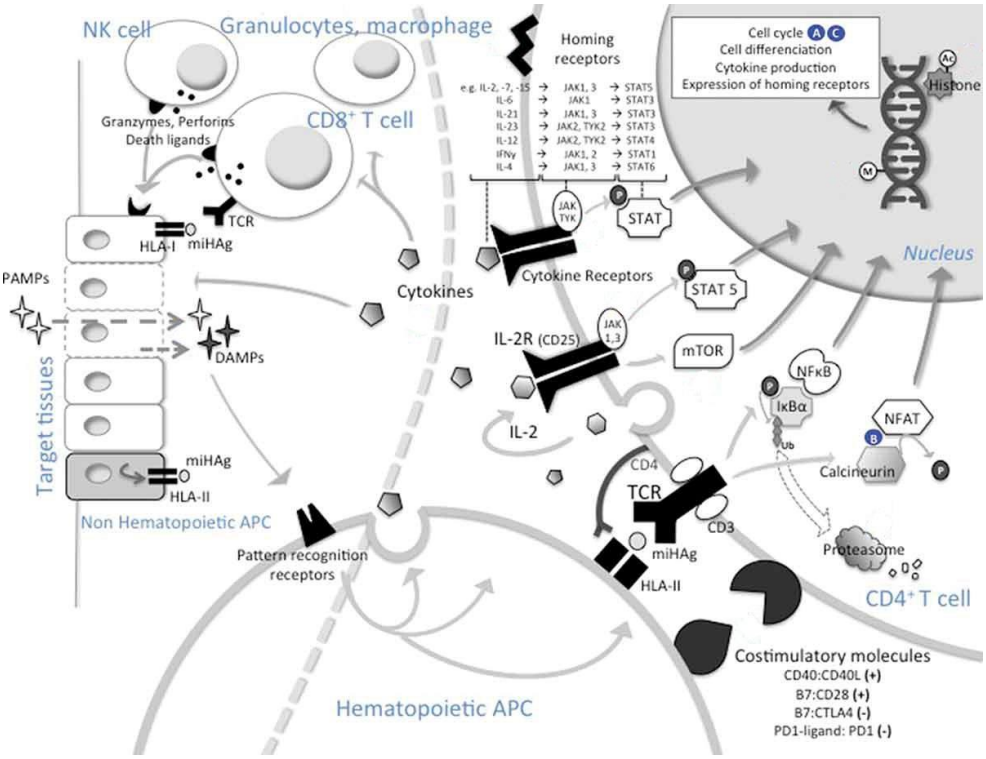

Figure 10: Signaling pathways during GVHD. Events on the left side from discontinued grey line mostly occur in peripheral tissues, events on the right side mostly occur in secondary lymphoid organs. Sites of action of standard prophylaxis regimens are depicted in circles (A = methotrexate. B = calcineurin inhibitors. C = mycophenolate mofetil). Ac, acetyl. APC, antigen-presenting cell. CTLA4, cytotoxic T-lymphocyte-associated protein 4. DAMPs, damage-associated molecular patterns. HLA, human leukocyte antigen. IL, interleukin. IL-2R, IL-2 receptor. IFN, interferon. IκBα, NFκB inhibitor alpha. JAK, janus kinase. M, methyl. miHAg, minor histocompatibility antigen. mTOR, mechanistic Target of Rapamycin. NFAT, nuclear factor of activated T-cells. NFκB, nuclear factor 'kappa-light-chain-enhancer' of activated B-cells. NK cells, natural killer cells. P, phosphate. PAMPs, pathogen-associated molecular patterns. PD1, programmed cell death 1. STAT, signal transducer and activator of transcription. TCR, T-cell receptor. TYK2, tyrosine kinase 2. Ub, ubiquitine. (modified from Servais et al. 2016).[59]

In the effector phase, activated (alloreactive) donor T cells infiltrate the typical GVHD target organs GI tract, skin and liver through tissue homing molecules and receptors (e.g. integrin α4β7, macrophage inflammatory protein 1α (MIP-1α), CC-chemokine ligands 2-5 (CCL2-5), CXC-chemokine ligands 2,9-11 (CXCL2,9-11)). A cascade of cellular and soluble inflammatory mediators results in target organ destruction. Activated APCs and T cells release various cytokines (i.a. interferon γ (IFN-γ), TNF-α, IL-1), which lead to further expansion of T cells and recruitment of innate effector cells as macrophages and NK cells amplifying local inflammation and tissue damage. The main cellular mediators causing tissue damage are NK cells and cytotoxic T cells. Due to large expression of Fas on hepatocytes, cytotoxic T cells mainly mediate GVHD liver damage through lysis and caspase activation in target cells using the Fas/FasL pathway. In skin and GI tract GVHD, cytotoxic T cells mainly use the perforin/granzyme pathway to target host cells. Inflammatory mediators include TNF-α or microbial products as LPS leaking through the damaged intestinal mucosa or skin and stimulating secretion of inflammatory cytokines trough Toll-like receptors (**Figure 9**).[59,70,80,86] However, alloreactive T cells cannot only attack host tissues (leading to GVHD) but also the tumor leading to the beneficial GVT effect.[3]

4.2.2 Clinical manifestations of acute GVHD

The clinical manifestations of acute GVHD occur as severe inflammatory lesions mainly of the skin, liver and GI tract. At the onset of acute GVHD, patients show 81 % skin, 54 % GI and 50 % liver involvement.[87] There is growing evidence that other organs can be targeted and damaged, i.a. the lungs,[84] the thymus[88,89] and the bone marrow niche.[90] To assess the incidence of severity, acute GVHD is scored from grade I-IV depending on the site and extent of manifestation (**Table 6**) and histology of organ biopsies can help to confirm the diagnosis especially if symptoms are unspecific.[80]

Table 6: Organ staging of acute GVHD. (from Ball et al. 2008).[80]

Stage	Skin	Liver	GI tract
0	No rash due to GVHD	Bilirubin <2 mg per 100 ml or 35 µmol/l	None (<280 ml/m^2)
I	Maculopapular rash <25 % of body surface area without associated symptoms	Bilirubin from 2 to <3 mg/100 ml or 35–50 µmol/l	Diarrhea >500–1000 ml/day (280–555 ml/m^2); nausea and emesis
II	Maculopapular rash or erythema with puritis or other associated symptoms >25 % of body surface area or localized desquamation	Bilirubin from 3 to <6 mg/100ml or 51–102 µmol/l	Diarrhea >1000–1500 ml/day (556–833 ml/m^2); nausea and emesis
III	Generalized erythroderma; symptomatic macular, papular or vesicular eruption with bullous formation or desquamation covering >50 % of body surface area	Bilirubin 6 to <15 mg/100 ml or 103–225 µmol/l	Diarrhea >1500 ml/day (>833 ml/m^2); nausea and emesis
IV	Generalized exfoliative dermatitis or bullous eruption	Bilirubin >15mg/100 ml or >225 µmol/l	Diarrhea >1500 ml/day (> 833 ml/m^2); nausea and emesis. Abdominal pain or ileus

The overall grades (**Table 7**), classified as I (mild), II (moderate), III (severe) and IV (very severe) are associated with prognosis of transplantation-related mortality.[70] While severe acute GVHD carries poor prognosis (25 % and 5 % long-term survival for grade III and IV, respectively),[91] mild acute GVHD (grade I) is associated with better survival because of decreased risk of disease relapse due to a sufficient GVT effect.[79,92,93]

Table 7: Overall clinical grading of acute GVHD. (from Ball et al. 2008).[80]

Grade	Skin	Liver	GI tract
0	0	0	0
I	1-2	0	0
II	1-3	1	1
III	2-3	2-3	2-3
IV	2-4	2-4	2-4

Commonly, the skin is the first organ involved often coinciding with engraftment. The characteristic maculopapular rash is pruritic, sometimes painful and can spread from the palms of the hands and soles of the feet to the face, neck, upper chest and trunk. Severe stage III includes generalized erythroderma which can progress to blistering and exfoliating of the epidermal skin layers in grade IV. Histopathologic features include apoptosis at the base of epidermal rete ridges, dyskeratosis, exocytosis of lymphocytes and perivascular lymphocytic infiltration in the dermis.[70,80]

GI involvement manifests as secretory and often severe diarrhea (>2 liters per day) accompanied by anorexia and nausea. In severe stages, abdominal pain, ileus and bleeding due to mucosal ulceration can occur. Radiologic diagnostic can picture luminal dilatation with thickening of the wall in small bowel as well as air/ fluid levels suggesting an ileus. Histopathologic findings are patchy ulcerations, apoptotic bodies in the base of crypts, crypt abscesses and flattening or loss of mucosal epithelium.[70,80]

Damage of the liver is characterized by an isolated hyperbilirubinemia, and increase in alkaline phosphatase in peripheral blood testing is more frequently than liver enzyme abnormalities. However, damage caused by acute GVHD is difficult to distinguish from other causes of liver complications after allo-HSCT (SOS, drug toxicity, viral infection, sepsis or iron overload). Although characteristic histopathological features (endothelialitis, portal lymphocytic

infiltration, pericholangitis and bile duct destruction) can ensure the diagnosis of hepatic GVHD, hepatic biopsies are rarely performed as thrombocytopenia early after allo-HSCT increases the risk of complications of this procedure. Therefore, identifying hepatic GVHD is often a diagnosis of exclusion.[70,80]

4.2.3 GVHD prophylaxis and treatment

Since the 1980´s, the standard GVHD prophylaxis for patients after allo-HSCT from HLA-matched sibling or unrelated donor combines the use of the folate antagonist methotrexate (MTX), which inhibits T cell proliferation, with the calcineurin inhibitors Cyclosporin A (CSA) or Tacrolimus, which inhibit the TCR-induced intracellular activation cascade.[94,95] The combination of CSA and MTX compared to the single use of CSA was shown to reduce incidence of acute GVHD, however leukocyte engraftment was delayed.[96] Side effects of CSA and Tacrolimus include hypomagnesemia, hyperkalemia, hypertension, nephrotoxicity and thrombotic microangiopathy.[97] As MTX can show severe toxicities (neutropenia and mucositis) it is sometimes replaced by Mycophenolate mofetil (MMF), especially after allo-HSCT with reduced intensity conditioning. The MMF metabolite, mycophenolic acid, inhibits lymphocyte proliferation by blocking the de novo synthesis of guanosine nucleotides.[59]

Another approach, T cell depletion, includes three principal methods: 1) negative selection of T cells *ex vivo*; 2) Positive selection of CD34+ stem cells *ex vivo*; and 3) anti-T cell antibodies *in vivo*.[70] Although these approaches mostly showed a significant reduction of acute GVHD, the outcome was hampered by increased graft failure, relapse of malignancy and infections.[70] Anti-T cell antibodies include e.g. anti-thymocyte globulins (ATG), polyclonal IgG antibody preparations generated from horses or rabbits, that were immunized with human thymocytes or the human T cell line Jurkat.[59] ATG induces T cell depletion through complement-dependent lysis and activation-associated apoptosis.[59] Alemtuzumab, a humanized monoclonal antibody against CD52 (widely expressed on T, NK and B cells), was shown to deplete T and B cells and prevent acute GVHD, especially after reduced intensity conditioning; however success was limited by delayed immune recovery, infections and delayed T cell chimerism.[59]

Still 40-60 % of patients develop GVHD after allo-HSCT despite current standard GVHD prophylaxis. Therefore new approaches are under investigation and development. This includes 1) further, more specific T cell depleting approaches (e.g. suicide gene therapies, post-transplant cyclophosphamide, depletion of specific T cell subsets); 2) functional inhibition of donor T cell activation by e.g. proteasome, mTOR or JAK inhibitors; 3) epigenetic modulation in immune cells (e.g. demethylating agents, histone deacetylase inhibitors); 4) inhibition of extracellular mediator pathways (IL-6, CCR5); 5) B cell depletion (anti-CD20); and more recently 6) the infusion of specific cell subsets to promote immune tolerance (e.g. infusion of

regulatory T cells, mesenchymal stem cells, invariant natural killer T cells or myeloid-derived suppressor cells).[59]

The standard therapy for acute GVHD treatment includes the continued treatment with calcineurin-based prophylaxis[98] and the application of steroids, which exhibit potent anti-lymphocyte and anti-inflammatory activities.[70] However, steroid treatment leads in less than half of the patients to a complete remission of GVHD and more severe GVHD is less likely to respond to the treatment. Although, there are some immune suppressive drugs and monoclonal antibodies available during this so called ‘steroid-refractory GVHD’, the outcome is still poor.[99]

The reliance of GVHD prophylactic and therapeutic treatment on the suppression of host-reactive T cells, harbours significant disadvantages. It favours the development of secondary immune deficiencies leading to an increased risk for tumor relapse and fatal infections.[62,63] GVHD treatment failure or immunosuppressive treatment-associated complications still lead to significant mortality in GVHD patients underlining the urgent medical need for alternative therapies, which do not attenuate the immune system.

4.2.4 Mouse models of acute GVHD

Studies in experimental models, especially in mice, have been clinically relevant for the development of allo-HSCT in humans.[85] Several main advances in fundamental understanding of allo-HSCT and GVHD were generated in murine models (see chapter 4.1.1).[2] Still, developing new treatment strategies or adding mechanistic understanding to the development of GVHD relies on the use of experimental murine GVHD models.[72,85]

As in human acute GVHD, alloreactive, disease-inducing T cells are activated through their TCR via foreign MHC or minor antigens. In mouse models, this is achieved by MHC class I and II differences between donor and recipient strains activating CD8+ or CD4+ T cells, respectively. These so called MHC-mismatched acute GVHD models are frequently used, the most commonly studied model is the C57BL/6 (H-2^b) donor in BALB/c (H-2^d) recipient transplantation.[72] Generally, a MHC-mismatched model develops a bi-phasic pathogenesis, with a hyper acute disease pattern within the first 7 days after allo-HSCT, a short recovery phase turning into acute GVHD progression.[48,100,101] However, this “full MHC mismatch” is not required in humans, as after a HLA-matched transplantation also acute GVHD occurs (with constant disease progression). MiHA-mismatched acute GVHD models represent human allo-HSCT more closely, as MHC-mismatched transplantations are not the first choice in humans. Similar to the human setting, acute GVHD is induced by activated CD4+ and CD8+ T cells responding to minor antigens in miHA-mismatched mouse models, leading to less morbidity compared MHC-mismatched model, but still developing lethal acute GVHD.[72]

In most acute GVHD mouse models, recipient mice are conditioned with myeloablative TBI, either in a single or split dose (range from 800-1300 cGy). These lethally irradiated recipients receive donor stem cells isolated from the bone marrow from tibia and femur of 8-12 week old donor mice. Depending on the model, the bone marrow can be T cell depleted. To induce GVHD, donor lymphocytes from the spleen or lymph nodes are supplemented to the bone marrow cells. Whole splenocytes or already selected T cell subsets (CD3+, CD4+, CD8+) can be transplanted. The severity of acute GVHD can be influenced in the mouse models by several factors: 1) MHC disparity due to selection of recipient and donor strains; 2) Dose and type of transplanted donor lymphocytes; 3) dose of TBI, as dose is proportional to the degree of tissue damage and GVHD-related mortality in mice; 4) different radiation susceptibility of inbred strains (e.g. BALB/c>C3H>C57BL/6); and 5) different environmental pathogens in housing facilities.[72,85,102]

4.3 Angiogenesis and the endothelium in inflammation

4.3.1 Angiogenesis

The formation of blood vessels (neovascularization) can occur through two mechanisms: 1) vasculogenesis, in which bone marrow derived endothelial precursor cells (EPCs) incorporate into vessels, differentiate and proliferate;[103-105] and 2) angiogenesis, the de novo formation of capillaries from pre-existing blood vessels involving endothelial cells (ECs), which layer the lumen of blood vessels. Both mechanisms are present in embryonic development and in the adult; however angiogenesis is the predominant process in adult neovascularization.[106] Angiogenic processes are tightly linked to inflammation, whether in physiological conditions as wound healing or ovulation; or in pathological processes as tumour growth, cardiovascular or inflammatory diseases.[104,105,107]

Angiogenesis is a tightly orchestrated process, which involves the activation of quiescent ECs, the degradation of the extracellular matrix, the vessel sprouting relying on migratory, guiding “tip” cells and elongating, proliferative “stalk” cells, morphogenesis and the vessel stabilization by recruitment of pericytes.[104,107,108]

Quiescent ECs form monolayers and are connected by tight, adherens and gap junctions.[109] They are surrounded by periendothelial mural cells (smooth muscle cells for large vessels, pericytes for small vessels) which support ECs through cell-survival signals and suppress their proliferation.[110] Both ECs and pericytes produce the basement membrane, mainly consisting of laminin, (HSPGs), type IV collagen and nidogen/ entactin.[111] ECs are anchored in this basement membrane by integrins.[112] Several maintenance signals preserve the EC quiescence, e.g. vascular endothelial growth factors (VEGF), angiopoietin-1, fibroblast growth factors (FGFs) or Notch signaling (**Figure 11**).[113]

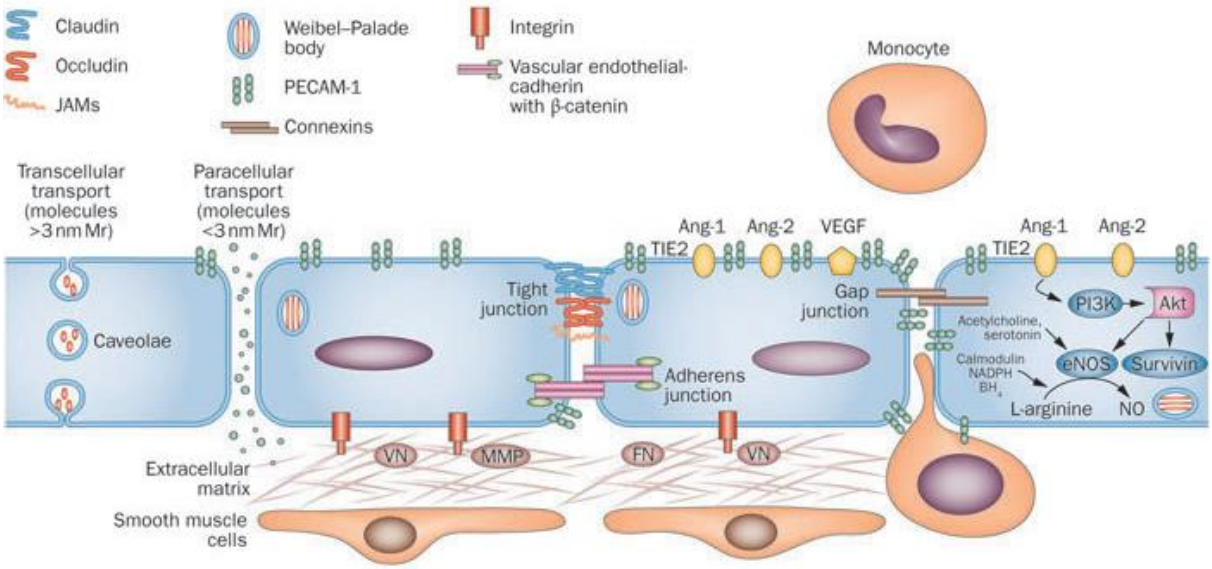

Figure 11: The quiescent endothelium. Ang, angiopoietin. BH4, 5,6,7,8-tetrahydrobiopterine. eNOS, endothelial nitric oxide synthase. FN, fibronectin. JAMs, junctional adhesion molecules. MMP, membrane metalloproteinases. Mr, molecular radius. NADPH, nicotinamide adenine dinucleotide phosphate. NO, nitric oxide. PECAM-1, platelet/endothelial cell adhesion molecule 1. PI3K, phosphoinositide 3-kinase. VEGF, vascular endothelial growth factor. VN, vitronectin. (from Otsuka et al. 2012).[109]

During angiogenesis, ECs within the vessel wall are selected for sprouting and become activated through the stimulation by angiogenic factors and chemokines released from fibroblasts, tumor or inflammatory cells, e.g. through hypoxia-inducible factor-1α (HIF-1α) mediated signaling.[114] The major activation mechanisms includes the activation of receptor tyrosine kinases, especially VEGFA→VEGFR2, bFGF2→FGFR1 and angiopoietin-2→Tie2, leading to intracellular activation of mainly the rat sarcoma (Ras)/ extracellular-signal regulated kinase (ERK1/2), phosphoinositide 3-kinase (PI3K)-AKT and Ca^{2+}-phospholipase Cγ (PLCy) pathways.[104] Activation in the selected ECs, called tip cells which will lead the angiogenic front, is spatially restricted by i.a. increased Delta-like 4 (DLL4) expression in these cells (**Figure 12**). DLL4 binds to Notch receptors on the surface of neighbouring ECs (called stalk cells), which lead to the transcriptionally downregulation of *Vegfr2*, enhancing unresponsiveness to VEGF.[115] The sprouting tip cells acquire an invasive and motile behaviour by changing their phenotype fundamentally;[115,116] this includes the degradation of the basement membrane by activated secreted or surface-anchored proteases (e.g. matrix metalloproteases (MMPs)), disruption of EC junctions (downregulation of e.g. vascular endothelial (VE)-cadherin, Zonula occludens-1 (ZO-1)) and pericyte detachment (regulated by angiopoietin-2). The apical-basal polarity is reversed as new sprouts need to emerge from the basal (outer) side of the endothelium. Sprout elongation is also characterized by polarization and directional changes in the cytoskeleton. Tip cells show extensive filopodia protrusions, which sense positive and negative guidance signals through e.g. VEGFA/VEGFR2, semaphorin-neuropilin, plexin, netrins and SLIT protein signaling (**Figure 12**). VEGFA increases the vessel permeability leading to the extravasation and deposition of plasma

proteins like fibronectin and fibrinogen, which build a provisional matrix layer enabling tip cell migration in the direction of the growth factor gradient. Release of platelet-derived growth factor B (PDGFB) from tip cells recruits PDGF receptor β expressing pericytes, which can stabilize the growing sprouts (**Figure 12**).[115,116] While tip cells polarize towards the angiogenic front, following stalk cells proliferate and elongate the sprout (stimulated by Notch, Wnts, placental growth factor and FGFs).[113] By encountering tip cells of other sprouts, tip cells suppress their motile behaviour and establish strong adhesive interactions and EC-EC junctions to form new vascular connections (**Figure 12**).[115] To establish a blood flow the formation of a vascular lumen is required, which occurs in the stalk cells before and after sprout joining. This process includes pinocytosis ("cell drinking") and vacuole formation, regulated by establishment of the apical basal polarity (by e.g. integrin cell-matrix adhesion machinery and guanosine triphosphate (GTP)ases CDC42 and Ras-related C3 botulinum toxin substrate 1 (Rac1))[115,117] and cell-cell contacts (e.g. adhesion receptors as E-cadherin).[118] Established perfusion promotes maturation processes as vessel stabilization by pericyte attachment, stabilization of EC junctions and deposition of a new basement membrane by ECs and pericytes (**Figure 12**).[119,120] It also improves the oxygen supply and thereby reduces hypoxia-induced proangiogenic signaling. Growth factor withdrawal can also trigger sprout retraction and EC apoptosis avoiding extensive sprouting and persistence of non-functional sprouts. In the new mature vasculature, ECs readopt their quiescent status.[115]

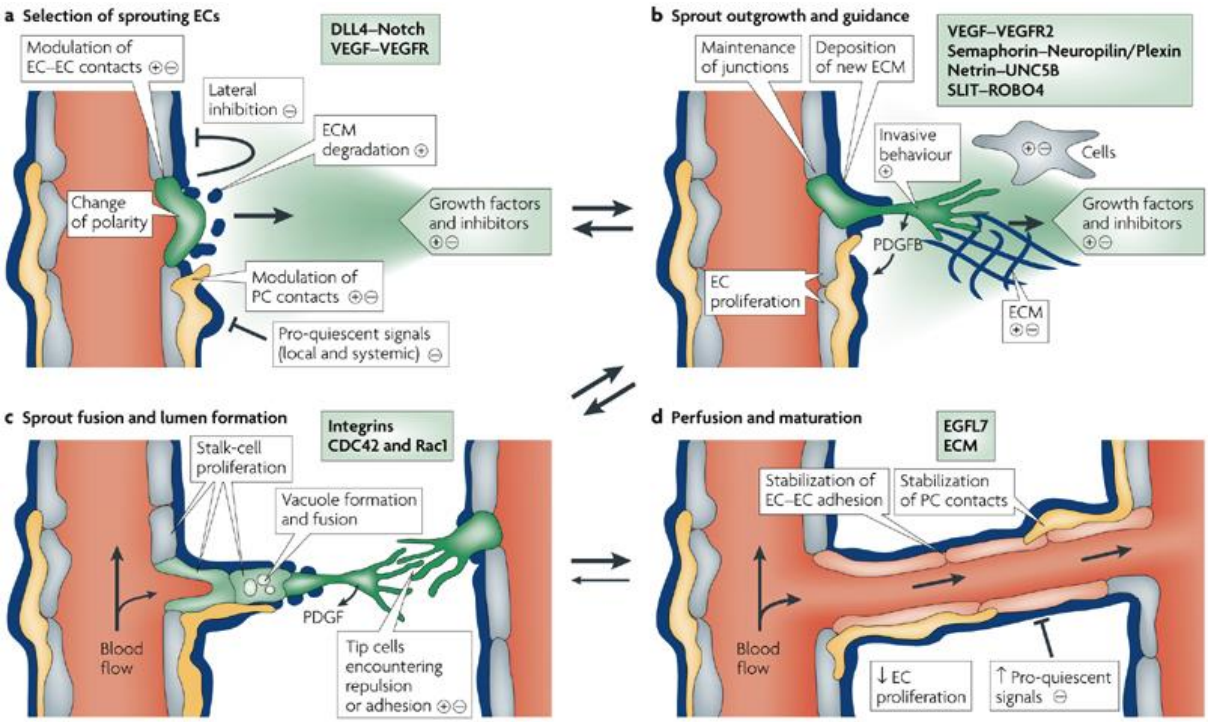

Figure 12: Schematic overview of angiogenic sprouting. DLL4, delta-like-4 ligand. EC, endothelial cell. ECM, extracellular matrix. EGFL7, epidermal growth factor ligand-7. PC, pericytes. PDGFB, platelet-derived growth factor B. Rac1, Ras-related C3 botulinum toxin substrate 1. ROBO4, roundabout homologue-4. UNC58, uncoordinated protein 58. VEGF, vascular endothelial growth factor. VEGFR2, VEGF receptor-2. (from Adams et al. 2007).[115]

4.3.2 Cellular and molecular mediators of angiogenesis

There is a wide range of molecules that can induce angiogenesis in either physiological or pathological conditions; however activated intracellular pathways often overlap. Many of these molecular mechanisms modulate angiogenic, endothelial activating and inflammatory processes and activating or targeting one can induce or modify the other (**Figure 13**).[104,121] Therefore the crosstalk between angiogenesis and inflammation is well-established, however it is still not clear if angiogenesis is a consequence or the cause of inflammation.[122] Hypoxia-induced translation of growth factors and other mediators as well as pro-inflammatory mediators released by immune and stromal cells are believed to be main drivers of these mechanisms.[104,107,121]

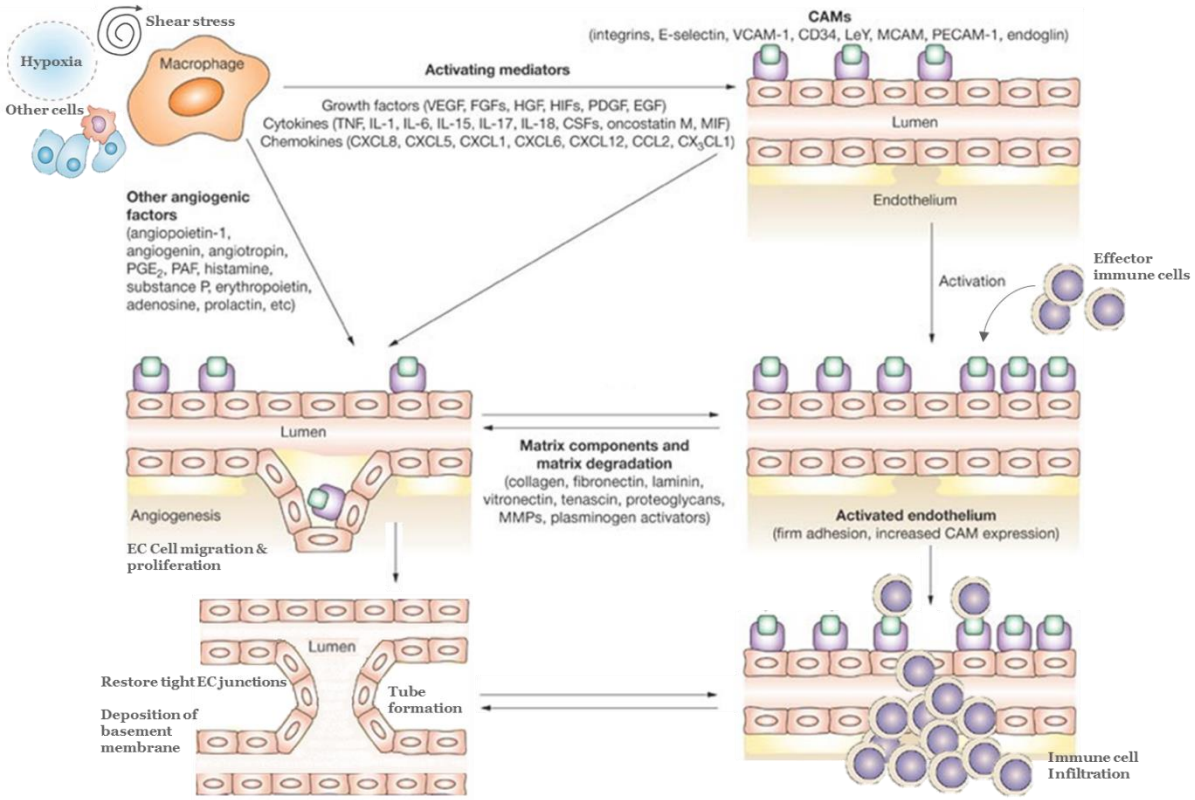

Figure 13: Interplay between inflammation and angiogenesis. CAM, cell adhesion molecule. CCL, CC-chemokine ligand. CSF, colony-stimulating factor. CXCL, CXC-chemokine ligand. CX_3CL, CX_3C-chemokine ligand. EGF, endothelial growth factor. FGF, fibroblast growth factor. HGF, hepatocyte growth factor. HIF, hypoxia inducible factor. IL, interleukin. LeY, Lewis Y antigen. MCAM, melanoma cell adhesion molecule. MIF, macrophage migration inhibitory factor. MMP, matrix metalloproteinase. PAF, platelet-activating factor. PDGF, platelet-derived growth factor. PECAM-1, platelet/endothelial cell adhesion molecule-1 (CD31). PGE2, prostaglandin E2. TNF, tumor necrosis factor. VCAM-1, vascular cell adhesion molecule-1. VEGF, vascular endothelial growth factor. (modified according to Szekanecz et al. 2007).[121]

During hypoxia, a poor oxygen concentration within a tissue, the transcription factors HIFs and NFκB can translocate to the nucleus as oxygen-sensing prolyl hydroxylases (PHDs) are inhibited (**Figure 14**). Hypoxia-induced HIF- and NFκB-dependent transcriptional activation include proangiogenic and pro-inflammatory factors as VEGF and VEGFR1, PDGF, intercellular adhesion molecule 1 (ICAM-1), vascular cell adhesion protein 1 (VCAM-1),

inducible nitric oxide synthase (iNOS), cyclooxygenase 1 and 2 (COX-1 and -2), IL-1β, CXCL12, IL-6, TNF-α, IL-8, MIP-2.[104,107]

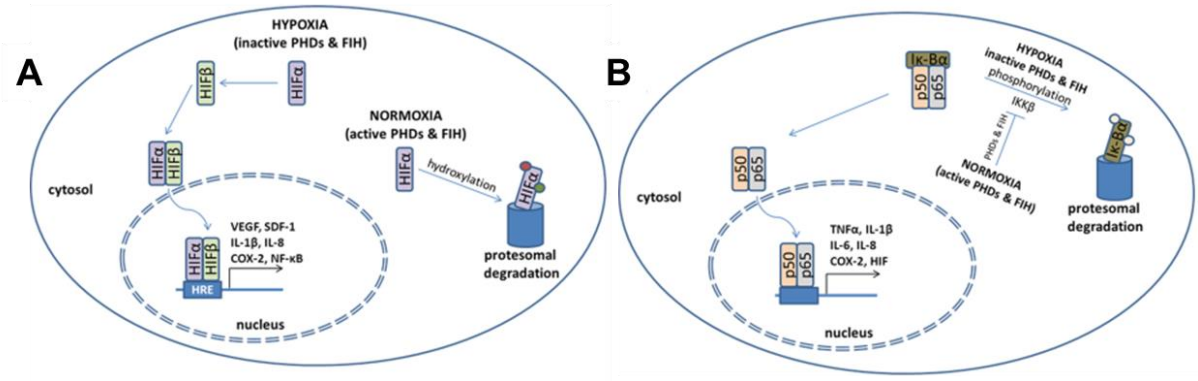

Figure 14: Regulation of HIF (A) and NFκB (B) activity in normoxia and hypoxia. In normoxia, PHDs and FIH hydroxylate HIFα subunit, targeting it to proteasomal degradation. Inactivation of these enzymes in hypoxic condition allows for HIF heterodimerization and enables its transcriptional activity (A). Unlike in hypoxia, PHDs and FIH modify IKKβ at normal oxygen level, inhibiting its phosphorylation and protecting from degradation. PHDs, oxygen-sensing prolyl hydroxylases. FIH, factor inhibiting HIF. HIF, hypoxia-inducible factor. IKKβ, inhibitor of nuclear factor kappa-B kinase subunit beta. IκBα, NFκB inhibitor alpha. VEGF, vascular endothelial growth factor. IL, interleukin. TNF, tissue necrosis factor. COX, cyclooxygenase. SDF-1, stromal cell-derived factor 1 NFκB, nuclear factor 'kappa-light-chain-enhancer' of activated B-cells (from Szade et al. 2015).[107]

Fibroblasts and several immune cells are described to release angiogenic factors; macrophages are key players in this process, especially M2 macrophages and tumor-associated macrophages show proangiogenic properties by releasing cytokines and chemokines.[104,107,121] Precursors of resident macrophages, circulating CD14+CD16+ monocytes can also induce angiogenic responses.[123] Several pro-inflammatory cytokines are considered to be also proangiogenic as TNF-α, IL-1, IL-6, IL-8, IL-15, IL-17, IL-18, G-CSF, GM-CSF or oncostatin M (**Figure 13**). These factors can either directly exhibit proangiogenic activities or act indirectly through VEGF-dependent pathways, upregulation of expression of adhesion molecules and MMPs or mediating Angiopoietin-TIE-dependent pathways. Chemokines as CXCL1, 5, 6, 8, 12 exhibit proangiogenic properties and can also indirectly promote angiogenesis by attracting further immune cells to inflammatory sites; e.g. CCL2 attracts monocytes and macrophages, the major source of proangiogenic mediators, CX_3CL1 can promote vessel formation but also recruits leukocytes.[104]

Tissue remodelling is found in inflammatory tissues and is a critical step during angiogenesis and involves extracellular matrix components, adhesion receptors and proteases. The pro-inflammatory environment promotes the degradation of matrix components, e.g. through MMPs, required for EC migration during angiogenic sprouting.[121]

4.3.3 Endothelial activation

In non-inflamed tissues, quiescent ECs 1) maintain blood fluidity by controlling coagulation, 2) regulate blood flow by controlling the vessel muscle tonus, 3) regulate vessel permeability; and 4) quiesce circulating leukocytes. During inflammatory processes, ECs are active participants and regulators. The inflammatory activation of ECs consist of three main components that

underlie the four cardinal signs of inflammation: 1) increase in blood flow accounting for red color (rubor) and warmth (calor) of inflamed tissues; 2) leakage of plasma-protein-rich fluid accounting for swelling (tumor) of inflamed tissues; and 3) recruitment and activation of circulating leukocytes entering the damaged tissue accounting for pain when released mediators excite C-type sensory nerve fibers.[124]

EC activation divides into two types: the fast type I activation (also called stimulation) which is independent of gene expression changes, and the slower (hours as opposed to minutes) type II activation, which is dependent on gene expression.[125] Type I activation is mediated by ligands binding heterotrimeric G-protein-coupled receptors (GPCR), however degree of inflammation and neutrophil extravasation caused by this activation is limited and spontaneously resolves as GPCR signals last for 10-20 minutes after which the receptors are desensitized to prevent restimulation (**Figure 15**). Type II activation arise slower but more persistent providing a more sustained inflammatory response. Prototypic signaling mediators of this activation are TNF-α and IL-1, mainly derived from activated leukocytes and binding on their corresponding receptors on the EC surface (**Figure 16**). Type II activation can persist as long as activating signals are present. However, it can be inhibited by the removal of the inflammatory stimulus or by multiple negative feedback mechanisms targeting activated gene expression.[124]

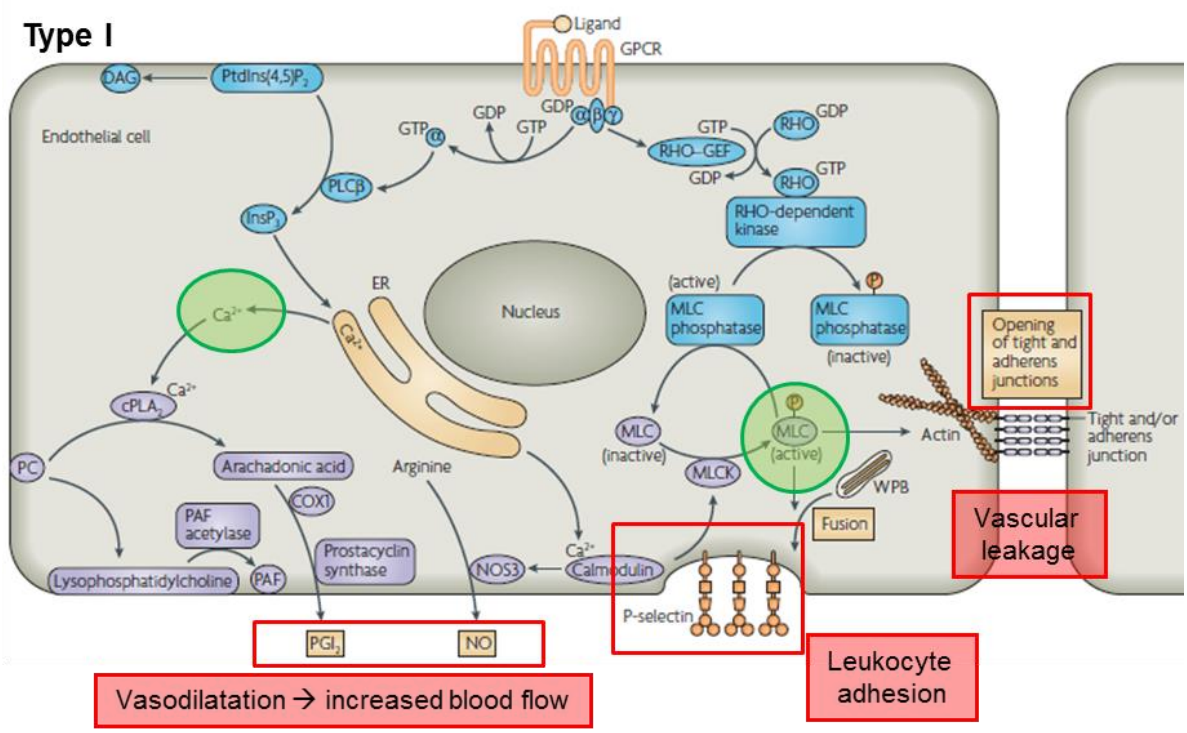

Figure 15: Type I endothelial activation. GPCR**,** G-protein-coupled receptor. GTP, guanosine triphosphate. GDP, guanosine diphosphate. PLCβ, phospholipase Cβ. PtdIns(4,5)P_2, phosphatidylinositol-4,5-bisphosphate. DAG, diacylglycerol. InsP3, inositol-1,4,5-trisphosphate. ER, endoplasmic reticulum. Ca^{2+}, calcium. cPLA2, cellular phospholipase A2. PC, phosphatidylcholine. COX1, cyclooxygenase-1. PGI2, prostaglandin I2. PAF, platelet-activating factor. NOS3, nitric-oxide synthase 3. NO, nitric oxide. MLCK, myosin-light-chain kinase. MLC, myosin light chain. RHO–GEF, RAS homology-guanine nucleotide exchange factor. WPB, Weibel–Palade bodies. (modified according to Pober et al. 2007)[124]

Activated GPCRs in type I stimulation lead to Ras homologue (RHO) activation and cytosolic calcium (Ca^{2+}, released from endoplasmic reticulum stores)-mediated responses (**Figure 15**). Ca^{2+} activates cellular phospholipase A_2, which cleaves phosphatidylcholine into arachidonic acid, which is finally converted by COX-1 and prostacyclin synthase to prostaglandin I_2 (PGI_2; also prostacyclin), a potent vasodilatator that relaxes smooth muscle vascular tone. Ca^{2+} also activates via the adaptor protein calmodulin nitric-oxide synthase 3 to produce nitric oxide (NO), which synergizes with PGI_2 to increase blood flow and leukocyte delivery. The combination of myosin-light-chain kinase activation (mediated by the Ca^{2+}-calmodulin complex) and myosin light chain (MLC) phosphatase inhibition (by RHO-dependent kinase) increases MLC phosphorylation. This initiates contraction of actin filaments attached to tight and adherens junction proteins, leading to the opening of gaps between neighboring ECs and increased vascular leakage. In addition, MLC activation by Ca^{2+} initiates exocytosis of Weibel-Palade bodies leading to the expression of P-selectin on the luminal EC surface. P-selectin and the EC-derived acyl form of platelet-activating factor (PAF) provide a juxtacrine signal initiating neutrophil extravasation, as circulating neutrophils are tethered by P-selectin followed by integrin activation and cell regulation by PAF.[124]

Type II activation induces new gene transcription mediated by the transcription factors NFκB and activator protein 1 (**Figure 16**). These transcription factors are activated by IL-1R1

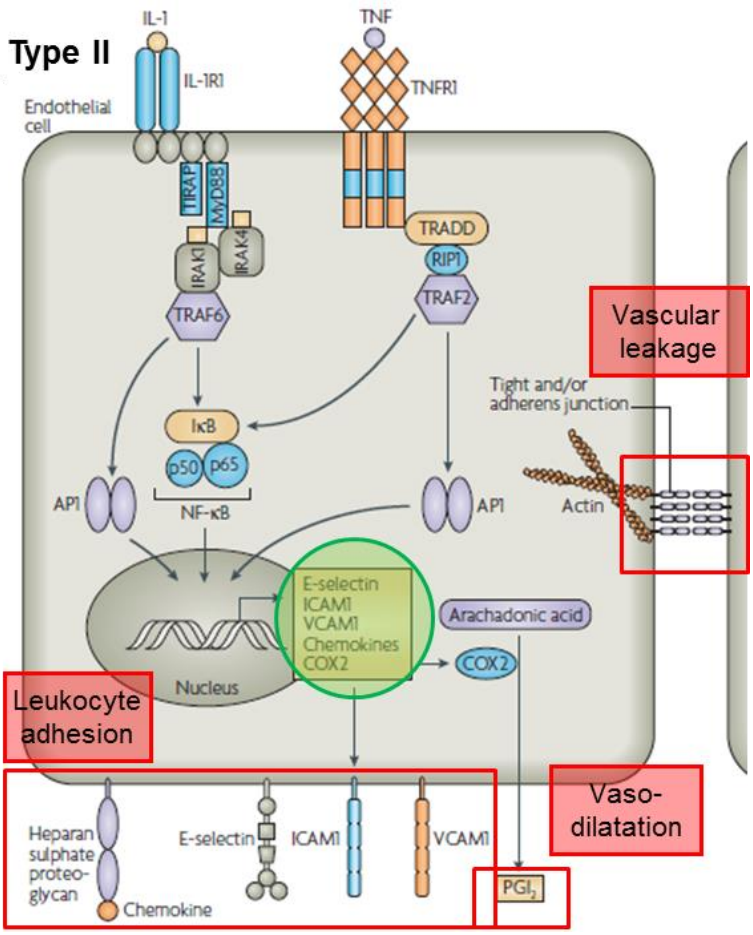

Figure 16: Type II endothelial activation. IL-1, interleukin-1. TNF, tumor-necrosis factor. IL-1R1, type 1 IL-1 receptor. TNFR1, TNF receptor 1. Myd88, myeloid differentiation primary-response gene 88. TIRAP, Toll/IL-1 receptor accessory protein. IRAK1/4, IL-1R-associated kinase 1/4. TRAF2/6, TNFR-associated factor 2/6. TRADD, TNFR-associated via death domain protein. RIP1, receptor-interacting protein 1. NFκB, nuclear factor 'kappa-light-chain-enhancer' of activated B-cells. AP1, activating protein 1. ICAM-1, intercellular adhesion molecule 1. VCAM-1, vascular cell-adhesion molecule 1. COX, cyclooxygenase. PGI_2, prostaglandin I_2. IκB, inhibitor of NF-κB. (modified according to Pober et al. 2007).[124]

(myeloid differentiation primary-response gene 88 (MyD88) and IL-1R-associated kinase (IRAK)-dependent) and TNFR1 (TNFR-associated via death domain protein (TRADD)-dependent) signaling. Transcription of specific gene results in the expression of pro-inflammatory proteins, including COX-2, leading to enhanced PGI_2 synthesis and therefore vasodilatation; leukocyte adhesion molecules as E-selectin, VCAM-1 and ICAM-1; chemokines and so far unknown effector proteins that reorganize actin filaments leading to the opening of intracellular junctions and vascular leakage. Chemokines are bound to HSPGs on the EC surface where they interact with cytokine-induced adhesion molecules on leukocytes, promoting their entry in the inflamed tissue.[124]

Leukocyte recruitment is the main mediator for tissue infiltration of inflammatory cells, a hallmark in various inflammatory diseases. Different kinetics in expression of adhesion molecules on the EC surface after activation and the more effective recruitment following the slower type II activation leads to a transition from primary neutrophil-rich infiltrates to mononuclear-cell-rich infiltrates, typically arising after 6-24 hours after cytokine-mediated activation.[124] The leukocyte-EC adhesion cascade involves several steps: capture and tethering, rolling, activation and adhesion of the leukocytes to the ECs resulting in diapedesis, the migration of the leukocytes across the endothelial layer by squeezing through the junctions between adjacent ECs. This cascade is performed through reciprocal binding and activation of multiple adhesion molecules on both ECs and leukocytes as seen in **Figure 17**.[126]

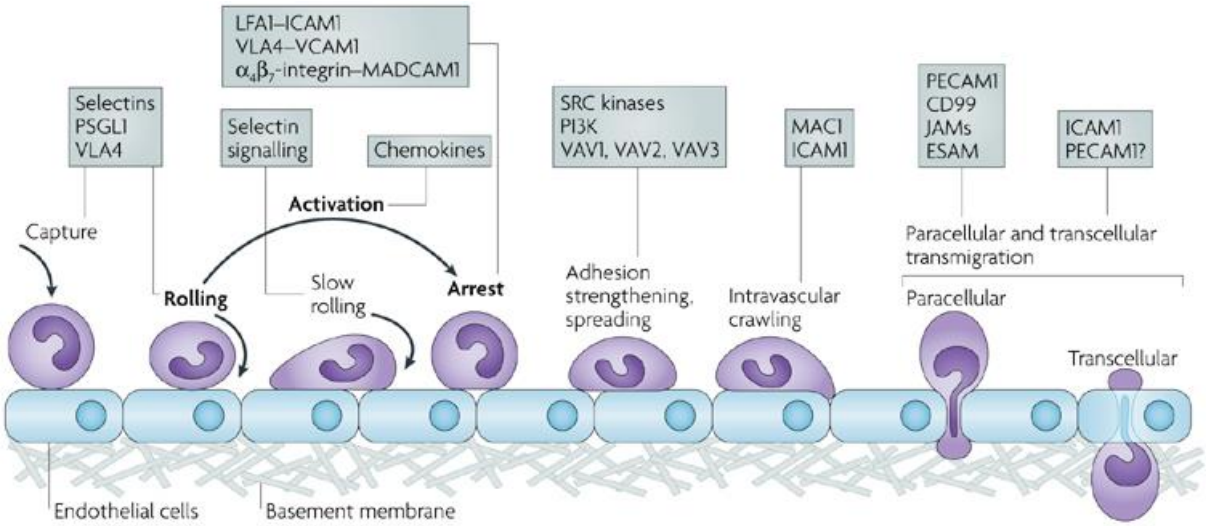

Figure 17: Leukocyte adhesion cascade. ESAM, endothelial cell-selective adhesion molecule. ICAM1, intercellular adhesion molecule 1. JAM, junctional adhesion molecule. LFA1, lymphocyte function-associated antigen 1 (also known as αLβ2-integrin). MAC1, macrophage antigen 1. MADCAM1, mucosal vascular addressin cell-adhesion molecule 1. PSGL1, P-selectin glycoprotein ligand 1. PECAM1, platelet/endothelial-cell adhesion molecule 1. PI3K, phosphoinositide 3-kinase. VCAM1, vascular cell-adhesion molecule 1. VLA4, very late antigen 4 (also known as α4β1-integrin). (from Ley et al. 2007).[126]

4.3.4 Angiogenesis in GVHD

As explained in chapter 4.2, there is an urgent medical need for alternative GVHD therapies, as current prophylactic and therapeutic approaches are limited in their efficiency and produce significant risks by creating a secondary immune deficiency. Penack et al. identified such a novel approach. The inhibition of angiogenesis reduced GVHD morbidity and mortality as well as tumor growth after allo-HSCT.[127]

It is well-established that angiogenesis and inflammation are tightly linked to each other.[104,107,121,122] Since 1971, when Judah Folkman postulated that angiogenesis is critical for tumour growth, [128] intense research established the reciprocal regulation of both processes. Angiogenesis is involved in the development of cancer and various inflammatory diseases, e.g. rheumatoid arthritis, psoriasis, inflammatory bowel disease as well as in ocular and metabolic disorders.[122] This important role is emphasized by the immense number of angiogenesis-targeting compounds being already approved or under investigation in clinical and preclinical trials for several cancer entities and inflammatory diseases.[104,108]

Evidence for angiogenesis in allogeneic immune reactions was already found in the mid 1970´s by Sidky and Auerbach, who analyzed local GVH reactions after irradiation and intracutaneous allogeneic lymphocyte transfer. They found that a network of blood vessels surrounded the scar region as early as 48 hours after injection. Interestingly, the number of injected allogeneic splenocytes correlated directly with the amount of neovascularization.[129]

Despite these early studies, the role of vascular proliferation and endothelial function during GVHD has not been studied experimentally until some years ago. There is increasing evidence that the vascular endothelium plays a major role in GVHD.[130] Clinical reports showed endothelial changes in cutaneous GVHD[131,132] and involvement of soluble biomarkers for endothelial injury in GVHD, e.g. increased serum levels of adhesion molecules,[133] von Willebrand factor,[134,135] thrombomodulin[136-138] and endothelial-cell-derived microparticles.[139] The toxicity of the conditioning can lead to endothelial damage and early complications after allo-HSCT include the endothelial syndromes transplant-associated microangiopathy,[140] SOS,[141,142] diffuse alveolar haemorrhage,[143,144] engraftment syndrome[145,146] and capillary leak syndrome.[147,148] Late endothelial events after allo-HSCT were identified, including cytotoxic T cells mediated endothelial injury and rarefaction of microvessels[149] as well as arterial events and atherosclerosis.[150] Furthermore, endothelial pathology was specifically connected to mortality in patients with GVHD.[136,137]

Penack et al. identified increased vessel density during established acute GVHD in the target organs skin, liver and GI tract in murine models.[127] The association of GVHD to the formation of new blood vessels, was confirmed in humans, e.g. showing increased vascular density in gastric and skin biopsies of acute GVHD patients.[127,151-153] Penack et al. pictures the involvement of the endothelium and angiogenesis in GVHD as a three-step process: 1) There is an initial endothelial damage due to the conditioning regimen irradiation or chemotherapy; followed by 2) a considerable neovascularization during the inflammation phase of GVHD facilitating migration of inflammatory cells to the target organs. During later stages of GVHD, 3) the vasculature is targeted and damaged by alloreactive donor T cells, leading to fibrosis and rarefaction of blood vessels (**Figure 18**).[152] First mechanistic studies in murine GVHD models involved therapeutic targeting of angiogenesis by inhibiting the endothelial adhesion molecule VE-cadherin and α_v integrin. The inhibition showed beneficial results in decreasing neovascularization and GVHD mortality and morbidity as well as decrease in tumour growth and increase of GVT activity, which potentially opened a new field of GVHD treatment options.[127,151,152]

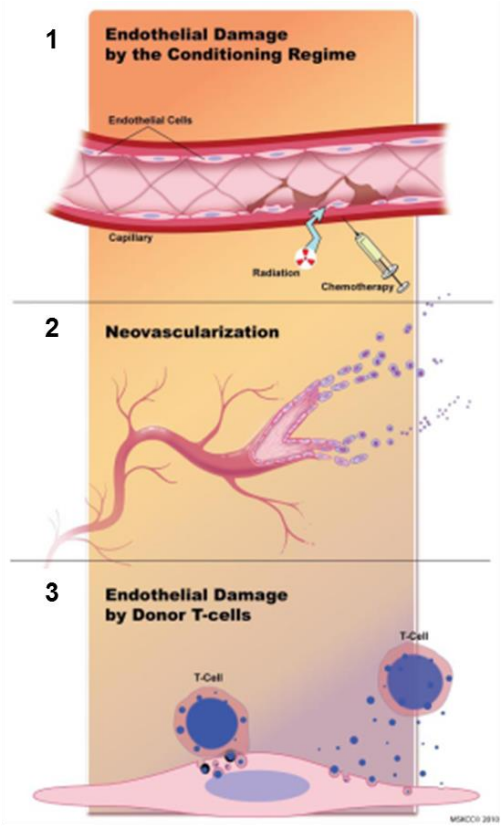

Figure 18: The endothelium during GVHD. (from Penack et al. 2011).[137]

4.4 Objective of the work

Allo-HSCT is the only curative treatment option for many patients suffering from hematological malignancies, and therefore the last hope for many leukemia patients. Accordingly, the number of allo-HSCTs performed worldwide has increased greatly in the past decades.[4,5] However, despite the maximum use of existing prophylactic and therapeutic strategies, the mortality after allo-HSCT is high. More than half of the patients die within the first two years after allo-HSCT because of GVHD and GVHD-associated complications.[60] GVHD treatment is based on suppressing effector T cell functions, which disadvantageously creates secondary immune deficiencies in allo-HSCT patients, increasing the risk for tumor relapse and fatal infections.[62,63] Most GVHD-associated deaths are related to treatment failure and toxicities of the immunosuppressive agents, underlining the urgent clinical need for alternative treatment strategies, which do not extenuate the immune response.

Recent work identified such a novel approach: the inhibition of pathologic angiogenesis offered the ideal possibility to modulate both GVHD and tumor growth after allo-HSCT.[127] The crosstalk between angiogenesis and inflammation is well-established and used in anti-angiogenic treatment strategies. However, it is still not clear if angiogenesis is a consequence or the cause of inflammation. This obstacle and missing suitable targets, that are differentially regulated during pathologic and physiologic angiogenesis limit the efficacy of current anti-angiogenic therapies and hinder the development of novel therapeutic approaches.

The objective of this cumulative study was to study GVHD-initiating mechanisms related to angiogenesis and provide potential new therapeutic targets being involved in early GVHD and aiming at the endothelium.

The study is divided into two parts and the published manuscripts are related to each purpose:

1) For a better translation of the experimental results into the human setting of allo-HSCT, a more clinical relevant, experimental acute GVHD mouse model should be developed and characterized as the most commonly used GVHD models are MHC-mismatched and only use lethal TBI as conditioning, which is in sharp contrast to clinical allo-HSCT. The features of the new model should mimic the most common features of clinical allo-HSCT, including MHC-matched donor transplantation, chemotherapy conditioning and GVHD progression and manifestation similar to patients.

2) To clarify if angiogenesis or inflammatory infiltration is the initial event in GVHD, the time course of angiogenesis and leukocyte infiltration should be determined in the novel developed acute GVHD model. Early and late changes in endothelial cells should be characterized to evaluate disease-initializing mechanisms and distinguish early from established GVHD. Finally, genes and proteins should be identified being responsible for molecular mechanisms in pathological angiogenesis during early GVHD to provide potential targets for pursuing therapeutically development and mechanistic studies.

5. Selected scientific publications

5.1 Article I

This research was originally published in Bone Marrow Transplantation.

Katarina Riesner, Martina Kalupa, Yu Shi, Sefer Elezkurtaj, Olaf Penack

A preclinical acute GVHD mouse model based on chemotherapy conditioning and MHC-matched transplantation

Bone Marrow Transplantation. March 2016. Volume 51 (3). pp. 410-417

https://www.nature.com/bmt/journal/v51/n3/full/bmt2015279a.html

5.1.1 Synopsis

Despite advances in prophylactic and therapeutic approaches, still 40-60 % and 60-80 % of patients receiving transplants from HLA-identical sibling[3] or one antigen HLA-mismatched unrelated donors[70,71] respectively develop acute GVHD. The mortality from acute GVHD can be as high as 50 %, representing one of the major complications after allo-HSCT.[60] Multiple murine models are used to investigate mechanisms of this systemic inflammatory disease *in vivo* and to identify possible targets for clinical treatment. However, current well-established murine acute GVHD models have their clinical limitations as they are based on MHC-mismatched transplantation and use only lethal irradiation as conditioning.[72] In sharp contrast, current clinical conditioning protocols mainly use chemotherapy with busulfan and cyclophosphamide.[42] HLA-matched family or unrelated donor transplantations improved the outcome of allo-HSCT compared to HLA-mismatched donor transplantation and are common clinical practice.[42] The availability of a more clinically relevant murine model would forward the transfer of experimental results into the human setting and the translational development of new treatment options.

To reflect the clinical situation of allo-HSCT and GVHD, we established a new murine GVHD model, which is based on chemotherapy conditioning and MHC-matched transplantation. Donor LP/J and recipient C57BL/6 mice share the same haplotype (H-2^b) with only mismatches at different minor histocompatibility loci. In the LP/J→C57BL/6 mouse model, the established chemotherapy transplantation protocol resulted in stable full donor chimerism and development of acute GVHD. The clinical pattern and timing of acute GVHD resembled the clinical situation of HLA-matched allo-HSCT with GVHD prophylaxis and differed from the hyper acute, bi-phasic GVHD that is observed in currently used TBI-based MHC-mismatched murine models[48,100,101] but not in the majority of allo-HSCT patients.

C57BL/6 recipients were conditioned with a 7-day busulfan-cyclophosphamide chemotherapy protocol and were transplanted with 1.5 x 10^7 bone marrow and 2 x 10^6 splenic T cells from

LP/J donors. Recipients showed profound engraftment with already 80 % donor chimerism in peripheral blood at day+15 after transplantation.

Allogeneic transplanted mice developed typical features of acute GVHD including decreased survival, GVHD-typical weight loss and significant increased clinical GVHD scoring consisting of five clinical parameters: weight loss, posture, activity, fur and skin. Pronounced acute GVHD was established between day+15 and +25 after transplantation. Survivors of acute GVHD, developed scleroderma-like chronic GVHD between day+50 and +60 after transplantation. Likewise in GVHD patients, skin changes were the first phenotypic changes in our model, and GVHD mice exhibited extensive scurf spreading over the whole body combined with fur loss. Histopathologic and immune fluorescence analyses of GVHD organs (large bowel, liver and skin) confirmed typical GVHD pathology and T cell infiltration, respectively. CD4+ and CD8+ T cell infiltration was significantly elevated in GVHD animals, however CD8+ T cell infiltration was more prominent concluding that CD8+ T cells play a prominent role in acute GVHD phase in our model. Additionally, GVHD mice showed increased mRNA expression of suppression of tumorigenicity 2 (ST2, an IL-33 receptor, effector molecule for Th2 response), a novel candidate biomarker for acute GVHD in patients.

Strong systemic inflammation included T cell and monocyte/granulocyte expansion. CD8+ T cells were significantly increased in GVHD mice in acute phase (day+15), whereas CD4+ T cells were elevated in late phase (day+50-60), confirming the development of an acute CD8-driven and a late, chronic CD4-driven phase. Likewise in patients, B cells, NK cells and regulatory T cells were decreased in acute GVHD mice. At the onset of GVHD (d+8/11), pro-inflammatory cytokines IFN-γ and TNF-α were elevated in the serum of GVHD mice.

In summary, we established a novel chemotherapy-based, MHC-matched GVHD model, which shows 1) profound engraftment, 2) typical clinical features of acute GVHD, and 3) systemic and target organ-specific inflammation. Our murine GVHD model closely resembles the clinical situation of patients undergoing HLA-matched allo-HSCT and GVHD prophylaxis; which may help to better understand pathogenic mechanisms in GVHD as well as to develop and translate new treatment approaches.

5.1.2 Personal contribution

I designed this study and performed all experiments, including all experimental handling of GVHD mice and subsequent analyses of blood, serum, bone marrow and target organs. I analyzed the data and prepared all figures and tables. I wrote and revised the manuscript.

Contribution of co-authors:

O. Penack helped designing the study and writing/correcting the manuscript. M. Kalupa experimentally helped to perform GVHD experiments in mice and subsequent target organ analyses. Y. Shi performed Real-Time PCR. S. Elezkurtaj performed histopathological scoring of GVHD target organs.

5.1.3 Manuscript 1 [redacted]

5.1.4 Supplemental Material 1

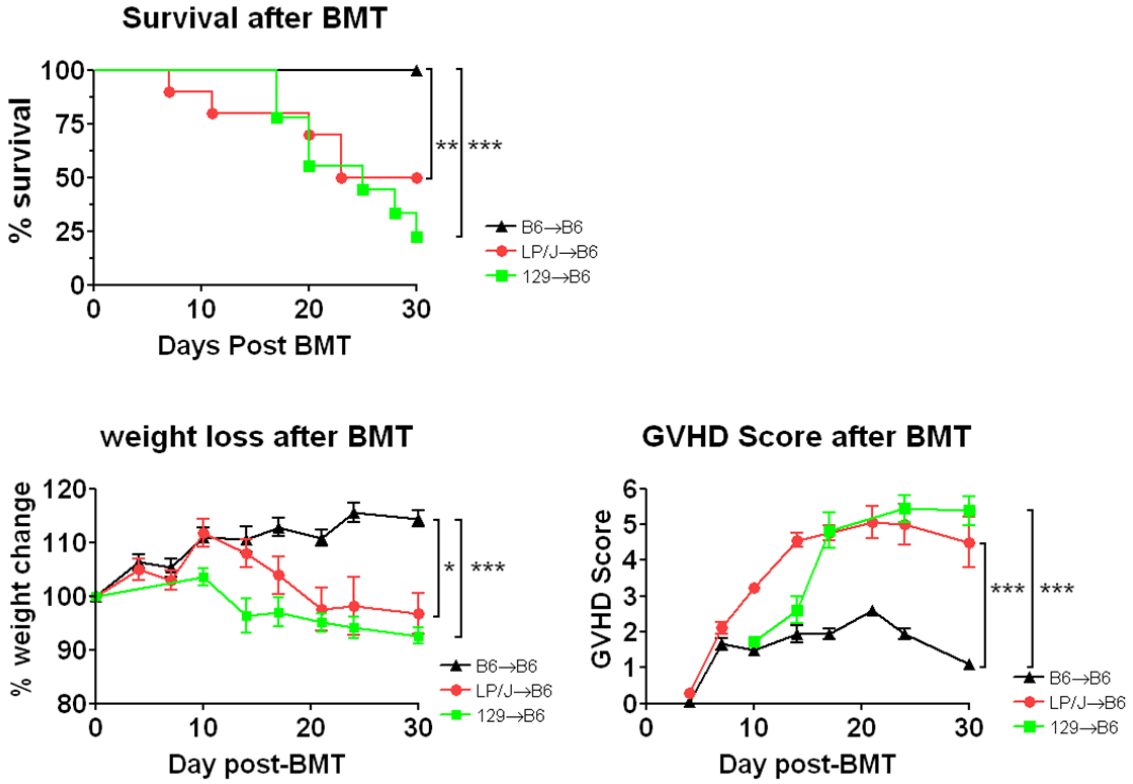

Figure 1S. Comparison of clinical GVHD in two chemotherapy-based, miHA-mismatched allo-HSCT models (LP/J→C57BL/6 and 129S2/SvPasCrl→C57BL/6). Survival, weight loss and GVHD Score after BMT in syngeneic and allogeneic transplanted mice. Allogeneic transplanted animals of both miHA-mismatched allo-HSCT models showed similarities in GVHD progression. Survival data was analyzed using Mantel-Cox log-rank test. Animals were regularly scored for five clinical parameters (weight loss, posture, activity, fur and skin) on a scale from 0 to 2. Clinical GVHD score was generated by summation of these five parameters. N=10 per group. ($P<0.05$ *, $P<0.01$ **, $P<0.001$ ***).

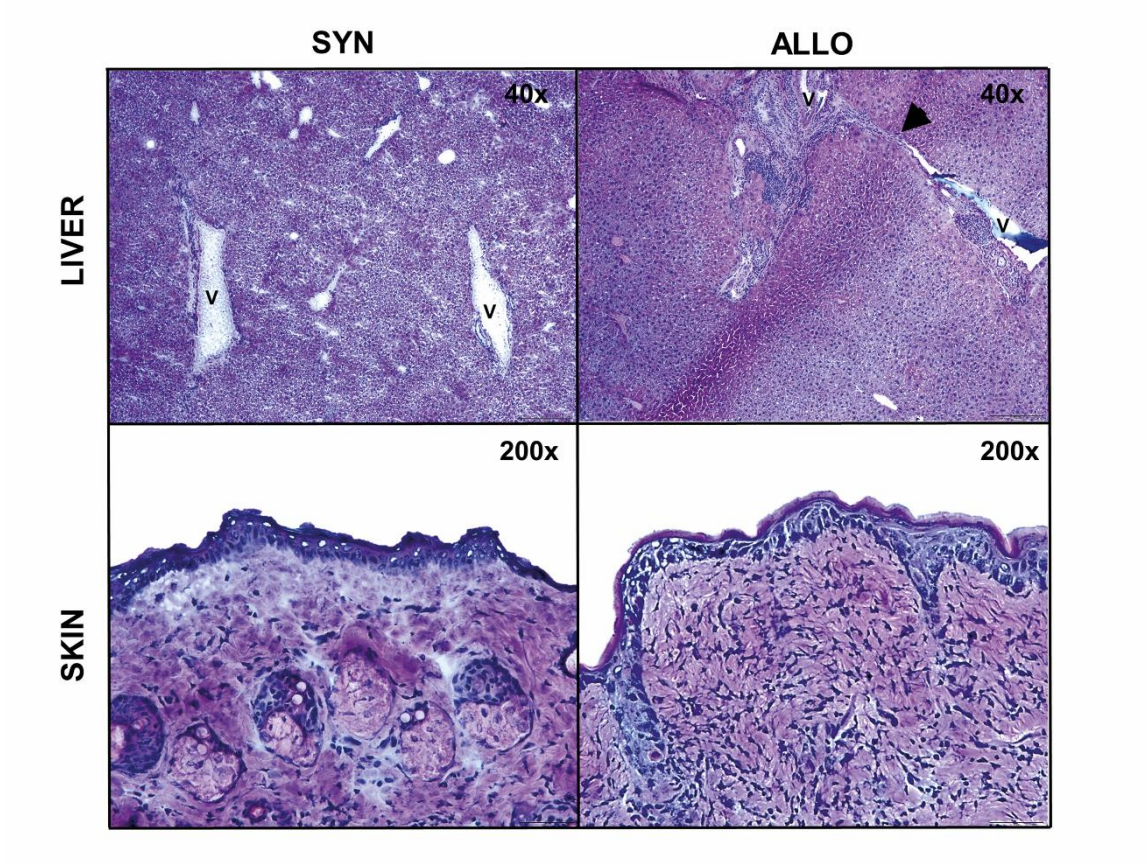

Figure 2S. Allogeneic transplanted mice showed histopathologic signs of chronic GVHD in liver and skin. 64 days after BMT, syngeneic and allogeneic transplanted animals were sacrificed for histologic examination. Representative H&E-stained sections of liver and abdominal skin from each group are shown. Liver of allogeneic transplanted mice exhibited periportal mononuclear infiltration and fibrosis with beginning of septum formation (black arrow). Whereas skin of syngeneic transplanted mice showed normal skin structure with adnexae and low cell density, skin of allogeneic transplanted mice showed fibrosis with high cell and fibrous density and atrophy of adnexal structures. V=Vein. Original magnification was 40x for liver samples and 200x for skin samples.

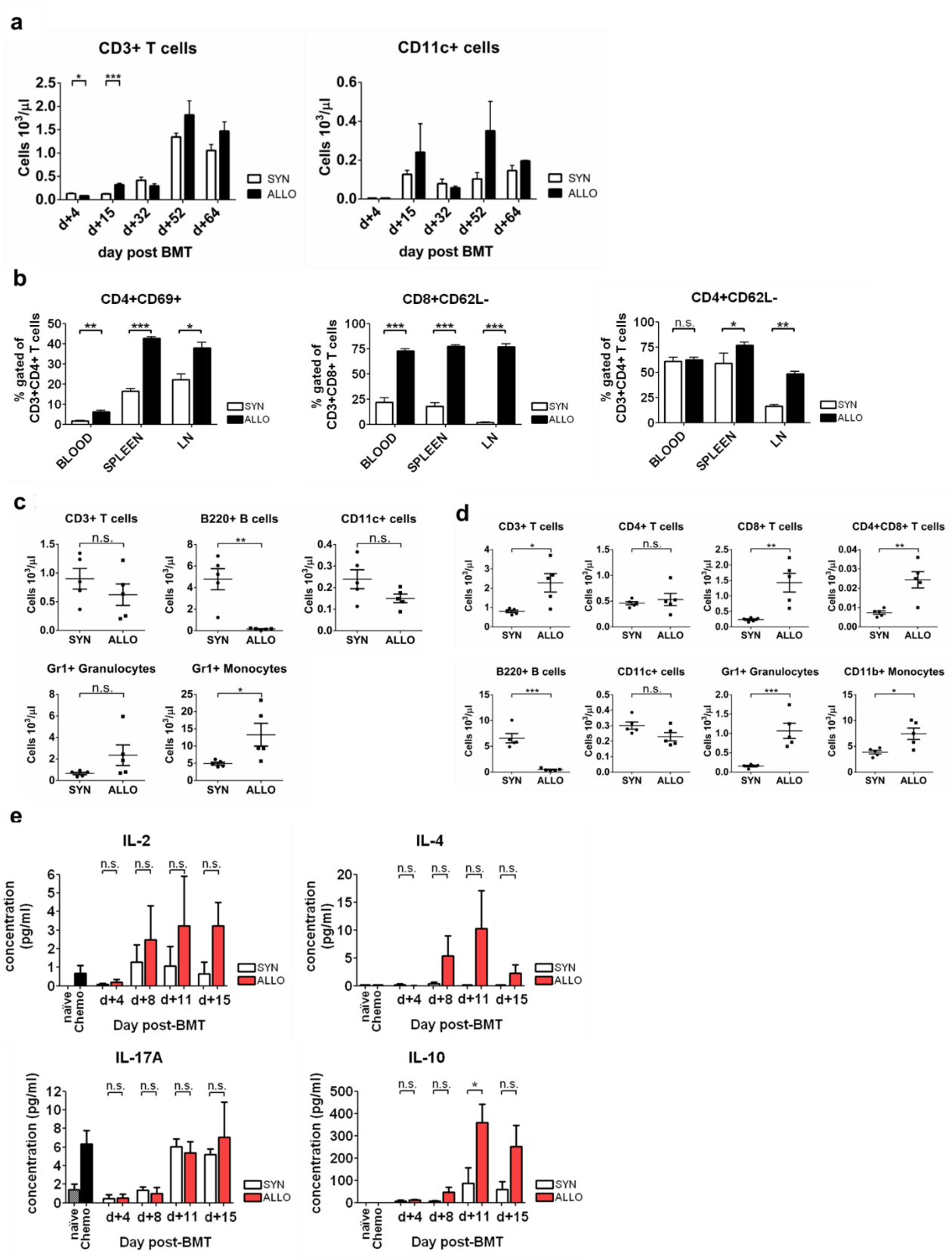
a
CD3+ T cells
CD11c+ cells
Cells 10³/µl
day post BMT
d+4
d+15
d+32
d+52
d+64
SYN
ALLO
b
CD4+CD69+
CD8+CD62L-
CD4+CD62L-
% gated of CD3+CD4+ T cells
% gated of CD3+CD8+ T cells
BLOOD
SPLEEN
LN
c
CD3+ T cells
B220+ B cells
CD11c+ cells
Gr1+ Granulocytes
Gr1+ Monocytes
d
CD4+ T cells
CD8+ T cells
CD4+CD8+ T cells
CD11c+ cells
Gr1+ Granulocytes
CD11b+ Monocytes
e
IL-2
IL-4
IL-17A
IL-10
concentration (pg/ml)
naïve
Chemo
Day post-BMT

Figure 3S. Systemic Inflammation during GHVD. **(a)** FACS analysis of CD3, CD11b in peripheral blood of syngeneic and allogeneic transplanted animals on different days after BMT. Absolute numbers are shown. Immune cell populations were gated on donor cells. Data from 1 representative of 3 individual experiments, N=3-10 per group. **(b)** CD4+CD62L-, CD8+CD62L-, CD4+CD69+ T cells were increased in allogeneic transplanted mice at d+15 after BMT. FACS analysis was performed in blood, spleen and lymph nodes. Percentage of gated cells from CD3+ cells are shown. Data pooled from two individual experiments. N=5 per group. **(c)** FACS analysis of different immune cell subsets in bone marrow at d+15 after BMT. Cell concentrations in the bone marrow cell preparation are shown. Immune cell populations were gated on donor cells. Data from 1 representative of 2 individual experiments, N=5 per group. **(d)** FACS analysis of different immune cell subsets in spleen at d+15 after BMT. Cell concentrations in the splenic cell preparation are shown. Immune cell populations were gated on donor cells. Data from 1 representative of 2 individual experiments, N=5 per group. **(e)** Serum levels of IL-2, IL-4, IL-17A and IL-10 after BMT. Serum was collected from naive C57BL/6, chemotherapy-treated and allogeneic and syngeneic transplanted animals 4, 8, 11 and 15 days after BMT. Three individual experiments were performed, N=5-8 per group. (n.s.= not significant, P<0.05*, P<0.01 **, P<0.001***).

Score	Posture	Fur	Activity	Skin	Weight loss
0.5	mild kyphosis, only at rest	mild ruffling	mild decreased	reddish, irritated areas	>5%
1	moderate kyphosis	moderate ruffling (>20 %)	Moderate decreased, isolation	scaling, dry skin areas (<20 %)	>10%
1.5	strong kyphosis. slightly impaired movement	severe ruffling (>40 %), mild loss of fur	stationary until stimulated, coordination disorders, stereotypes	scaling, dry skin areas (>20 %)	>15%
2 =abort	Severe kyphosis, distinct impaired movement	severe ruffling (>60 %), poor grooming, moderate to severe loss of fur	lethargy, paralysis, staggering	scaling, dry skin areas (>40 %), open, bloody skin areas	>20%

Table 1S. GVHD Scoring. Mice were individually scored twice a week for five clinical parameters (posture, activity, fur, skin and weight loss) on a scale from 0-2. Clinical GVHD score was assessed by summation of these parameters. Animals were sacrificed when reaching a single score of 2 or exceeding clinical GVHD score of 6.

Thymus Sample	CD3+ Count x10^4 (mean±SEM)	CD4+/CD8+ % gated (mean±SEM)	CD4-/CD8- % gated (mean±SEM)	CD4+/CD8- % gated (mean±SEM)	CD4-/CD8+ % gated (mean±SEM)
Acute Phase (d+15)					
SYNGENEIC	6.69 ± 1.50	22.08 ± 3.25	8.10 ± 1,49	57.42 ± 2.17	12.40 ± 2.09
ALLOGENEIC	1.09 ± 0.29	4.48 ± 2.30	19.54 ± 5,64	46.48 ± 3.41	29.52 ± 3.31
P-Value		P=0.002	P=0.026	P=0.085	P=0.002
Late Phase (d+52-64)					
SYNGENEIC	25.54 ± 5.51	27.38 ± 4.25	10.06 ± 4.18	51.98 ± 2.32	10.62 ± 2.26
ALLOGENEIC	20.51 ± 10.31	27.85 ± 7.60	5.45 ± 2.12	54.13 ± 7.68	12.57 ± 1.18
P-Value		P=0.921	P=0.332	P=0.789	P=0.396

Table 2S. Recovery of thymopoiesis at late phase after BMT. FACS analysis of thymus cell preparations of transplanted mice at d+15 and d+52-64 after BMT revealed recovered CD3+ T cell number in transplanted mice at late phase. Allogeneic transplanted mice showed recovery of CD4/CD8 thymocytes ratio. Cell count of CD3+ T cells in 10 mg thymus and percentage of CD4/CD8 gated cells from CD3+ cells are shown. Data pooled from two individual experiments. N=5 per group. FACS data from d+52 and d+64 showed similar values and were summarized in one group.

5.2 Article II

This research was originally published in BLOOD.

Katarina Riesner, Yu Shi, Angela Jacobi, Martin Kräter, Martina Kalupa, Aleixandria McGearey, Sarah Mertlitz, Steffen Cordes, Jens-Florian Schrezenmeier, Jörg Mengwasser, Sabine Westphal, Daniel Perez-Hernandez, Clemens Schmitt, Gunnar Dittmar, Jochen Guck and Olaf Penack

Initiation of acute graft-versus-host disease by angiogenesis

BLOOD. April 2017. Volume 129 (14). pp. 2021-2032

http://www.bloodjournal.org/content/129/14/2021?sso-checked=true

5.2.1 Synopsis

Successful outcome of allo-HSCT is still hampered by post-transplant complication-associated morbidity and mortality, mainly because of GVHD development. In this area there is an urgent medical need for new therapeutic approaches. Recently, such a novel approach was identified: GVHD is associated to angiogenesis and the inhibition of angiogenesis ameliorated GVHD mortality in murine models.[127] Increased angiogenesis was confirmed in GVHD patients and endothelial pathology was specifically connected to mortality in patients with GVHD.[136,137] As described in other inflammatory diseases, angiogenesis and inflammation are two closely related processes and inhibition of angiogenesis can ameliorate inflammatory diseases by reducing the recruitment of tissue infiltrating leukocytes.[104,107,121,122] However, there is limited evidence on initial mechanisms of both processes and it is unknown if angiogenesis contributes to initiation of inflammation or is a mere consequence, hindering the development of therapeutic approaches.

In this study, we provided novel evidence on a primary involvement of angiogenesis in the initiation of tissue inflammation in GVHD and found that during initial angiogenesis classical inflammation-associated endothelial activation signs were absent, but metabolic and cytoskeletal alterations occurred. We identified potential novel targets for pursuing mechanistic studies and the development of anti-inflammatory therapies aiming at angiogenesis.

In murine GVHD models, we found that angiogenesis preceded infiltration of inflammatory leukocytes particularly in GVHD target organs liver, skin and intestines. Whereas leukocytes began to infiltrate around day+7 after transplantation, increase in vessel density occurred already at day+2 and was dependent on the proliferation of resident tissue ECs, termed angiogenesis. We confirmed our findings in an experimental model of inflammatory bowel disease, implicating a broader significance of our results surpassing the field of transplantation biology.

To identify pathways being relevant for initiating angiogenesis during GVHD, we first investigated the VEGFA/VEGFR1+2 axis. We found no consistent upregulation of *Vegfa* and *Vegfr2* expression levels in GVHD target organs during initiation of GVHD or later time points, and VEGFR1+2 or VEGFA inhibition with monoclonal blocking antibodies in murine GVHD models had no positive effects on GVHD, suggesting that the VEGFA/VEGFR2 pathway is not a major mechanism for initiation of pathological angiogenesis in GVHD target organs.

Additionally, we demonstrated that initial endothelial activation followed a different pattern as compared to established GVHD. In a highly inflammatory environment at d+15, we found typical increased expression levels of adhesion molecules and MHC class II molecules on ECs of GVHD mice, whereas in a leukocyte infiltration-free environment at d+2, significant downregulation of gene expression of adhesion molecules and no MHC class II upregulation occurred.

To identify alternative pathways during initial angiogenesis in GVHD, we performed microarray and mass spectrometry (MS) proteome analyses and revealed especially metabolic and cytoskeleton changes in ECs during early GVHD (day+2). Other most striking genes and proteins were involved in angiogenic pathways, immune response, ATP-dependent pathways and RNA/DNA cell machinery. These changes in ECs had functional consequences, shown by significantly higher deformation of liver ECs from GVHD mice at d+2, measured by Real-Time deformability cytometry.

In summary, we demonstrated that angiogenesis initiates GVHD in target organs and plays a major role in disease development. We revealed novel genes and proteins, for further mechanistic studies, regulating migration and proliferation of ECs in initial angiogenesis during GVHD. This amends the knowledge on the interplay between the vasculature and inflammation opening a new window to develop therapeutic strategies targeting the endothelium.

5.2.2 Personal contribution

I designed this study and performed nearly all experiments, including all experimental handling of GVHD mice and subsequent analyses of target organs (fluorescence-activated cell sorting (FACS), Immune fluorescence staining, Real-time PCR, microarray analysis). I analyzed the data and prepared all figures and tables. I wrote and revised the manuscript.

Contribution of co-authors:

O. Penack, Y. Shi and J. Mengwasser helped designing the study. M. Kalupa, A. McGearey, S. Mertlitz, S. Cordes, J. Mengwasser and S. Westphal experimentally helped to perform GVHD and colitis experiments in mice and subsequent target organ analyses. J.-F. Schrezenmeier performed FACS sorting. D. Perez-Hernandez and G. Dittmar performed MS proteome analysis. A. Jacobi, M. Kräter, and J. Guck performed Real-Time deformability analysis and prepared the corresponding figure and manuscript text. C. Schmitt provided advices concerning the manuscript. O. Penack helped writing and correcting the manuscript.

5.2.3 Manuscript 2 [redacted]

5.2.4 Supplemental Material 2

Supplemental Material and Methods

Protein quantification by dimethylation labeling

Cells were digested in solution and labeled by dimethylation according to Boersema *et al.*[21] Endothelial cells were pelleted and were resuspended in 75 µl of denaturation buffer [6M urea (Sigma-Aldrich), 2M thiourea (Sigma-Aldrich), 10mM HEPES (pH=8)]. They were sonicated 30 pulses of limit microtip sonication at 30% on duty cycle. The remained cell pellet was erased by centrifugation at 14000 rpm for 15 minutes. After removing the supernatant, the protein concentration was calculated by Bradford. Each sample had 15-20 µg of protein (approximately 0.4 mg/ml). They were reduced by incubating with 5 µl of 10mM *tris*(2-carboxyethyl)phosphine (TCEP) (Sigma-Aldrich) for 30 min at RT, followed by an alkylation step using 5 µl of 55mM Cloroacetamide (Sigma-Aldrich) for 60 min at RT. The samples were first digested using 0.25 mg/ml endopeptidase LysC (Wako, Osaka, Japan) for 3 hours. The samples were diluted by adding 100 µl of 50 mM ammonium bicarbonate (pH=8.5), and finally digested with 0.25 mg/ml trypsin (Promega, Germany) for 16h. The digestion was stopped by acidifying each sample to pH<2.5 by adding 10% trifluoroacetic acid solution. The peptide extracts were purified and stored on stage tips according to Rappsilber *et al.*[22] The samples were reconstituted in 100 µl of 20 mM HEPES buffer pH=7.5. The samples were differentially labelled adding 8 µl of 8% of light label formaldehyde (Pierce, Thermo Scientific) in ECV (+28Da), medium label formaldehyde (Cambridge Isotope Laboratories) (+32Da) and heavy label formaldehyde (Sigma-Aldrich, Germany) (+36Da) cells (45). We added 8 µl of 0.6M $NaBH_3CN$ (Sigma-Aldrich, Germany) to the light and medium labelled samples and 8 µl of 0.6M $NaBD_3CN$ (Sigma-Aldrich, Germany) to the heavy labelled simple, incubating at 20ºC. The reaction was quenched after 1 hour adding 30 µl of 1% ammonia solution. All the samples were mixed and acidified to pH<2.5 by adding 10% trifluoroacetic acid solution.

High through-put LC-MS/MS analysis

After Stage-Tip extraction, the eluted peptides were lyophilized and resuspended in 1% trifluoro-acetic acid and 3% acetonitrile buffer. Peptides were separated on a Eksigent nLC-415 system (Eksigent Technologies, CA), resolved with a reversed-phase column (30 cm in length, 75 mm ID [inner diameter of the fused silica capillary tubing used to make the column], 3 mm, Dr. Maisch GmbH C18) by a gradient from 4 to 42% B in 240 min. MS and MS/MS spectra were analysed coupled to a QExactive mass spectrometer (Thermo Scientific). The mass spectrometer was operated in a data-dependent acquisition mode with dynamic exclusion enabled (30 s). Survey

scans (mass range 300-1700 Th) were acquired at a resolution of 70,000 with the ten most abundant multiply charged (z ≥ 2) ions selected with a 4 Th isolation window for HCD fragmentation. MS/MS scans were acquired at a resolution of 17,500 and injection time of 60 ms.

Processing of mass spectrometry data

Protein and peptide quantitation information were extracted from MaxQuant 1.5.2.8.[23] All the samples were searched against the Uniprot mouse database 2014-10 (*ftp://ftp.uniprot.org/pub/databases/uniprot*). Cleavage specificity was set for trypsin/P. Search parameters were two missed cleavage sites, cysteine carbamidomethylation as fixed modification and methionine oxidation as variable modification. Quantification data of labeled peptides were measure considering N-termini and lysine dimethylation on light (+28Da) or medium (+32Da) or on heavy (+36Da) modification per free primary amine.[21] The mass accuracy of the precursor ions was set by the recalibration algorithm of MaxQuant, fragment ion mass tolerance was set as default. The false discovery rate (FDR) was determined using statistical methods contained in MaxQuant software package v.1.5.2.8 and uses the multiple hypotheses testing (Cox et al.[23] and Elias et al.[24]). The maximum false discovery rate (FDR) was 1% for proteins and peptides, the minimum peptide length was 7 amino acids for valid identification. All other parameters are settings by default in MaxQuant. Quantitative ratios were calculated and normalized by Max Quant software package. R software (Version 3.0.0., www.r-project.org) was used to calculate log2 ratios between syn and allo-transplanted groups, log10 of signal intensities and p-values of protein abundance changes. p-values <0.05 were chosen as statistically significant. Normalized ratios were used for differential expression analysis (up ≥1.3 or down ≤0.44).

Real-Time Deformability Cytometry

For measurements, cells were re-suspended in PBS containing 0.63% methylcellulose at a concentration of 1-2 x 10^6 cells/ml and filtered through a 70 µm cell strainer. The cell suspension was drawn into a syringe and connected to a microfluidic chip consisting of two reservoirs separated by a channel constriction (15 x 15 μm^2 cross-section, 330 µm length). Using a syringe pump, cells were flushed through the channel at a constant flow rate of 0.048 µl/sec and imaged at the end of the constriction. The cells were deformed by hydrodynamic shear stresses and pressure gradients into a characteristic bullet-like shape. Cell cross-sectional area ($A = \pi r^2$) and circularity ($c = 2\sqrt{\pi A/l}$), where l is the cell perimeter ($l = 2\pi r$), were determined in real-time using an algorithm implemented in C/LabVIEW. The results were displayed as scatter plots of deformation ($D = 1 - c$), which defines the deviation of the cell shape from a perfect circle ($c = 1$), and size[3]. To exclude pre-deformation or size misinterpretation we measured the cells in an area

of the microfluidic chip where no shear stress was applied (reservoir). Deformation was close to zero indicated by round shaped, non-deformed cells and cell size was the same as in the micro-channel (Fig. 4f insert). Statistical comparison of deformation was carried out with 1-dimensional linear mixed model analysis. One fixed and one random effect was considered, in order to analyze the difference between subsets of cells and to consider the replicates' variance, respectively. *P* values were determined by a likelihood ratio test, comparing the full model with a model lacking the fixed effect term.

Supplemental Figures

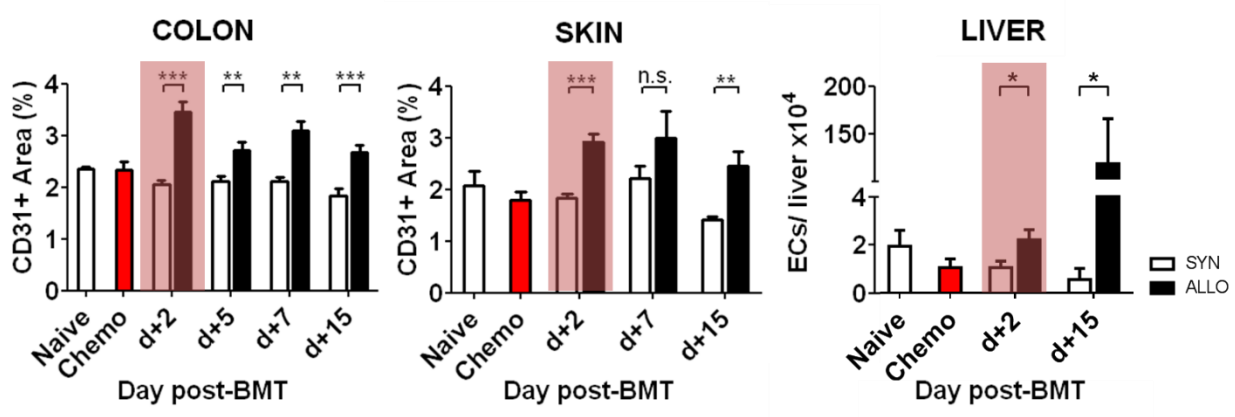

Figure S1. Time course of angiogenesis in GVHD target organs colon, skin and liver of syngeneic and allogeneic transplanted mice (LP/J→C57BL/6). Vascular density: Percentage of CD31 positive area in colon and skin and endothelial cell (EC) number in liver of syngeneic (SYN) and allogeneic (ALLO) transplanted mice at day+2, +5, +7 and +15 after BMT. The red box marks the earliest significant increase in positive CD31 areas or endothelial cell (EC) number in allogeneic transplanted mice. Untreated (Naive) and only chemotherapy-conditioned (Chemo) mice served as control and showed no increase in vascular density. Data pooled from two independent experiments (naive, chemo n=5 per group; SYN, ALLO n=10-12 per group). Error bars indicate mean ± s.e.m. $^{*}P < 0.05$, $^{**}P < 0.01$, $^{***}P < 0.001$, n.s. not significant by Student's *t* test (two-tailed).

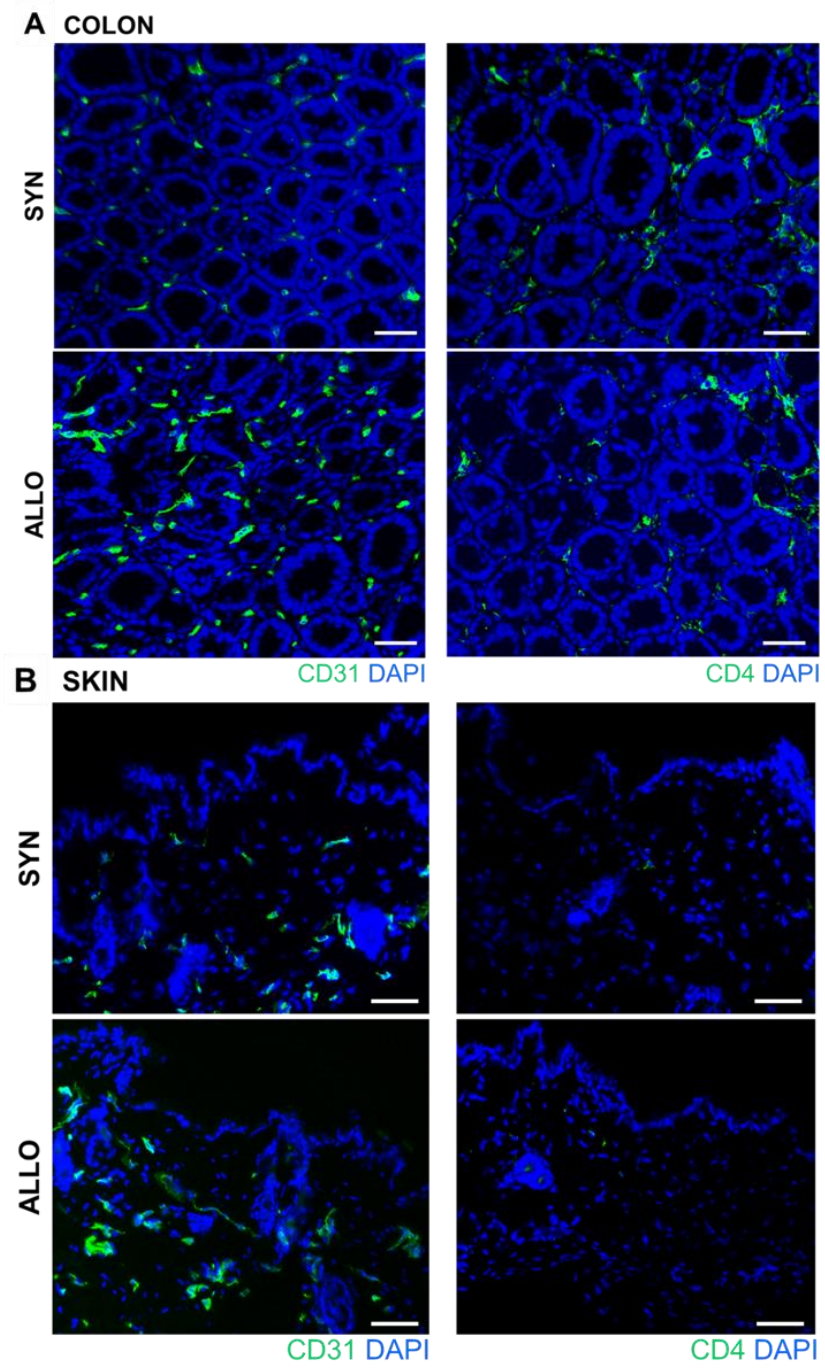

Figure S2. Increased vascular density and no CD4+ lymphocyte infiltration in colon and skin of allogeneic transplanted mice at day+2 after BMT. Representative pictures from colon (A) and skin (B) of SYN and ALLO mice at day+2 after BMT (LP/J→C57BL/6). Sections are stained against CD31 (green-A488) and CD4 (green-A488) and counterstained with 4´,6-Diamidino-2-phenylindole (DAPI). Scale bar, 30 µm.

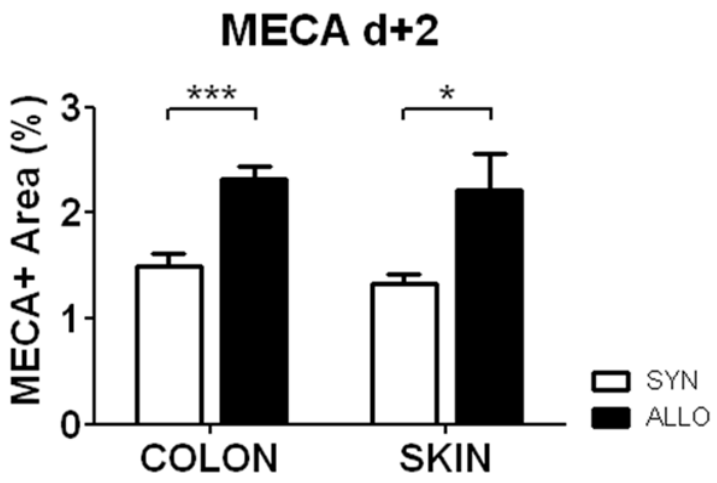

Figure S3. Staining with another endothelial cell marker MECA-32 confirms early angiogenesis in GVHD target organs. Increase in vascular density was determined by elevated positive areas of the stained endothelial cell marker MECA-32 in colon and skin of ALLO mice at day+2 after BMT (LP/J→C57BL/6). Representative data from one of two independent experiments (n=6 per group). Error bars indicate mean ± s.e.m. *$P < 0.05$, ***$P < 0.001$ by Student's *t* test (two-tailed).

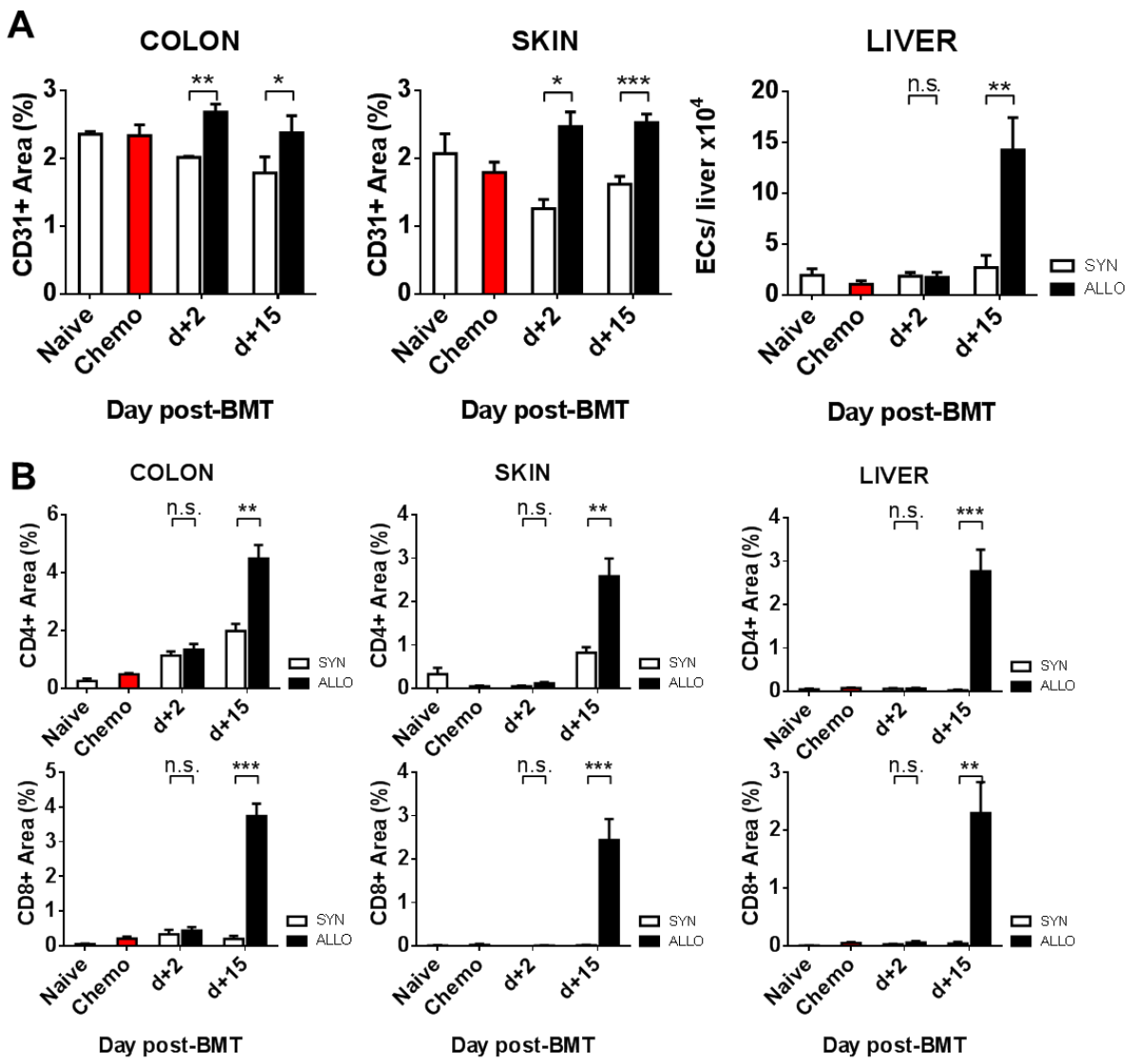

Figure S4. Angiogenesis precedes lymphocyte infiltration in another chemotherapy-based MHC-matched, miHA-mismatched murine GVHD model (129S2/SvPasCrl→C57BL/6). Time course of angiogenesis and lymphocyte infiltration in GVHD target organs colon, skin and liver of SYN and ALLO mice at day+2 and +15 after BMT. (A) Vascular density: Percentage of CD31 positive area in colon and skin and EC number in liver of SYN and ALLO mice. (B) Lymphocyte infiltration: Percentage of CD4 and CD8 positive area in colon, skin and liver of SYN and ALLO mice. Untreated (Naive) and only chemotherapy-conditioned (Chemo) mice served as control and showed no increase in vascular density or infiltration. Representative data from one of two independent experiments (n=5 per group). Error bars indicate mean ± s.e.m. *$P < 0.05$, **$P < 0.01$, ***$P < 0.001$, n.s. not significant by Student's *t* test (two-tailed).

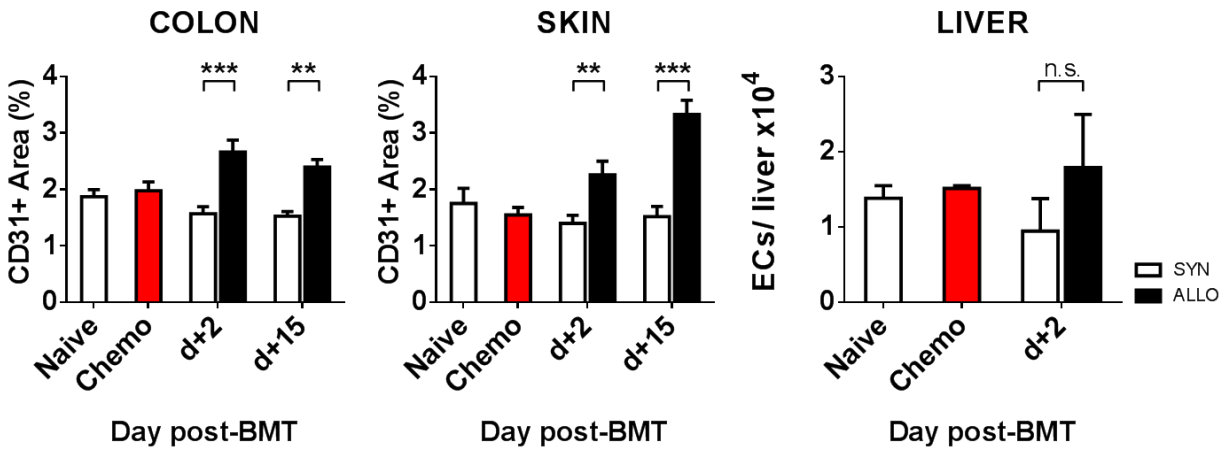

Figure S5. Early Angiogenesis in another chemotherapy-based MHC -mismatched murine GVHD model (C57BL/6→B6D2F1). Time course of angiogenesis in GVHD target organs colon, skin and liver of SYN and ALLO mice at day+2 and +15 after BMT. Vascular density: Percentage of CD31 positive area in colon and skin and EC number in liver of SYN and ALLO mice. CD4+ and CD8+ lymphocyte infiltration in GVHD target organs colon, skin and liver of ALLO mice was observed at day+15 but not at day+2 after BMT (data not shown). Untreated (Naive) and only chemotherapy-conditioned (Chemo) mice served as control and showed no increase in vascular density or infiltration. Representative data from one of two independent experiments (n=7 per group). Error bars indicate mean ± s.e.m. $^{**}P < 0.01$, $^{***}P < 0.001$, n.s. not significant by Student's *t* test (two-tailed).

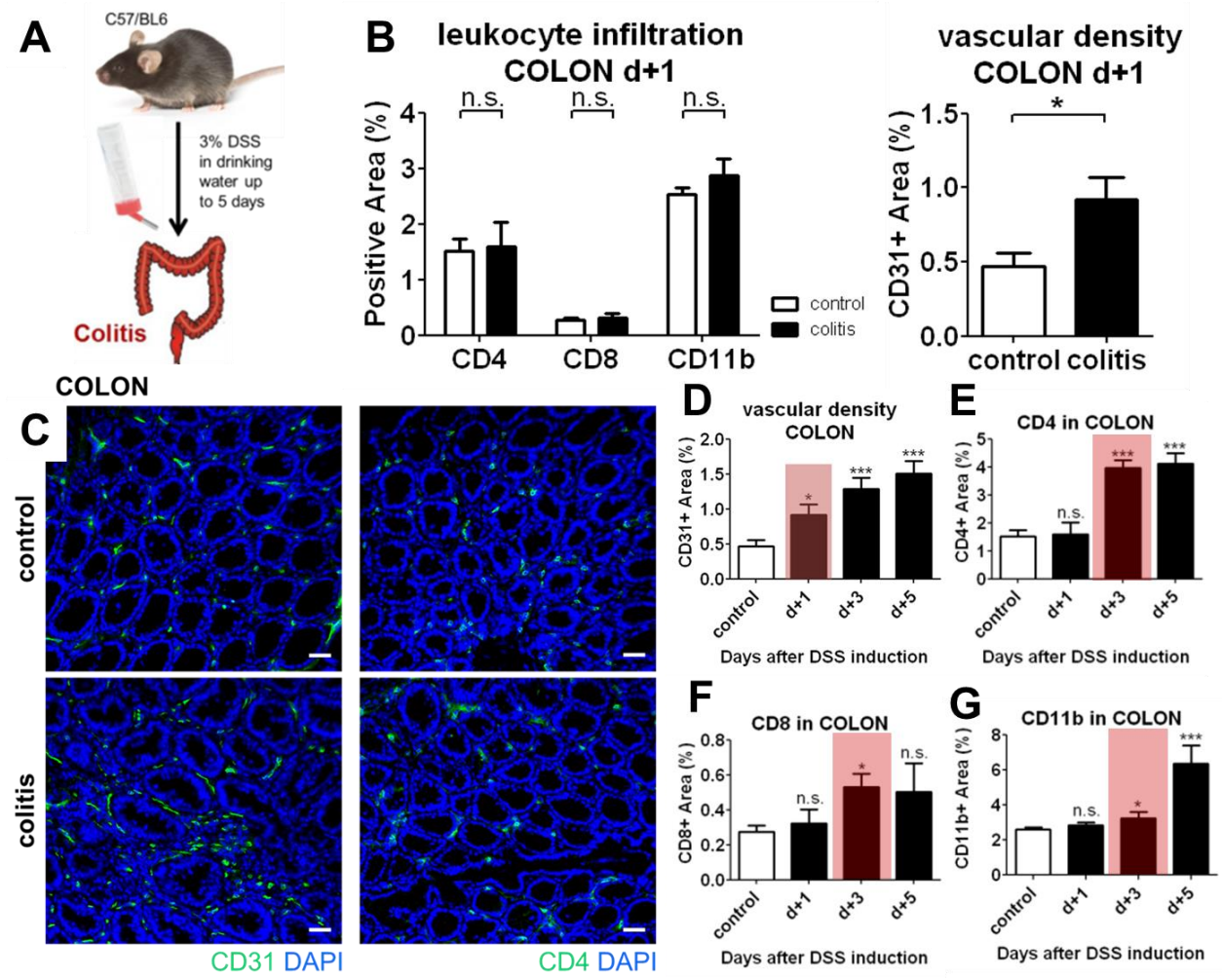

Figure S6. Angiogenesis precedes leukocyte infiltration during experimental colitis. (A) Schematic representation of induction of colitis with 3% dextran sulfate sodium (DSS). (B) Percentage of CD4, CD8, CD11b and CD31 positive area in colon of colitis bearing compared to control mice one day (d+1) after DSS induction. (C) Representative pictures from colon of colitis bearing and control mice at day+1 after DSS induction. CD31 (green-A488), CD4 (green-A488) and counterstained with DAPI. Scale bar, 30 µm. (D) Time course of angiogenesis in colon of colitis bearing mice compared to control mice. Control mice exhibited at all time points same percentage of CD31+ area. The red box marks the earliest significant increase in positive CD31 area in colitis bearing mice. (E, F, G) Time course of CD4+, CD8+, CD11b+ leukocyte infiltration. Red box marks the first significant increase in positive CD4, CD8 or CD11b area in colitis bearing mice. Representative data from one of two independent experiments (n=5-7 per group). Error bars indicate mean ± s.e.m. *$P < 0.05$, ***$P < 0.001$, n.s. not significant by Student's *t* test (two-tailed).

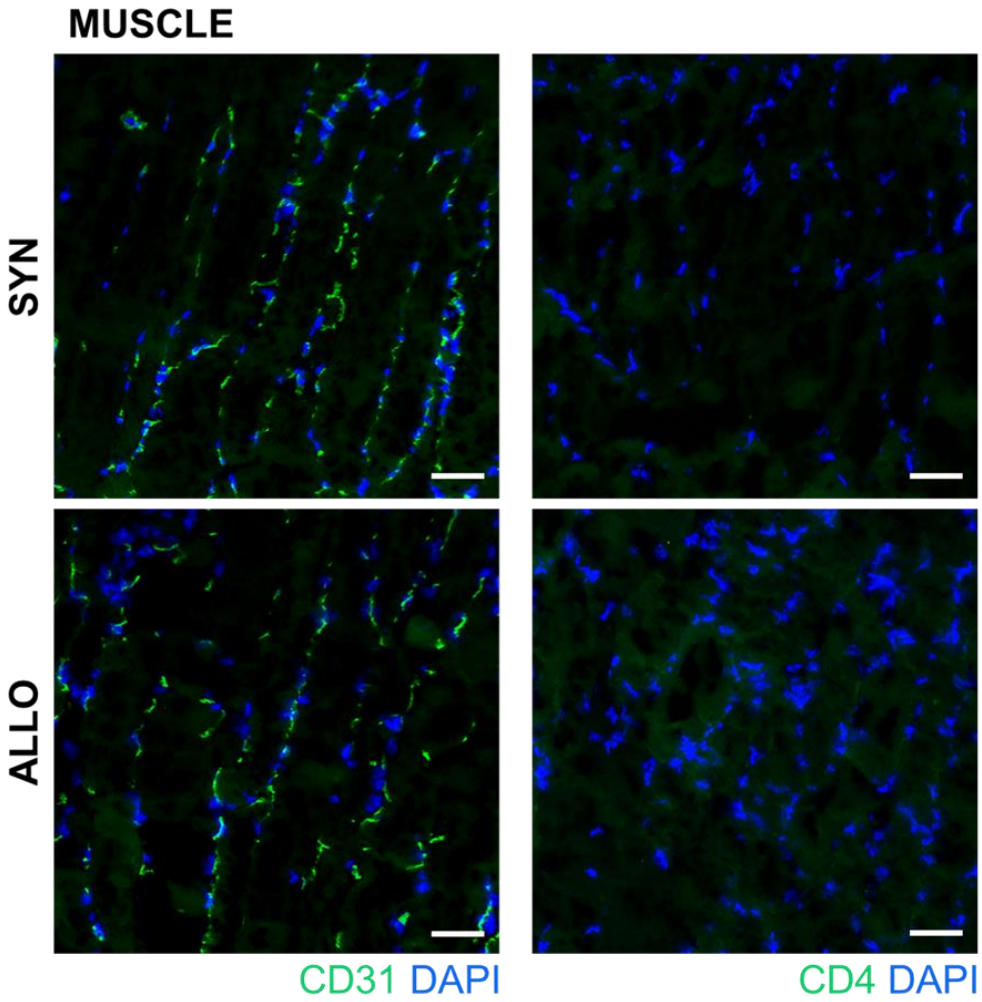

Figure S7. Non-target organs show no lymphocyte infiltration and no increase in vascular density. Representative pictures from skeletal muscle sections of SYN and ALLO mice at day+2 after BMT (LP/J→C57BL/6). Sections are stained against CD31 (green-A488) and CD4 (green-A488) and counterstained with DAPI. Scale bar, 30 µm.

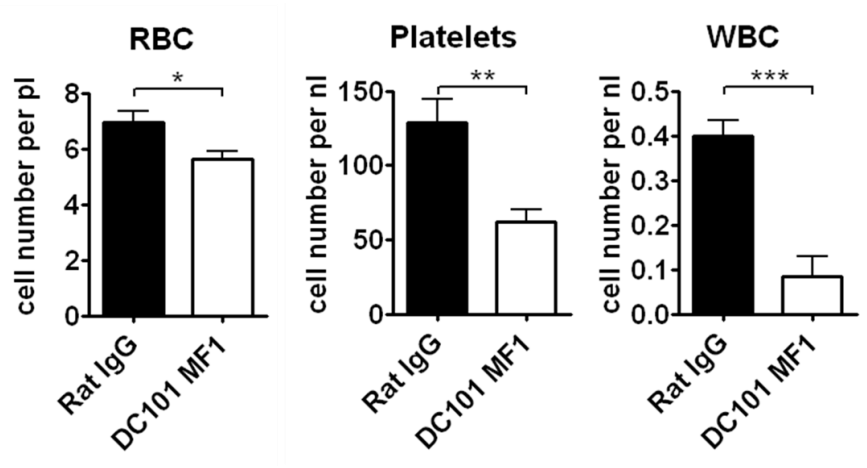

Figure S8. DC101+MFI treated mice showed significantly decreased hematological parameters suggesting defects in hematopoietic reconstitution. Hematological analysis of red blood cells (RBC), platelets and white blood cells (WBC) in peripheral blood of DC101+MF1 (VEGFR1+2 inhibitor) and rat IgG control treated mice at d+10 after BMT (C57BL/6→BALB/c). n=5 per group. Error bars indicate mean ± s.e.m. *$P < 0.05$, **$P < 0.01$, ***$P < 0.001$ by Student's *t* test (two-tailed).

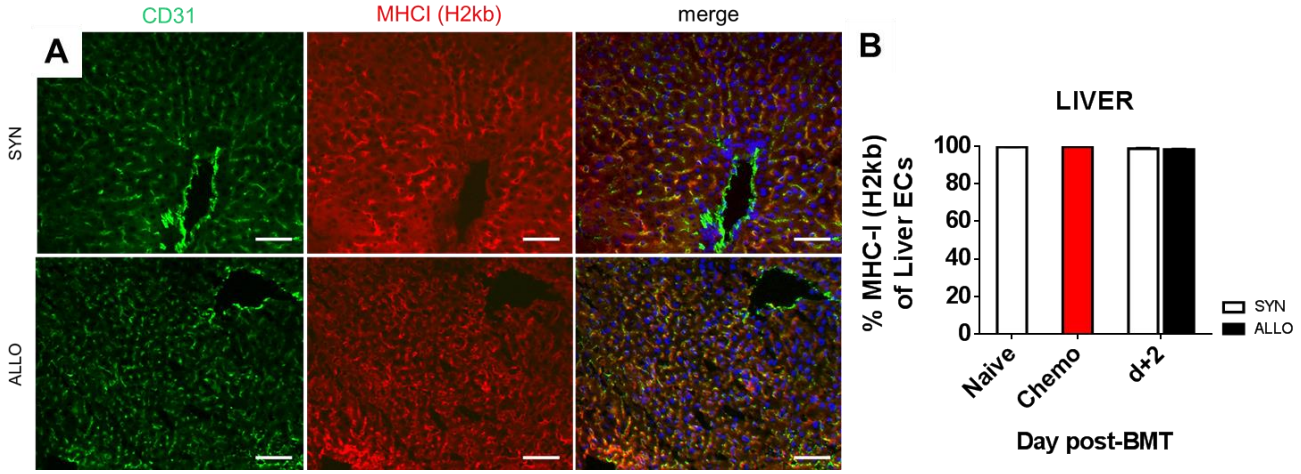

Figure S9. MHC-I expression in liver ECs (LP/J→C57BL/6). (A) Representative pictures from liver sections of SYN and ALLO mice at day+2 after BMT. Sections are stained against CD31 (green-A488), MHC-I (H2kb) (red-A555) and counterstained with DAPI. Scale bar, 30 µm. (B) FACS analysis of MHC-I (H2kb) on liver ECs of untreated (naive), chemotherapy-treated (Chemo) or SYN and ALLO mice at day+2 after BMT.

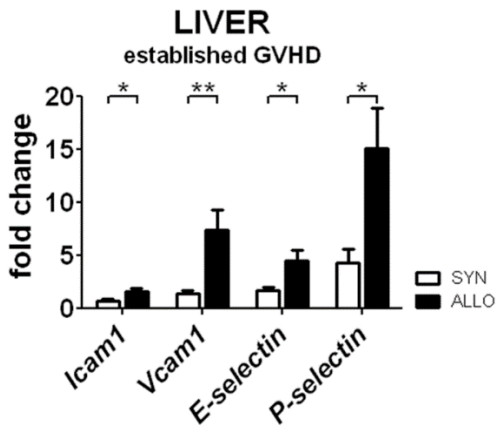

Figure S10. Increased expression of adhesion molecules in liver of allogeneic transplanted mice during established GVHD. Expression of adhesion molecules Intercellular Adhesion Molecule 1 (*Icam1*), vascular cell adhesion molecule 1 (*Vcam1*), *E-selectin* and *P-selectin* in ALLO versus SYN mice during established GVHD (GVHD scores >5) (LP/J→C57BL/6). Gene expression levels were normalized to *Gapdh* expression and are shown relative to gene levels of a reference untreated sample. n=10 per group. Error bars indicate mean ± s.e.m. *$P < 0.05$, **$P < 0.01$ by Student's *t* test (two-tailed).

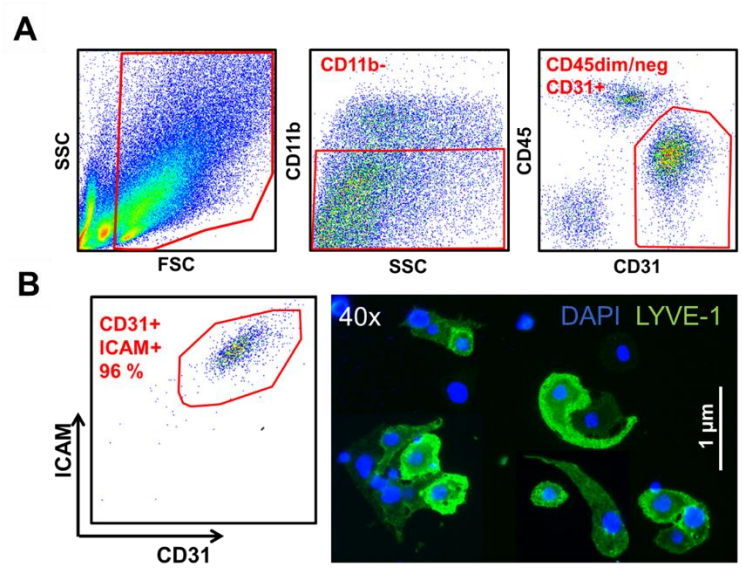

Figure S11. Gating Strategy and Purity check of MACS-isolated liver ECs and FACS-sorted colon ECs. (A) Endothelial cells were FACS-sorted as CD11b-CD45dim/-CD31+ cells. (B) Purity check by flow cytometry analysis of CD31 and ICAM1 revealed over 90 % purity. Some isolated ECs were plated on fibronectin-coated dishes. In 40x magnification isolated ECs exhibited positive LYVE-1 staining (green) and typical cell shape.

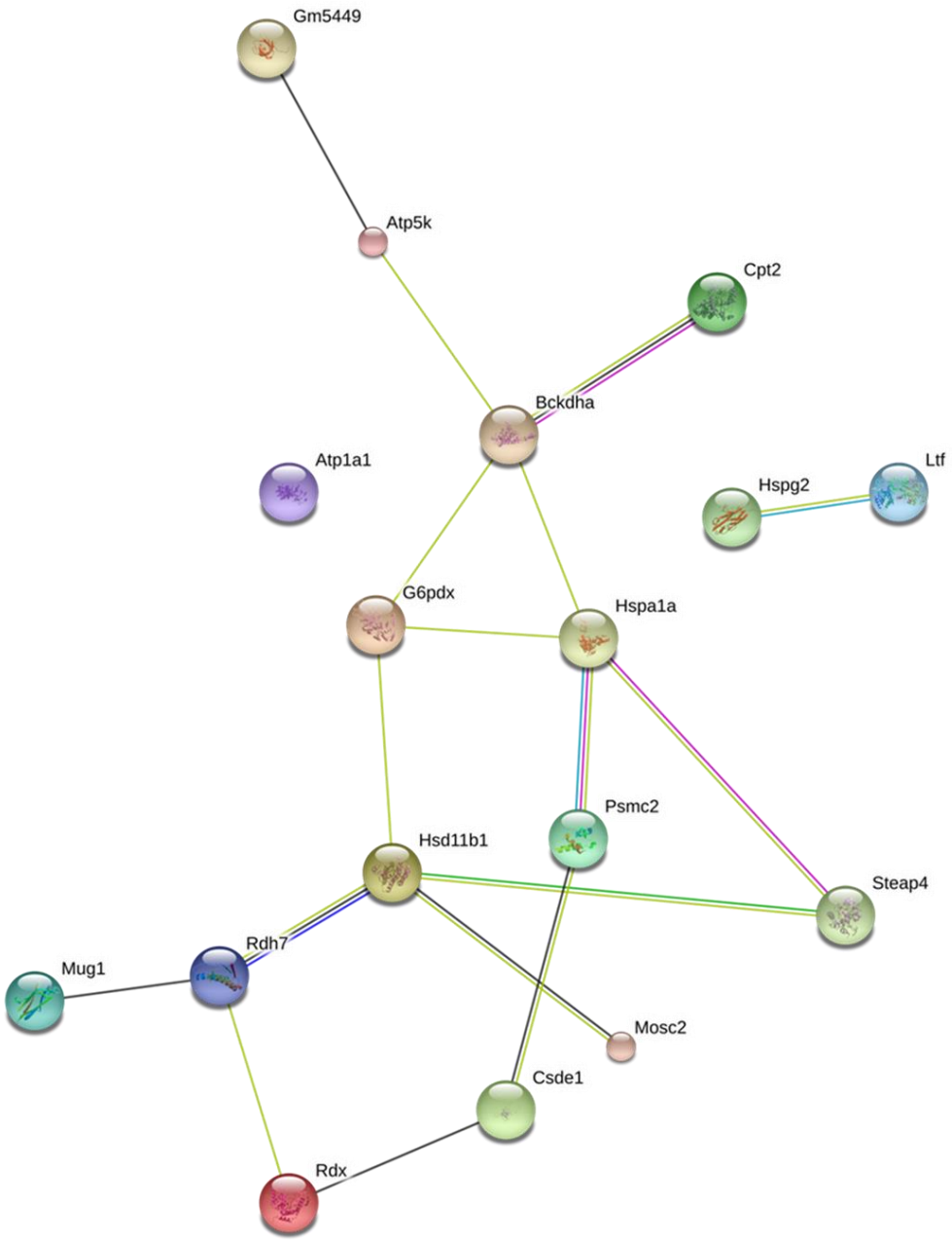

Figure S12. Network connections of the 18 upregulated proteins in liver ECs of allogeneic transplanted mice at day+2 after BMT. Network connections were analyzed with http://string-db.org. Colored lines represent different interactions: known interactions from curated databases (cyan) and experimentally determined (violet); predicted interactions by gene neighborhood (green) and by gene co-occurrence (blue); by textmining (yellow) and co-expression (black).

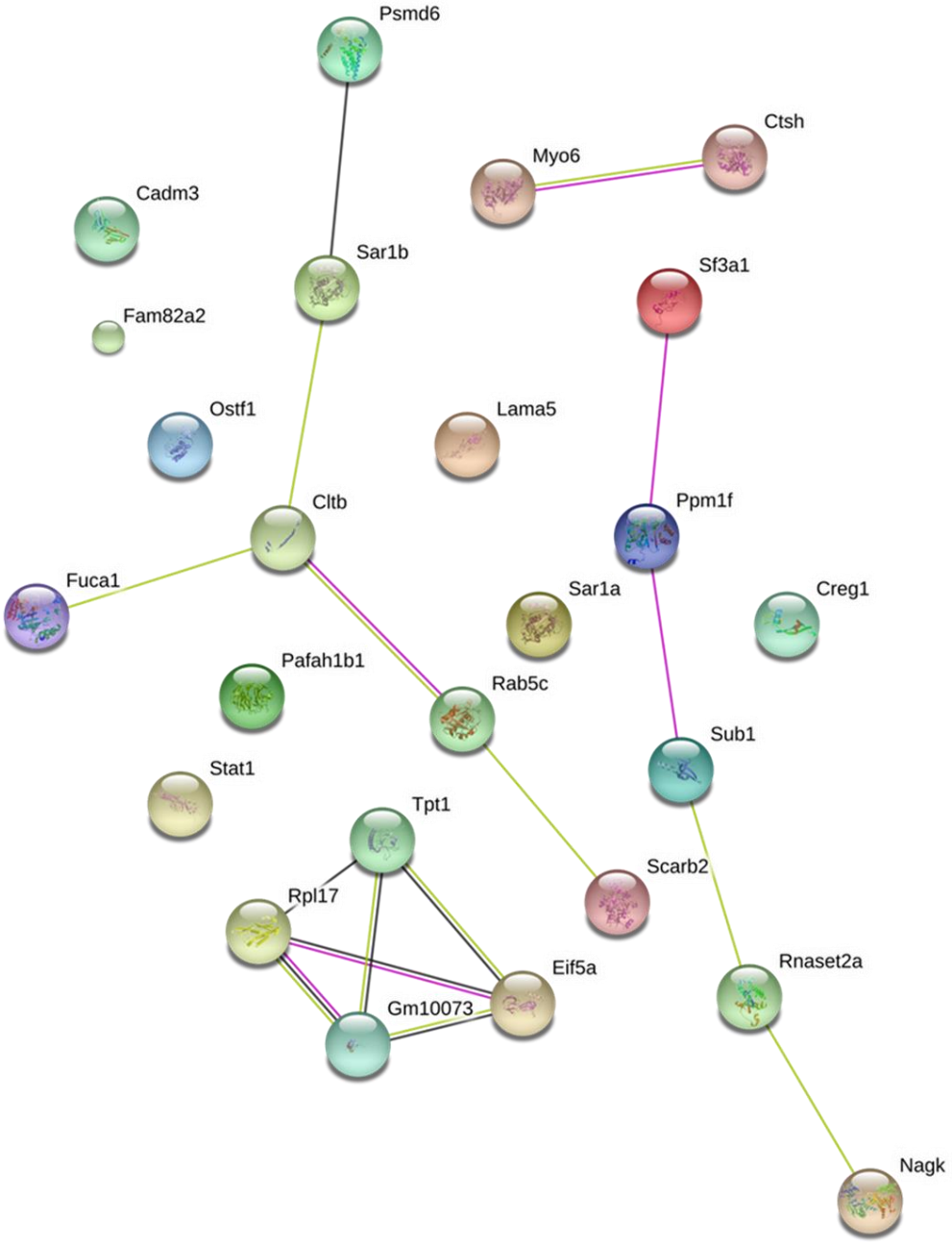

Figure S13. Network connections of the 25 downregulated proteins in liver ECs of allogeneic transplanted mice at day+2 after BMT. Network connections were analyzed with http://string-db.org. Colored lines represent different interactions: known interactions from experimentally determined (violet); by textmining (yellow) and co-expression (black).

Supplementary Table 1: Upregulated genes from Microarray of colon EC d+2

Transcript Cluster ID	COLON ALLO_d+2 Bi-weight Avg Signal (log2)	COLON SYN_d+2 Bi-weight Avg Signal (log2)	Fold Change (linear) COLON ALLO VS. SYN d+2	ANOVA p-value COLON ALLO VS. SYN d+2	FDR p-value COLON ALLO VS. SYN d+2	Gene Symbol	Description
17524944	5,91	4,71	**2,29**	0,020712	0,405681	**Zfp599**	zinc finger protein 599
17326567	5,64	4,43	**2,3**	0,000459	0,192066	**Gbe1**	glucan (1,4-alpha-), branching enzyme 1
17417115	6,36	5,16	**2,3**	0,014931	0,373285	**Gm24045**	predicted gene, 24045
17284636	4,31	3,11	**2,3**	0,021716	0,410783	**Ighv8-13**	immunoglobulin heavy variable 8-13
17330162	5,27	4,06	**2,31**	0,002101	0,259757	**BC117090**	cDNA sequence BC1179090
17246381	9,72	8,51	**2,31**	0,029469	0,437867	**Mettl7b**	methyltransferase like 7B
17212286	8,54	7,31	**2,33**	0,003438	0,281526	**Slc9a2**	solute carrier family 9 (sodium/hydrogen exchanger), member 2
17533755	9,36	8,14	**2,33**	0,004634	0,297099	**Slc6a14**	solute carrier family 6 (neurotransmitter transporter), member 14
17402350	10,96	9,75	**2,33**	0,011729	0,351792	**Fabp2**	fatty acid binding protein 2, intestinal
17419407	11,65	10,43	**2,33**	0,032395	0,445436	**Snora44**	small nucleolar RNA, H/ACA box 44; small nucleolar RNA host gene 12
17456247	8,6	7,37	**2,35**	0,007637	0,329623	**Cftr**	cystic fibrosis transmembrane conductance regulator
17266372	8,48	7,24	**2,36**	0,001115	0,220469	**Snord42b**	small nucleolar RNA, C/D box 42B
17501250	8,36	7,13	**2,36**	0,002128	0,259757	**Hpgd**	hydroxyprostaglandin dehydrogenase 15 (NAD)
17330799	9,16	7,92	**2,37**	0,006673	0,32298	**Gm5485**	predicted gene 5485
17319488	6,08	4,84	**2,37**	0,02279	0,411933	**LOC102634155**	uncharacterized LOC102634155; predicted gene 17025
17449447	7,82	6,57	**2,37**	0,031497	0,441571	**Igj**	immunoglobulin joining chain
17322750	8,75	7,5	**2,38**	0,003353	0,279815	**Abat**	4-aminobutyrate aminotransferase
17409343	10,22	8,97	**2,38**	0,012605	0,356876	**5330417C22Rik**	RIKEN cDNA 5330417C22 gene
17378685	7,97	6,7	**2,41**	0,027731	0,431447	**Tldc2**	TBC/LysM associated domain containing 2
17284913	6,77	5,51	**2,41**	0,032079	0,44446	**Tubal3**	tubulin, alpha-like 3
17378359	8,45	7,18	**2,42**	0,000679	0,198367	**Acss2**	acyl-CoA synthetase short-chain family member 2
17346401	8,21	6,94	**2,42**	0,002325	0,264313	**Acer1**	alkaline ceramidase 1
17411420	8,53	7,25	**2,43**	0,003019	0,271724	**Cth**	cystathionase (cystathionine gamma-lyase)
17412102	9,52	8,23	**2,44**	0,000536	0,196947	**Ggh**	gamma-glutamyl hydrolase
17488057	8,9	7,6	**2,47**	0,008457	0,332893	**Cyp2s1**	cytochrome P450, family 2, subfamily s, polypeptide 1
17300233	3,94	2,63	**2,49**	0,009461	0,340726	**Traj7**	T cell receptor alpha joining 7
17275223	7,05	5,73	**2,5**	0,007955	0,33102	**Immp2l**	IMP2 inner mitochondrial membrane peptidase-like (S. cerevisiae)
17366670	8,24	6,91	**2,51**	0,001485	0,244434	**Itih5**	inter-alpha (globulin) inhibitor H5
17414651	5,79	4,46	**2,51**	0,002486	0,264313	**Zfp618**	zinc finger protein 618
17550400	7,13	5,8	**2,51**	0,002575	0,264313	**Hottip**	Hoxa distal transcript antisense RNA; predicted gene 15053
17517349	7,61	6,28	**2,51**	0,028658	0,435007	**Slc35f2**	solute carrier family 35, member F2
17364872	6,19	4,84	**2,54**	0,001937	0,258287	**Pyroxd2**	pyridine nucleotide-disulphide oxidoreductase domain 2
17286540	5,97	4,6	**2,58**	0,038386	0,458152	**Gm16984**	predicted gene, 16984; uncharacterized LOC102640991
17280817	7,19	5,82	**2,59**	0,011888	0,352951	**Scin**	scinderin
17367473	6,2	4,82	**2,6**	0,028203	0,433033	**Myo3a**	myosin IIIA
17528934	7,67	6,28	**2,62**	0,001293	0,233058	**Tinag**	tubulointerstitial nephritis antigen
17396162	10,18	8,79	**2,63**	0,001178	0,224358	**Car2**	carbonic anhydrase 2
17496354	8,9	7,5	**2,63**	0,002038	0,258287	**Sult1a1**	sulfotransferase family 1A, phenol-preferring, member 1
17226655	6,62	5,21	**2,66**	0,030232	0,439549	**C4bp**	complement component 4 binding protein
17287175	8,31	6,88	**2,69**	0,004406	0,292895	**Ogn**	osteoglycin
17295278	8,83	7,4	**2,7**	0,000454	0,192066	**Hexb**	hexosaminidase B
17539110	6,15	4,7	**2,74**	0,004932	0,304259	**Smpx**	small muscle protein, X-linked
17213313	6,48	5	**2,79**	0,020158	0,401665	**Snord70**	small nucleolar RNA, C/D box 70
17260931	6,23	4,73	**2,83**	0,026916	0,427179	**Mir1933**	microRNA 1933
17517222	7,04	5,53	**2,85**	0,000661	0,197483	**Arhgap20**	Rho GTPase activating protein 20
17319707	8,21	6,7	**2,85**	0,005101	0,305895	**Cyp2d26**	cytochrome P450, family 2, subfamily d, polypeptide 26
17506532	10,79	9,27	**2,87**	0,000324	0,192066	**Dpep1**	dipeptidase 1 (renal)
17472114	8,98	7,46	**2,88**	0,001003	0,214752	**Plbd1**	phospholipase B domain containing 1
17314476	7,13	5,6	**2,89**	0,00018	0,17246	**Tmem117**	transmembrane protein 117
17482310	8,63	7,1	**2,9**	0,000891	0,213174	**Acsm3**	acyl-CoA synthetase medium-chain family member 3
17392401	10,51	8,96	**2,91**	0,030618	0,439931	**Snord17**	small nucleolar RNA, C/D box 17
17495320	6,01	4,45	**2,96**	0,016694	0,382242	**Cyp2r1**	cytochrome P450, family 2, subfamily r, polypeptide 1
17217035	7,9	6,33	**2,98**	0,003811	0,288753	**Ctse**	cathepsin E
17215370	7,41	5,82	**3,01**	0,029085	0,43639	**Atg16l1**	autophagy related 16-like 1 (S. cerevisiae); predicted gene, 25395
17482897	7,4	5,81	**3,02**	0,005933	0,311645	**Aqp8**	aquaporin 8
17488151	6,81	5,16	**3,14**	0,005214	0,306632	**Mia**	melanoma inhibitory activity; predicted gene 21983
17540378	7,45	5,75	**3,26**	0,000485	0,192997	**Maob**	monoamine oxidase B
17284396	6,04	4,33	**3,28**	0,025067	0,419462	**LOC101056284**	Ig heavy chain V region 5-84-like; immunoglobulin heavy variable 2-5; immunoglobulin heavy constant mu
17449346	7	5,26	**3,33**	0,006982	0,32298	**Ugt2b5**	UDP glucuronosyltransferase 2 family, polypeptide B5

Transcript Cluster ID	COLON ALLO_d+2 Bi-weight Avg Signal (log2)	COLON SYN_d+2 Bi-weight Avg Signal (log2)	Fold Change (linear) COLON ALLO VS. SYN d+2	ANOVA p-value COLON ALLO VS. SYN d+2	FDR p-value COLON ALLO VS. SYN d+2	Gene Symbol	Description
17374089	10,14	9,14	**2,01**	0,000568	0,197483	**Lin7c**	lin-7 homolog C (C. elegans)
17526982	6,18	5,18	**2,01**	0,001751	0,248333	**Gm684**	predicted gene 684
17530141	9,52	8,51	**2,01**	0,005744	0,311578	**Pccb**	propionyl Coenzyme A carboxylase, beta polypeptide
17504512	7,27	6,26	**2,01**	0,006878	0,32298	**Ces2c**	carboxylesterase 2C
17352517	5,69	4,68	**2,01**	0,007722	0,329876	**Mkx**	mohawk homeobox
17452578	9,55	8,55	**2,01**	0,010867	0,348605	**Hpd**	4-hydroxyphenylpyruvic acid dioxygenase
17518458	7,32	6,31	**2,01**	0,01112	0,349449	**Igdcc4**	immunoglobulin superfamily, DCC subclass, member 4
17530406	7,31	6,29	**2,02**	0,029659	0,437867	**Acpp**	acid phosphatase, prostate
17349552	6,36	5,35	**2,02**	0,036824	0,455549	**Snora74a**	small nucleolar RNA, H/ACA box 74A
17470060	6,74	5,73	**2,03**	0,000554	0,196947	**Rassf4**	Ras association (RalGDS/AF-6) domain family member 4
17255511	7,41	6,38	**2,04**	0,002761	0,265146	**Ttll6**	tubulin tyrosine ligase-like family, member 6
17392255	6,45	5,42	**2,04**	0,003908	0,288753	**Flrt3**	fibronectin leucine rich transmembrane protein 3
17363429	7,35	6,32	**2,05**	0,001373	0,238661	**Aldh1a7**	aldehyde dehydrogenase family 1, subfamily A7
17284919	7,8	6,75	**2,06**	0,000584	0,197483	**Akr1c14**	aldo-keto reductase family 1, member C14
17524077	5,89	4,85	**2,06**	0,003323	0,279384	**Fut4**	fucosyltransferase 4
17241676	6,14	5,1	**2,06**	0,008742	0,333064	**1700040L02Rik**	RIKEN cDNA 1700040L02 gene
17222777	8,49	7,45	**2,06**	0,034444	0,450559	**Slc40a1**	solute carrier family 40 (iron-regulated transporter), member 1
17212346	7,02	5,97	**2,07**	0,001812	0,251823	**AI597479**	expressed sequence AI597479
17515715	6,7	5,65	**2,07**	0,004272	0,292895	**Zbtb44**	zinc finger and BTB domain containing 44
17465170	7,68	6,63	**2,07**	0,02939	0,437867	**Slc13a1**	solute carrier family 13 (sodium/sulfate symporters), member 1
17252183	8,61	7,56	**2,08**	0,000296	0,192066	**Eno3**	enolase 3, beta muscle
17415570	7,3	6,24	**2,08**	0,021728	0,410783	**Hook1**	hook homolog 1 (Drosophila)
17307354	7,13	6,06	**2,09**	0,005134	0,305895	**Atp8a2**	ATPase, aminophospholipid transporter-like, class I, type 8A, member 2
17420064	8,99	7,92	**2,09**	0,006556	0,322403	**Tcea3**	transcription elongation factor A (SII), 3
17533474	9,9	8,83	**2,1**	0,007876	0,33102	**Maoa**	monoamine oxidase A
17213317	4,25	3,18	**2,1**	0,008111	0,33102	**Gm26287**	predicted gene, 26287
17248476	7,23	6,16	**2,1**	0,040458	0,463039	**Pank3**	pantothenate kinase 3
17443985	6,21	5,13	**2,11**	0,00267	0,264698	**Cyp2w1**	cytochrome P450, family 2, subfamily w, polypeptide 1
17326964	7,26	6,18	**2,11**	0,024533	0,416812	**Hunk**	hormonally upregulated Neu-associated kinase
17291241	7,4	6,32	**2,12**	0,027615	0,431298	**Slc17a4**	solute carrier family 17 (sodium phosphate), member 4
17255540	6,59	5,51	**2,12**	0,031001	0,440561	**Gm11538**	predicted gene 11538
17516997	7,06	5,97	**2,13**	0,037729	0,455745	**Gm5617**	predicted gene 5617
17295386	9,8	8,7	**2,14**	0,011436	0,350667	**Tmem171**	transmembrane protein 171
17520736	7,09	5,99	**2,15**	0,020286	0,402813	**A4gnt**	alpha-1,4-N-acetylglucosaminyltransferase
17547877	7,86	6,74	**2,16**	0,008517	0,332994	**Deptor**	DEP domain containing MTOR-interacting protein
17370799	4,73	3,62	**2,16**	0,008581	0,332994	**A430018G15Rik**	RIKEN cDNA A430018G15 gene
17282498	8,45	7,33	**2,17**	0,003163	0,273992	**Entpd5**	ectonucleoside triphosphate diphosphohydrolase 5
17236393	9,36	8,24	**2,17**	0,026518	0,425569	**Slc5a8**	solute carrier family 5 (iodide transporter), member 8
17540154	6,04	4,92	**2,17**	0,031265	0,441571	**Cybb**	cytochrome b-245, beta polypeptide
17354282	8,4	7,27	**2,18**	0,003291	0,277413	**Cdo1**	cysteine dioxygenase 1, cytosolic
17226049	7,71	6,59	**2,18**	0,023744	0,414239	**Kdsr**	3-ketodihydrosphingosine reductase
17404534	7,34	6,21	**2,19**	0,000766	0,204238	**Lrrc31**	leucine rich repeat containing 31
17284612	5,52	4,39	**2,19**	0,011358	0,350667	**Ighv8-9**	immunoglobulin heavy variable V8-9
17529990	8,92	7,79	**2,19**	0,020042	0,401205	**Gm1123**	predicted gene 1123
17405908	5,89	4,76	**2,2**	0,000407	0,192066	**Bche**	butyrylcholinesterase
17310673	7,72	6,58	**2,21**	0,000716	0,198367	**Ank**	progressive ankylosis
17351168	7,25	6,11	**2,21**	0,008912	0,333064	**Htr4**	5 hydroxytryptamine (serotonin) receptor 4
17336414	5,63	4,48	**2,22**	0,0301	0,438736	**H2-DMb2**	histocompatibility 2, class II, locus Mb2
17353256	8,18	7,02	**2,23**	0,000043	0,116899	**Gm6665**	predicted gene 6665
17316348	8,94	7,78	**2,23**	0,021236	0,408475	**Snord123**	small nucleolar RNA, C/D box 123
17250365	8,12	6,96	**2,24**	0,012121	0,352951	**Gid4**	GID complex subunit 4, VID24 homolog (S. cerevisiae)
17360406	10,11	8,94	**2,25**	0,000078	0,127951	**Pdcd4**	programmed cell death 4
17257906	6,5	5,33	**2,25**	0,015679	0,377934	**Map2k6**	mitogen-activated protein kinase kinase 6
17408336	7,32	6,15	**2,25**	0,044091	0,475027	**Hsd3b3**	hydroxy-delta-5-steroid dehydrogenase, 3 beta- and steroid delta-isomerase 3
17477384	8,94	7,76	**2,26**	0,008123	0,33102	**Klk1b5**	kallikrein 1-related peptidase b5
17252058	7,09	5,9	**2,28**	0,036773	0,455549	**Tm4sf5**	transmembrane 4 superfamily member 5
17458626	6,05	4,86	**2,29**	0,000122	0,145268	**Hottip**	Hoxa distal transcript antisense RNA; predicted gene 15053
17358103	9,28	8,09	**2,29**	0,007393	0,326276	**Aldh1a1**	aldehyde dehydrogenase family 1, subfamily A1

Transcript Cluster ID	COLON ALLO_d+2 Bi-weight Avg Signal (log2)	COLON SYN_d+2 Bi-weight Avg Signal (log2)	Fold Change (linear) COLON ALLO VS. SYN d+2	ANOVA p-value COLON ALLO VS. SYN d+2	FDR p-value COLON ALLO VS. SYN d+2	Gene Symbol	Description
17400862	11,59	9,83	**3,39**	0,037671	0,455745	**Hmgcs2**	3-hydroxy-3-methylglutaryl-Coenzyme A synthase 2
17435643	7,44	5,65	**3,46**	0,004621	0,297099	**Rnf32**	ring finger protein 32
17456710	6,8	4,99	**3,52**	0,003097	0,273769	**Tspan33**	tetraspanin 33
17348833	8,94	7,12	**3,55**	0,005357	0,306729	**Ttr**	transthyretin
17306143	9,11	7,27	**3,59**	0,038776	0,458152	**Ang4**	angiogenin, ribonuclease A family, member 4
17345066	7,78	5,92	**3,64**	0,003129	0,273992	**Mep1a**	meprin 1 alpha
17475870	10,19	8,33	**3,65**	0,000543	0,196947	**Sycn**	syncollin
17425233	8,59	6,67	**3,79**	0,003061	0,273386	**Aldob**	aldolase B, fructose-bisphosphate
17528924	7,34	5,39	**3,85**	0,002988	0,270369	**Fam83b**	family with sequence similarity 83, member B
17376191	7,42	5,46	**3,88**	0,001771	0,250164	**Tgm3**	transglutaminase 3, E polypeptide
17397923	7,41	5,44	**3,93**	0,002659	0,264698	**Aadac**	arylacetamide deacetylase (esterase)
17321780	9,27	7,24	**4,07**	0,028124	0,432767	**Cela1**	chymotrypsin-like elastase family, member 1
17477399	5,63	3,5	**4,39**	0,000406	0,192066	**Gm25386**	predicted gene, 25386
17219751	11,58	9,41	**4,48**	0,049364	0,491056	**Mptx1**	mucosal pentraxin 1
17408360	9,62	7,23	**5,24**	0,000429	0,192066	**Hao2**	hydroxyacid oxidase 2
17345989	7,9	5,44	**5,51**	0,005343	0,306632	**Sult1c2**	sulfotransferase family, cytosolic, 1C, member 2
17533253	7,63	5,15	**5,56**	0,001041	0,215688	**Otc**	ornithine transcarbamylase
17364403	6,36	3,87	**5,63**	0,00089	0,213174	**Cyp2c67**	cytochrome P450, family 2, subfamily c, polypeptide 67
17232438	5,87	3,27	**6,1**	0,00512	0,305895	**Gm25596**	predicted gene, 25596
17526663	9,31	6,7	**6,11**	0,000009	0,093803	**Nxpe2**	neurexophilin and PC-esterase domain family, member 2
17364440	6,07	3,28	**6,89**	0,000217	0,178839	**Cyp2c69**	cytochrome P450, family 2, subfamily c, polypeptide 69
17467486	8,77	5,9	**7,33**	0,00427	0,292895	**Igkv12-44**	immunoglobulin kappa variable 12-44; immunoglobulin kappa chain complex
17364414	8,22	4,52	**12,94**	0,000037	0,116899	**Cyp2c68**	cytochrome P450, family 2, subfamily c, polypeptide 68

Supplementary Table 2: Downregulated genes from Microarray of colon EC d+2

Transcript Cluster ID	COLON ALLO_d+2 Bi-weight Avg Signal (log2)	COLON SYN_d+2 Bi-weight Avg Signal (log2)	Fold Change (linear) COLON ALLO VS. SYN d+2	ANOVA p-value COLON ALLO VS. SYN d+2	FDR p-value COLON ALLO VS. SYN d+2	Gene Symbol	Description
17467554	5,4	9,61	**-18,48**	0,043008	0,47251	**Igkv6-13**	immunoglobulin kappa variable 6-13
17306968	4,31	8,15	**-14,38**	0,01045	0,346389	**Mcpt8**	mast cell protease 8
17262250	3,35	6,25	**-7,46**	0,020495	0,404885	**Tgtp2**	T cell specific GTPase 2; T cell specific GTPase 1
17350916	7,17	9,77	**-6,06**	0,020032	0,401205	**Gm4951**	predicted gene 4951
17318950	6,5	8,57	**-4,19**	0,024999	0,418743	**Csf2rb2**	colony stimulating factor 2 receptor, beta 2, low-affinity (granulocyte-macrophage)
17526707	5,51	7,49	**-3,95**	0,000827	0,210924	**Zbtb16**	zinc finger and BTB domain containing 16
17334638	6,19	8,12	**-3,81**	0,000656	0,197483	**Prss34**	protease, serine 34
17399823	3,13	5,02	**-3,7**	0,000086	0,127951	**S100a8**	S100 calcium binding protein A8 (calgranulin A)
17410905	9,51	11,4	**-3,7**	0,001719	0,247742	**AI747448**	expressed sequence AI747448
17438955	4,59	6,45	**-3,63**	0,000603	0,197483	**Cxcl5**	chemokine (C-X-C motif) ligand 5
17346150	8,06	9,9	**-3,58**	0,000226	0,178839	**Lrg1**	leucine-rich alpha-2-glycoprotein 1
17233329	5,74	7,49	**-3,37**	0,013165	0,359033	**Gm5423**	predicted gene 5423
17449710	7,46	9,18	**-3,3**	0,011174	0,349999	**Cxcl9**	chemokine (C-X-C motif) ligand 9
17428795	3,94	5,64	**-3,26**	0,011972	0,352951	**Gm22980**	predicted gene, 22980
17403205	7,15	8,85	**-3,26**	0,014732	0,372144	**Gbp5**	guanylate binding protein 5
17450461	8,31	10,01	**-3,25**	0,023048	0,412372	**Gbp4**	guanylate binding protein 4
17508188	7,4	9,07	**-3,18**	0,013399	0,359477	**Ido1**	indoleamine 2,3-dioxygenase 1
17403268	6,94	8,6	**-3,14**	0,006919	0,32298	**Gbp2**	guanylate binding protein 2
17305683	5,27	6,9	**-3,08**	0,012982	0,357733	**Gm22637**	predicted gene, 22637
17309061	3,22	4,83	**-3,06**	0,007262	0,326276	**Gm25831**	predicted gene, 25831
17450448	6,64	8,17	**-2,89**	0,014393	0,369294	**Gbp9**	guanylate-binding protein 9
17220919	5,06	6,57	**-2,84**	0,014287	0,368355	**A130010J15Rik**	RIKEN cDNA A130010J15 gene
17455954	5,15	6,66	**-2,83**	0,000012	0,093803	**Tac1**	tachykinin 1
17515074	6,84	8,34	**-2,83**	0,010388	0,346389	**Icam1**	intercellular adhesion molecule 1
17543572	6,38	7,87	**-2,8**	0,013554	0,361896	**Il2rg**	interleukin 2 receptor, gamma chain; predicted gene 20489
17283945	4,42	5,9	**-2,79**	0,018749	0,393856	**Gm22079**	predicted gene, 22079
17394153	5,98	7,45	**-2,78**	0,000636	0,197483	**Slpi**	secretory leukocyte peptidase inhibitor
17236525	6,34	7,81	**-2,77**	0,005886	0,311645	**Mir1931**	microRNA 1931
17308568	2,57	4,03	**-2,74**	0,044451	0,475453	**Rb1**	retinoblastoma 1
17403224	7,73	9,17	**-2,71**	0,006733	0,32298	**Gbp7**	guanylate binding protein 7
17337110	6,61	8,03	**-2,67**	0,007399	0,326276	**H2-Q5**	histocompatibility 2, Q region locus 5
17369950	9,06	10,46	**-2,65**	0,017688	0,38592	**Gm26236**	predicted gene, 26236
17221191	4,51	5,92	**-2,65**	0,032632	0,446054	**Snord87**	small nucleolar RNA, C/D box 87
17337122	9,09	10,49	**-2,64**	0,008472	0,332893	**H2-Q6**	histocompatibility 2, Q region locus 6; histocompatibility 2, Q region locus 8; histocompatibility 2, Q region locus 6-like
17494394	4,48	5,87	**-2,61**	0,043948	0,474578	**Trim30a**	tripartite motif-containing 30A
17262241	5,31	6,68	**-2,58**	0,037866	0,456066	**9930111J21Rik2**	RIKEN cDNA 9930111J21 gene 2
17450501	7,88	9,24	**-2,57**	0,009573	0,340726	**Gbp10**	guanylate-binding protein 10
17249034	8,62	9,96	**-2,52**	0,003133	0,273992	**Gm23813**	predicted gene, 23813
17372742	5,48	6,81	**-2,51**	0,001739	0,247742	**Gm23716**	predicted gene, 23716
17406450	4,13	5,46	**-2,51**	0,049835	0,493791	**Snord73a**	small nucleolar RNA, C/D box U73A
17253707	6,31	7,64	**-2,5**	0,007794	0,33074	**Nos2**	nitric oxide synthase 2, inducible
17312223	5,41	6,73	**-2,5**	0,011169	0,349999	**BC025446**	cDNA sequence BC025446
17249980	8,01	9,32	**-2,49**	0,011824	0,352121	**Igtp**	interferon gamma induced GTPase
17403237	5,97	7,28	**-2,48**	0,021414	0,410335	**Gbp3**	guanylate binding protein 3
17449718	4,83	6,12	**-2,45**	0,002532	0,264313	**Cxcl10**	chemokine (C-X-C motif) ligand 10
17337133	6,67	7,96	**-2,45**	0,006894	0,32298	**H2-Q7**	histocompatibility 2, Q region locus 7; histocompatibility 2, Q region locus 9
17278328	8,76	10,06	**-2,45**	0,014665	0,371821	**Serpina3n**	serine (or cysteine) peptidase inhibitor, clade A, member 3N
17547660	4,73	6,02	**-2,45**	0,015081	0,373285	**Gm20235**	predicted gene, 20235

Transcript Cluster ID	COLON ALLO_d+2 Bi-weight Avg Signal (log2)	COLON SYN_d+2 Bi-weight Avg Signal (log2)	Fold Change (linear) COLON ALLO VS. SYN d+2	ANOVA p-value COLON ALLO VS. SYN d+2	FDR p-value COLON ALLO VS. SYN d+2	Gene Symbol	Description
17549216	10,13	11,4	**-2,42**	0,004328	0,292895	**H2-Q7**	histocompatibility 2, Q region locus 7; histocompatibility 2, Q region locus 9; histocompatibility 2, Q region locus 5
17429632	7,83	9,1	**-2,41**	0,00481	0,299884	**Mfsd2a**	major facilitator superfamily domain containing 2A
17369925	8,47	9,74	**-2,41**	0,035941	0,454178	**Eng**	endoglin
17318089	7,02	8,27	**-2,38**	0,025247	0,420922	**Ly6c1**	lymphocyte antigen 6 complex, locus C1
17250744	6,42	7,66	**-2,36**	0,006071	0,313609	**Snord65**	small nucleolar RNA, C/D box 65
17404337	3,98	5,2	**-2,32**	0,011829	0,352121	**Cpa3**	carboxypeptidase A3, mast cell
17514834	7,42	8,64	**-2,31**	0,01918	0,396379	**Gm23455**	predicted gene, 23455; TATA box binding protein (Tbp)-associated factor, RNA polymerase I, D
17436791	5,55	6,76	**-2,31**	0,035323	0,453266	**Mir3097**	microRNA 3097
17353663	7,3	8,49	**-2,28**	0,001038	0,215688	**Tmem173**	transmembrane protein 173
17247225	8,09	9,27	**-2,26**	0,001057	0,215688	**Upp1**	uridine phosphorylase 1
17490622	5,47	6,65	**-2,26**	0,012251	0,352951	**Snord35a**	small nucleolar RNA, C/D box 35A
17254041	5,42	6,59	**-2,26**	0,017474	0,384495	**Ccl2**	chemokine (C-C motif) ligand 2
17450515	3,43	4,6	**-2,25**	0,039345	0,459803	**Gbp11**	guanylate binding protein 11
17238367	8,13	9,29	**-2,24**	0,001613	0,246222	**Stat2**	signal transducer and activator of transcription 2
17531001	7,09	8,25	**-2,23**	0,033961	0,449632	**Sema3f**	sema domain, immunoglobulin domain (Ig), short basic domain, secreted, (semaphorin) 3F
17375409	8,71	9,86	**-2,22**	0,006224	0,316651	**Duoxa2**	dual oxidase maturation factor 2
17270615	3,95	5,09	**-2,2**	0,000838	0,210924	**Gm22743**	predicted gene, 22743
17379873	3	4,13	**-2,2**	0,005766	0,311578	**Gm23201**	predicted gene, 23201; RIKEN cDNA 1500012F01 gene
17399374	5,87	7	**-2,19**	0,000082	0,127951	**Muc1**	mucin 1, transmembrane
17514687	5,67	6,8	**-2,19**	0,003671	0,285052	**Phxr4**	per-hexamer repeat gene 4
17350925	9,86	10,98	**-2,18**	0,024014	0,415142	**Iigp1**	interferon inducible GTPase 1
17350921	5,37	6,47	**-2,15**	0,035796	0,453972	**F830016B08Rik**	RIKEN cDNA F830016B08 gene
17346155	7,16	8,25	**-2,14**	0,026936	0,427301	**Sema6b**	sema domain, transmembrane domain (TM), and cytoplasmic domain, (semaphorin) 6B
17505478	7,34	8,42	**-2,12**	0,01043	0,346389	**Tat**	tyrosine aminotransferase
17514592	8,73	9,8	**-2,11**	0,00248	0,264313	**Mmp7**	matrix metallopeptidase 7
17383892	6,27	7,35	**-2,11**	0,003281	0,277171	**Lcn2**	lipocalin 2
17419411	6,26	7,33	**-2,1**	0,008388	0,332143	**Snord99**	small nucleolar RNA, C/D box 99; small nucleolar RNA host gene 12
17439805	3,66	4,74	**-2,1**	0,015805	0,379229	**Dmp1**	dentin matrix protein 1
17249990	8,25	9,32	**-2,1**	0,017743	0,386618	**Irgm2**	immunity-related GTPase family M member 2
17518318	6,61	7,68	**-2,1**	0,017931	0,388021	**Gm22455**	predicted gene, 22455
17318020	5,6	6,66	**-2,09**	0,001584	0,246222	**Ly6d**	lymphocyte antigen 6 complex, locus D
17387517	7,66	8,73	**-2,09**	0,033246	0,447305	**Serping1**	serine (or cysteine) peptidase inhibitor, clade G, member 1
17337100	5,97	7,01	**-2,07**	0,005138	0,305895	**H2-Q4**	histocompatibility 2, Q region locus 4
17462437	5,63	6,68	**-2,07**	0,045032	0,478369	**Usp18**	ubiquitin specific peptidase 18
17394993	6,78	7,83	**-2,06**	0,00149	0,244434	**Gm26489**	predicted gene, 26489
17411545	5,15	6,19	**-2,06**	0,003147	0,273992	**6330407A03Rik**	RIKEN cDNA 6330407A03 gene
17278268	4,6	5,64	**-2,05**	0,006994	0,32298	**Serpina3f**	serine (or cysteine) peptidase inhibitor, clade A, member 3F
17459196	7,07	8,09	**-2,04**	0,005258	0,306632	**Tnip3**	TNFAIP3 interacting protein 3
17336432	9,39	10,42	**-2,04**	0,00581	0,311578	**Tap1**	transporter 1, ATP-binding cassette, sub-family B (MDR/TAP)
17336458	6,49	7,52	**-2,04**	0,035257	0,453266	**Tap2**	transporter 2, ATP-binding cassette, sub-family B (MDR/TAP)
17448064	4,79	5,81	**-2,03**	0,005846	0,311578	**Lgi2**	leucine-rich repeat LGI family, member 2
17452054	6,12	7,14	**-2,02**	0,01499	0,373285	**Oas2**	2-5 oligoadenylate synthetase 2
17358219	4,36	5,37	**-2,02**	0,015904	0,379229	**Mir1192**	microRNA 1192
17221079	5,69	6,71	**-2,02**	0,042119	0,470508	**Gm25493**	predicted gene, 25493
17481260	4,24	5,25	**-2,01**	0,036087	0,454178	**Trim6**	tripartite motif-containing 6

Supplementary Table 3: Upregulated proteins from LC-MS/MS proteome analysis of liver EC d+2

UP	Protein	Protein name	Ratio norm.	Cellular location	Biological Process
METABOLIC PROCESS	**CPT2**	Carnitine palmitoyl-transferase II	**8,13**	mitochondrial inner membrane	fatty acid beta-oxidation cellular lipid metabolic process carnitine shuttle small molecule metabolic process
	G6pdx	Glucose-6-phosphate dehydrogenase	**6,81**	centrosome cytoplasm cytoplasmatic side of plasma membrane cytosol extracellular exosome intracellular membrane-bounded organelle membrane microtubule organizing center nucleus	glucose metabolic process pentose-phosphate shunt, oxidative branch carbohydrate metabolic process lipid metabolic process cholesterol biosynthetic process NADPH regeneration, NADP metabolic process oxidation-reduction process cellular response to oxidative stress negative regulation of protein glutathionylation response to ethanol,food, organic cyclic compounds small molecule metabolic process ribose phosphate biosynthetic process transcription initiation from RNA polymerase II promoter
	Hsd11b1	11-beta-hydroxy-steroid dehydro-genase, type I	**1,33**	ER membrane, single-pass type II membrane protein	glucocorticoid biosynthetic process steroid metabolic process small molecule metabolic process
	Bckdha	Branched-chain keto acid dehydrogenase e1, alpha polypeptide	**7,74**	mitochondrion matrix	branched-chain amino acid catabolic process cellular nitrogen compound metabolic process glyoxylate metabolic process small molecule metabolic process
	Marc2	Molybdenum cofactor sulfurase c-terminal domain-containing protein 2	**3,31**	Peripheral + mitochondrion outer membrane peroxisome	detoxification of nitrogen compound nitrate metabolic process oxidation-reduction process vitamin metabolic process
	Steap 4	Metalloreductase STEAP 4	**4,37**	cell membrane golgi membrane	copper ion import ferric iron import into cell iron ion homeostasis fat cell differentiation
EXTRACELLULAR MATRIX	**Hspg2**	Heparan sulfate proteoglycan of basement membrane	**2,76**	basement membrane extracellular matrix secreted	angiogenesis extracellular matrix organization glycosaminoglycan metabolic process lipoprotein metabolic process cellular protein metabolic process carbohydrate metabolic process fat-soluble vitamin metabolic small molecule metabolic process
CYTOSKELETON	**Rdx**	Radixin	**3,43**	cell membrane cytoskeleton	positive regulation of cell migration actin filament capping microvillus assembly establishment of endothelial barrier negative regulation of adherens junction organization negative regulation of homotypic cell-cell adhesion apical protein localization positive regulation of cellular protein catabolic process positive regulation of early to late endosome transport positive regulation of G1/S transition of mitotic cell cycle positive regulation of gene expression negative regulation of cell size regulation of cell shape negative regulation of GTPase activity protein kinase A signaling

UP	Protein	Protein name	Ratio norm.	Cellular location	Biological Process
IMMUNE RESPONSE	**Ltf**	Lactotransferrin	**7,1**	secreted cytoplasmatic granule note: secreted into most exocrine fluids by various endothelial cells	antibacterial, antifungal humoral response regulation of cytokine production positive regulation of NF-κB transcription factor activity positive regulation of TLR 4 signaling pathway regulation of TNF production negative regulation of apoptotic process negative regulation of ATPase activity regulation of protein serine/threonine kinase activity cell redox homeostasis cellular protein metabolic process ion transport transcription, DNA-templated
	Psmc2	PROTEASOME 26S SUBUNIT, ATPpase, 2	**4,9**	cytoplasm nucleus	MHC I peptide antigen processing and presentation innate immune response viral process T cell receptor signaling pathway TNF-mediated signaling pathway NIK/NF-κB signaling EGFR, FGFR, VEGFR, Insulin receptor signaling pathway activation of MAPKK activity cellular nitrogen compound metabolic process polyamine metabolic process regulation of cellular amino acid metabolic process small molecule metabolic process DNA damage response, signal transduction by p53 class mediator resulting in cell cycle arrest G1/S transition of mitotic cell cycle gene expression negative regulation of apoptotic process regulation of mRNA stability protein polyubiquitination positive regulation of proteasomal protein catabolic process
INTRACELLULAR SIGNALING/ CELL MACHINERY	**Hspa1a**	Heat-shock 70-kd protein 1a	**3,04**	cytoplasm	ATP metabolic process cellular response to oxidative stress regulation of mRNA stability regulation of protein ubiquitination protein refolding, stabilization negative regulation of apoptosis positive regulation of gene expression positive regulation of endoribonuclease activity positive regulation of interleukin-8 production positive regulation of NF-κB transcription factor activity positive regulation of TNF-mediated signaling pathway
	CSDE1	Cold-shock domain-containing e1, RNA-binding	**5,86**	cytoplasm	regulation of transcription, DNA-templated nuclear-transcribed mRNA catabolic process, no-go decay
	FAM 208a	Family with sequence similarity 208, member a	**2,83**	nucleus chromosome	regulation of transcription, DNA-templated transcription, DNA-templated
	Gm5449	Small nuclear ribonucleoprotein D2 pseudogene	**6,46**	splicosom	spliceosomal snRNP assembl

UP	Protein	Protein name	Ratio norm.	Cellular location	Biological Process
ATP DEPENDANT PROCESS	**Atp1a1**	ATPase, Na+/K+ transporting, alpha-1 polypeptide	3,8	cell membrane	ATP hydrolysis coupled proton transport membrane hyperpolarization, repolarization transmembrane transport cellular potassium ion, sodium ion homeostasis negative regulation of glucocorticoid biosynthetic process cellular response to steroid hormone stimulus response to drug response to glycoside regulation of blood pressure
	Atp5i	ATP synthase, H+ transporting, mitochondrial fo complex, subunit e	**5,44**	mitochondrion inner membrane	cellular metabolic process mitochondrial ATP synthesis coupled proton transport respiratory electron transport chain small molecule metabolic process
OTHER	**Rdh7**	Retinol dehydrogenase 7	**3,15**	microsome ER	retinol metabolic process catalytic activity retinol dehydrogenase activity
	Mug1	Murinoglobulin	**2,84**	secreted	serine-type endopeptidase inhibitor activity

DOWN	Protein	Protein name	Fold down	Cellular location	Biological Process
ADHERENS JUNCTIONS	**Cadm3**	Cell adhesion molecule 3	**2,31**	cell membrane cell junction	adherens junction organization cell-cell junction organization cell recognition protein localization
	SCARB2	Scavenger Receptor Class B, Member 2	**4,59**	Cell membrane Lysosome membrane	cell adhesion protein targeting to lysosome
	Ostf1 (SH3P2)	Osteoclast-stimulating Factor 1	**2,75**	cytoplasm	cell adhesion contact signal transduction
BASAL MEMBRANE	**Lama5**	Laminin, Alpha-5	**5,62**	Extracellular matrix Basal membrane secreted	angiogenesis endothelial cell differentiation extracellular matrix organisation, disassembly focal adhesion assembly regulation of cell adhesion establishment of protein localization to plasma membrane cell recognition integrin-mediated signaling pathway cytoskeleton organization cell differentiation, migration, proliferation
GENE EXPRESSION/PROLIFERATION	**CREG1**	Protein Creg1	**3,05**	secreted	cell proliferation multicellular organismal development negative regulation of nucleic acid-templated transcription regulation of growth regulation of transcription from RNA polymerase II promoter regulation of apoptosis, inflammation and wound healing of vascular endothelial cells inhibit NF-κB activation, TNF-α-induced inflammatory responses and hyperpermeability of endothelial cells
	Ppm1f	Protein Phosphatase 1	**3,63**	Cytosol Perinuclear region of cytoplasm Protein complex	cellular response to drug histone dephosphorylation negative regulation of peptidyl-serine phosphorylation negative regulation of protein kinase activity by regulation of protein phosphorylation negative regulation of transcription, DNA-templated peptidyl-threonine dephosphorylation positive regulation of cell-substrate adhesion positive regulation of chemotaxis positive regulation of cysteine-type endopeptidase activity involved in apoptotic process positive regulation of epithelial cell migration positive regulation of focal adhesion assembly positive regulation of gene expression positive regulation of growth positive regulation of stress fiber assembly
PROTEIN TRANSPORT	**Cltb**	Clathrin, Light Polypeptide B	**2,38**	cell membrane	clathrin-mediated endocytosis intracellular protein transport
	Rab5c	RAS-associated protein 5c	**2,63**	Cell membrane Early endosome membrane	endosome organization plasma membrane to endosome transport protein transport regulation of endocytosis small GTPase mediated signal transduction
	Sar1a/b	GTP-binding protein 1a/b	**2,27**	ER Golgi	intracellular protein transport negative regulation of cargo loading into COPII-coated vesicle vesicle-mediated transport antigen processing and presentation of exogenous peptide antigen via MHC class II antigen processing and presentation of peptide antigen via MHC class I cellular protein metabolic process COPII vesicle coating membrane organization ER to Golgi vesicle-mediated transport post-translational protein modification small molecule metabolic process

DOWN	Protein	Protein name	Fold down	Cellular location	Biological Process
IMMUNE RESPONSE	**STAT1**	Signal Transducer And Activator Of Transcription 1	**2,59**	Cytoplasm nucleus	cellular response to interferon-beta, gamma, TNF cytokine-mediated signaling pathway defense response to virus lipopolysaccharide-mediated signaling pathway negative regulation of macrophage fusion cellular response to organic cyclic compound response to peptide hormone response to exogenous dsRNA JAK-STAT cascade negative regulation of I-kappaB kinase/NF-kappaB signaling response to cAMP negative regulation of angiogenesis negative regulation of endothelial cell proliferation blood circulation negative regulation of mesenchymal to epithelial transition involved in metanephros morphogenesis positive regulation of mesenchymal cell proliferation positive regulation of smooth muscle cell proliferation apoptotic process positive regulation of transcription, DNA-templated positive regulation of transcription from RNA polymerase II promoter
	Ctsh	Pro-cathepsin H Heavy Chain	**3,84**	lysosome	adaptive immune response immune response-regulating signaling pathway antigen processing and presentation T cell mediated cytotoxicity zymogen activation cellular response to thyroid hormone stimulus bradykinin catabolic process response to retinoic acid positive regulation of angiogenesis negative regulation of apoptotic process positive regulation of apoptotic signaling pathway positive regulation of cell migration, proliferation positive regulation of epithelial cell migration positive regulation of gene expression positive regulation of peptidase activity protein destabilization membrane protein proteolysis ERK1 and ERK2 cascade cellular protein metabolic process
	Psmd6	Proteasome 26S Subunit, ATPase, 6	**2,51**	Cytoplasm nucleus	antigen processing and presentation of peptide antigen via MHC class I innate immune response viral process T cell receptor signaling pathway tumor necrosis factor-mediated signaling pathway NIK/NF-kappaB signaling EGFR, FGFR, VEGFR, Insulin receptor signaling pathway activation of MAPKK activity cellular nitrogen compound metabolic process polyamine metabolic process regulation of cellular amino acid metabolic process small molecule metabolic process DNA damage response, signal transduction by p53 class mediator resulting in cell cycle arrest G1/S transition of mitotic cell cycle gene expression negative regulation of apoptotic process regulation of mRNA stability protein polyubiquitination positive regulation of proteasomal protein catabolic process

DOWN	Protein	Protein name	Fold down	Cellular location	Biological Process
RNA CELL MACHINERY	**Sub1**	Activated RNA Polymerase II Transcription Cofactor 4	**2,38**	nucleus	regulation of transcription from RNA polymerase II promoter SMAD protein signal transduction
	Sf3a1	Splicing Factor 3a, Subunit 1	**2,70**	nucleus	gene expression mRNA 3'-splice site recognition mRNA processing mRNA splicing, via spliceosome
	Rnaset2	Ribonuclease T2	**2,23**	Secreted Lysosome lumen ER lumen	RNA catabolic process RNA phosphodiester bond hydrolysis
METABOLIC PROCESS / TRANSLATION	**Eif5a**	Eukaryotic Translation Initiation Factor 5a	**2,50**	Cytoplasm Nucleus ER membrane	apoptotic process cellular protein metabolic process mRNA export from nucleus nucleocytoplasmic transport peptidyl-lysine modification to peptidyl-hypusine positive regulation of cell proliferation positive regulation of translational elongation, termination post-translational protein modification protein export from nucleus translational frameshifting
	Rplp1	Ribosomal Phosphoprotein, Acidic	**2,32**	Cytoplasm Cytosol Extracellular exosome Focal adhesion	cellular nitrogen compound metabolic process cellular protein metabolic process gene expression nuclear-transcribed mRNA catabolic process, nonsense-mediated decay translational initiation, elongation, termination selenocysteine metabolic process small molecule metabolic process SRP-dependent cotranslational protein targeting to membrane viral process, transcription, life circle
	Rpl17	Ribosomal Protein L17	**4,14**	Cytosol Nucleus Cytosolic large ribosomal subunit	cellular nitrogen compound metabolic process cellular protein metabolic process gene expression nuclear-transcribed mRNA catabolic process, nonsense-mediated decay selenium compound metabolic process small molecule metabolic process SRP-dependent cotranslational protein targeting to membrane translational elongation, initiation, termination viral life cycle, process, transcription

DOWN	Protein	Protein name	Fold down	Cellular location	Biological Process
METABOLIC PROCESS	**Fuca1**	Fucosidase, Alpha-l, Tissue	**2,24**	lysosome	cellular protein metabolic process fucose metabolic process glycosaminoglycan catabolic process glycoside catabolic process
	Nagk	N-acetylglucosamine Kinase	**3,11**	Extracellular exosome	carbohydrate phosphorylation N-acetylglucosamine metabolic process N-acetylmannosamine metabolic process N-acetylneuraminate catabolic process
	Pafah1b 1	Platelet-activating Factor Acetylhydrolase, Isoform 1b, α Subunit	**2,79**	Cytoplasm Nucleus membrane	platelet activating factor metabolic process lipid catabolic process positive regulation of cytokine-mediated signaling pathway actin cytoskeleton organization microtubule cytoskeleton organization organelle organization vesicle transport along microtubule regulation of microtubule cytoskeleton organization regulation of microtubule motor activity brain morphogenesis cerebral cortex,hippocampus development neuroblast proliferation positive regulation of embryonic development stem cell division positive regulation of mitotic cell cycle establishment of mitotic spindle orientation G2/M transition of mitotic cell cycle nuclear migration negative regulation of JNK cascade protein secretion regulation of GTPase activity
CYTOSKELETON	**MYO6**	Unconventional Myosin VI	**2,57**	Golgi Nucleus Cytoplasm Membrane (clatherin-coated pits)	actin filament-based movement intracellular protein transport endocytosis membrane organization protein targeting glutamate secretion, regulation of secretion cellular response to electrical stimulus DNA damage response, signal transduction by p53 class mediator positive regulation of transcription from RNA polymerase II promoter auditory receptor cell differentiation inner ear morphogenesis dendrite development regulation of synaptic plasticity synapse assembly synaptic transmission
CALCIUM HOMEOSTASIS	**Tpt1**	Tumor Protein, Translationally-controlled 1	**2,40**	cytoplasm	calcium ion transport cellular calcium ion homeostasis negative regulation of apoptotic process response to virus
	Rmdn3	Regulator of microtubule dynamics 3	**3,23**	Mitochondrial membrane Nucleus cytoplasm	apoptotic process cell differentiation cellular calcium ion homeostasis interaction with microtubules

6. Discussion

6.1 The limitations of mouse models of allo-HSCT and GVHD

In the last decades, most of our understanding of acute GVHD has developed from experimental models, in particular mouse models. Appropriate preclinical models of allo-HSCT provide the unique opportunity to study mechanistic pathways in detail, simplify complex systems, image pathological events more facile than in humans, perform genetic modifications and screen for suitable therapeutic interventions.[72,85,102,154] However, there is an ongoing debate if genomic responses in mice fully mimic human inflammatory diseases[155,156] questing the rightfully use as translational models; and predicting effectiveness of treatment strategies is hampered if critical disparities between experimental and clinical features of the disease exist.[157] Indeed, there are many limitations to current preclinical models of allo-HSCT and not all findings may be directly extrapolated into clinical applications;[154] emphasized by several GVHD studies in which findings from mouse models failed to correlate with the clinical scenario: e.g. keratinocyte growth factor (KGF) ameliorated murine GVHD and inhibited the rejection of pan-T-cell-depleted donor bone marrow allografts,[158] whereas in a subsequent randomized, placebo-controlled clinical trial palifermin, a recombinant human KGF, had no significant effect on engraftment, acute GVHD and survival in allo-HSCT patients.[159,160] In another example, animal models supported the notion that inhibiting IL-1 may ameliorate or prevent GVHD,[161] however a double-blind, placebo-controlled randomized trial of recombinant human IL-1 receptor antagonist (IL-1Ra) showed no improvement of survival or reduction of GVHD and conditioning-related toxicity in allo-HSCT patients.[162] Therefore, it is from utmost importance to select a preclinical GVHD model that recapitulates the complex clinical scenario as close as possible.

Our established GVHD model overcomes some of the major limitations of the most currently used mouse models. Many mouse models of GVHD involve mismatches in MHC antigens, which is in contrast to human allo-HSCT.[72] On the account that the incidence of acute GVHD is directly related to the degree of HLA-mismatch,[70] HLA-identical or HLA-matched transplantations are mainly performed; made possible by detailed HLA typing of the major transplantation antigens HLA-A, HLA-B, HLA-C, HLA-DR and HLA-DQ. However, GVHD still develops in these recipients due to genetic differences laying outside the MHC loci and encoding for miHAs.[70,80] Our MHC-matched strain combination (LP/J→C57BL/6) mimics the most prevalent form of donor selection, as the development of GVHD in this models also relies on miHAs.

The second advantage of our established model includes the use of busulfan and cyclophosphamide as conditioning regimen, which are commonly used for clinical conditioning.[42] Conditioning regimens vary in their intensity and toxicity so that before allo-

HSCT, the appropriate conditioning is chosen depending on the patient´s age and disease-related factors.[163] In contrast, the majority of used GVHD murine models only includes myeloablative TBI in large fraction doses and high dose rates.[85] Although the administration of TBI is faster and easier compared to chemotherapy, we achieved the same main advantages of established TBI-based mouse model: sustained engraftment with full donor chimerism and reliable GVHD. Of note, by using busulfan and cyclophosphamide we do not only mimic the most common clinical conditioning protocol, we also overcome the known fact that mice are more radio-resistant (and therefore needing higher TBI doses) than humans.[154] Radiosensitivity also varies greatly across different mouse strains due to strain-specific alterations in DNA repair mechanisms mending ionizing radiation-related DNA damage.[154] As conditioning results in tissue damage, release of pro-inflammatory mediators and stimulation of APCs,[164] it influences the development of GVHD. Therefore differing conditioning regimens between mice and humans can lead to disparate GVHD phenotypes.[72]

Third, our model mimics the clinical pattern and timing of GVHD, and both acute and chronic GVHD arise. Established GVHD mouse models are used to investigate either acute or chronic GVHD individually,[72,154] although chronic GVHD in patients often progress from acute GVHD-related inflammatory responses leading to characteristic tissue pathology mainly characterized by severe target organ fibrosis.[165] GVHD development in humans relies on both CD4+ and CD8+ T cell interactions, whereas common mouse models are either CD4+ or CD8+ T cell-mediated, depending on the MHC disparities.[72] We could show in our model that both T cell subsets are involved in the development of GVHD. Additionally, our model lacks the hyper acute disease pattern in the first 7-10 days after allo-HSCT, which is characteristic for the most common used mouse models[48,100,101] but not seen in most patients as the majority undergo immunosuppression and GVHD prophylaxis. Instead, we found a constant progression to acute GVHD, which resembles the clinical setting of HLA-matched allo-HSCT with GVHD prophylaxis. However, one significant contrast to the clinical practice remains, as mice did not receive immunosuppressive regimens such as tacrolimus, CSA, MMF[94,95] or steroids,[99] which are used in patients to control GVHD. Immunosuppression after allo-HSCT is rarely performed in mouse models, primary to allow analysis of GVHD development at a single-variable level in a controlled and reproducible manner. However it harbours the risk that immunological mechanisms in GVHD progression and tumor growth/ relapse after allo-HSCT differ in mice compared to patients, as mice show faster immune recovery and enhanced anti-pathogen capabilities.[154]

Although, our model overcomes some major limitations, there are still some caveats of murine GVHD models that have to be considered. In human allo-HSCT, donor cells derive from the bone marrow or the peripheral blood (number, origin and type of circulating immune cells can differ depending on the mobilization reagent).[1] In mouse experiments, donor bone marrow

cells are supplemented with T cells isolated from the lymph nodes or spleen to induce GVHD. As T cells are originated from different sources, they might have different homing capacities and composition affecting the GVHD phenotype.[72,85,154]

GVHD mouse models mainly use healthy, lean and young mice (typically 8 to 14 weeks old, having a 2-year life span) being equivalent to healthy early-adolescent humans.[72] However, the majority of allo-HSCTs is performed in adult or elderly humans, and patient populations show high diversity in age and health status including body mass index and co-morbidities.[154] Recipient age was shown to influence immune reconstitution after allo-HSCT and being a risk factor for the incidence of acute GVHD in mice[166] and humans.[167] These observations could be related to alterations in immunological and physiological mechanisms with increasing age, including increased immune senescence, impaired tissue repair, altered APC capacity, and impaired thymopoiesis and peripheral T cell recovery.[168,169] Epidemiological studies revealed that obesity in patients is associated to a higher incidence of developing acute and chronic GVHD.[170] Additionally, as allo-HSCT often represents the last hope for patients with hematological malignancies, most of the patients already received chemotherapy or other anti-tumor agents to initially treat the malignancy.[171-173] The indications for allo-HSCT are various,[1,42] which increases the range of possible malignancies and their corresponding pretreatments. This variety is hard to mimic in an experimental mouse model.

Although the mouse model can mimic MHC-matched allo-HSCT, genetic differences between murine and human species will remain as inbred mice exhibit a homozygous MHC haplotype whereas “outbred” humans show a heterozygous HLA haplotype.[45] This leads to a higher diversity of MHC alleles (see Table 2, Chapter 4.1.3) increasing possible disparities between the donor and recipient. Therefore, humans may have “different degrees” of HLA-identical transplantation compared to mice.[154] Outbred large animal GVHD models, the canine and primate model, can overcome or diminish these genetic differences as their MHC loci closely resemble that of humans with also exhibiting the high MHC allele diversity. However these models show significant performance limitations including smaller sample size, longer duration of experiments and follow-up, limited reagents and very high costs.[154]

The gastrointestinal tract microbiota can influence the severity and kinetics of GVHD,[85,154] as it can modify the intestinal barrier damage during conditioning and later the target organ damage during the effector phase.[70,164] Manipulations of the microbiome were found to have dramatic impact on the severity of GVHD in mice and humans.[174] However, as the mice used for experimental allo-HCST are kept under specific pathogen-free (SPF) conditions, they exhibit an over-simplified microbiome differing from that of humans, which are exposed to various immunological challenges and microorganisms throughout life. Additionally, whereas mice are housed under constant living conditions, humans develop a greater diversity in their commensal flora due to dynamic environmental influences including lifestyle, age, obesity and

disease status.[154] Observations show that strict SPF conditions to achieve more “clean” mouse colonies have indeed adverse effects on experimental GVHD and reproducibility.[154] This may be overcome by co-housing inbred mice with free-living feral mice and pet store mice. These mice showed immune systems which closer resembled human ones, as blood cell gene expression shifted to patterns that more closely reflect human immune signatures.[175] However, this co-housing harbours significant challenges in the organization of experimental animal facilities.

Despite limitations, GVHD mouse models offer a valuable tool to study the complex scenario of allo-HSCT and GVHD in a controlled, reproducible and simplified environment.[154] Our established mouse model represents a good option to study clinically relevant features of allo-HSCT, as it has overcome some major limitations of commonly used models. However, it still remains a “tool”, as before described caveats must be taken into account when translating experimental results into the clinical setting.

6.2 Transfer of experimental results concerning initial angiogenesis into the clinical setting of GVHD

Our experimental data, showing that angiogenesis is an initial event during GVHD, was mainly obtained in the established MHC-matched, chemotherapy-based LP/J→C57BL/6 model, to achieve maximum similarity to the clinical setting. However, as our model does not claim to be the only valid model and to increase the experimental significance, e.g. by increasing the MHC and minor antigens spectrum seen in human transplantations, we confirmed our results in additional chemotherapy-based GVHD mouse models: another MHC-matched one (129S2/SvPasCrl→C57BL/6) with a different inbred donor and influenced by other miHAs; and the C57BL/6→B6D2F1 model, relying on parent-to-F1 transplantation. As pointed out in chapter 6.1, the used GVHD mouse models overcome some major limitations and resemble the clinical pattern of GVHD, but still differences between mice and humans have to be considered when interpreting our preclinical results. Therefore, for translating experimental results, human data on angiogenesis preceding leukocyte infiltration after allo-HSCT would be preferable.

Important clinical evidence on the role of angiogenesis during established human GVHD has been published already. Findings from preclinical models, demonstrating that GVHD is associated to the formation of new blood vessels,[127,151] were confirmed in humans.[152,153] Furthermore, there is accumulating evidence on the significance of endothelial factors, such as Angiopoietin 2,[176] Thrombomodulin[136,138] and the endothelial activation and stress index, EASIX[177] for the clinical course of GVHD.

Clinical evidence on the role of angiogenesis in initial GVHD has to be established by presenting data on target organ histology from human allo-HSCT recipients before clinical GVHD onset, being comparable to our experimental results. However, this approach is very challenging as the performance of organ biopsies during the early post-transplant period in absence of clinical GVHD signs is no standard procedure. Given the absence of any direct use for the individual patient as well as the relatively high complication risk, including infections (because of immunosuppression and that biopsies cannot be performed on the stem cell ward) and bleeding risk (due to thrombocytopenia),[178] a prospective clinical study to generate these data is ethically very challenging. There is currently no access to a sufficient number of GVHD target organ biopsies at day+2 or any other early time points with still absent immune cell infiltration or GVHD symptoms, as GVHD target organ biopsies are mostly performed for diagnosis or exclusion of GVHD when clinical symptoms are present,[80] which is typically later than day+10 after allo-HSCT. Analyses of human biopsies at later time points during established GVHD, which are present in transplantation centres, will be of no value to confirm our preclinical data and will lead to false interpretations. This is demonstrated by our finding of different patterns of endothelial cell activation (**Figure 3**, **Supplemental Figure 10, Article II**) and different endothelial gene expression early after allo-HSCT (d+2) vs. established GVHD (d+15) (**Appendix Figure 21**). We performed microarray analyses of liver endothelial cells at d+2 and d+15 and found significant different expression profiles between these two time points. 4073 genes were differentially expressed, with 3644 genes upregulated and 429 genes downregulated showing changes in various, important endothelial pathways: i.a. regulation of actin cytoskeleton, glycolysis and gluconeogenesis, fatty acid β-oxidation (FAO), adhesion-PI3K-AKT-mTOR-signaling, mitogen-activated protein kinase (MAPK) signaling, epidermal growth factor receptor 1 (EGFR1) signaling, complement and coagulation cascades and matrix metalloproteinases. This observation goes in line with publications showing differing kinetics of gene expression over the time course of GVHD.[179,180]

To achieve the long-term aim of the translational development of GVHD therapies aiming at angiogenesis, our preclinical findings need to be correlated to the clinical setting. However, as prospective clinical studies on early angiogenesis and its mechanisms harbour significant hindrances, due to ethical considerations of performing biopsies in asymptomatic patients with high bleeding and infection risk, further preclinical research is needed to better determine mechanisms and optimal molecular targets. This includes elucidating connections between allo-HSCT and angiogenesis in target organs by e.g. soluble factors (see chapter 6.3); and performing functional analyses of pathways of possible targets identified with proteome and gene array analyses in article II (see chapter 6.4-6.6), prior to the transfer to the human setting.

6.3 Connection between allo-HSCT and initial target organ angiogenesis by cellular and soluble factors

In murine GVHD models, we detected early increased EC proliferation specifically after allo-HSCT[181] and analysing how angiogenesis can be initiated rapidly and specifically in allo-HSCT would further dissect functional mechanisms.

We showed that prior to angiogenesis no infiltrated leukocytes were present in the particular target organs[181] which disqualify them to be the angiogenic initiators in this context. However, with this analysis approach we cannot fully exclude that circulating immune cells may activate endothelial cells; either by reciprocal binding and activation of leukocyte adhesion molecules to their ligands on ECs;[126] or by endothelial activation through released cytokines and chemokines.[104,121,124] Though, these reactions seem to be unlikely as we could show that adhesion molecules on ECs during early GVHD at d+2 were indeed downregulated in allogeneic transplanted mice (**Figure 3, Article II**). Downregulation of adhesion molecules was confirmed in our microarray analyses in ECs at day+2, showing a significant downregulation of *Icam-1* and a tendency for *Vcam-1* and *E-Selectin* (**Appendix Table 8**). Released cytokines and chemokines can bind to their corresponding receptors and initiate type II endothelial activation (**Figure 16**). Prototypic mediators of type II activation are TNFα and IL-1, which are released by activated leukocytes.[125] However, our microarray data from ECs at d+2 does not show upregulated expression of genes involved in type II activation (**Appendix Table 8**) in allogeneic compared to syngeneic transplanted mice. Most of the involved genes showed no significant change, and gene expression of *Myd88*, involved in the intracellular signaling complex of IL-1R1, and *Tnfr1* was even decreased. Gene expression of *Nfκb*, one of the main transcription factors regulating intracellular responses in inflammatory-associated endothelial activation and angiogenesis, was also not significantly changed in GVHD mice at d+2. Although these observations are not an entire proof, they point in the direction, that circulating leukocytes and their released mediators are also not initial activators of angiogenesis in GVHD target organs.

The innate immune system is activated in the first phase of GVHD pathogenesis (see chapter 4.2.1) as conditioning-damaged tissues release inflammatory mediators, which are recognized by pathogen recognition receptors on host innate immune cells leading to increased expression of adhesion, antigen-presenting (MHC) and co-stimulatory molecules.[70] Main pro-inflammatory mediators including i.a. TNF-α, IL-1 or IL-6 are known to exhibit proangiogenic capacities.[121] However, considering that we did not find increased angiogenesis in only chemotherapy-treated mice and syngeneic transplanted mice, which also were conditioned before transplantation, makes it less likely that factors of the innate immune response are responsible for the allogeneic-specific increase in EC proliferation. Additionally, although we

found the in literature well-established cytokine dysregulation during acute GVHD[164,182-184] in our mouse model, we could not detect an early increase of the main pro-inflammatory cytokines TNF-α, IL-6 and IFN-γ in GVHD mice (**Figure 4c, Article I**). Serum cytokine levels of TNF-α and IFN-γ increased in allogeneic transplanted mice, but temporally after initial angiogenesis and associated with the beginning of immune cell target organ infiltration at day+8. Although IL-6 levels increased due to chemotherapy conditioning, no significant serum levels were detected between allogeneic compared to syngeneic transplanted mice; suggesting that these cytokines may not play a major role in initial angiogenesis exclusively arising in allo-HSCT. The rather late increase of these cytokines at the onset of acute GVHD characteristic infiltration in our mouse model correlates with clinical data showing that 1) TNF-α levels in conditioned patients did not raise until later after allo-HSCT,[185-189] 2) IL-6 levels in patients increased shortly after HSCT and later in both GVHD and non-GVHD bearing patients,[186-188,190] and 3) IFN-γ levels were increased in already GVHD symptoms bearing patients.[191-193] In mouse models as well as in clinical allo-HSCT, the role of cytokines as regulators or inducers of GVHD severity depends on the degree of HLA-mismatch, the intensity of conditioning and different T cell subsets involved after transplantation,[102] explaining the temporal differences in the cytokine profile of MHC-mismatched mouse models, where cytokine serum levels increase strongly and early after transplantation.[164,183] In severe combined immunodeficiency (SCID) mice[161] as well as in patients,[194] TBI resulted in a prominent release of TNF-α, whereas busulfan conditioning did not increase TNF-α levels shortly after HSCT. In SCID mice, a MHC-mismatched transplantation resulted in a stronger release of cytokines, just as TBI was followed by increased cytokine levels compared to non-TBI. Busulfan/ cyclophosphamide treated SCID mice showed the lowest cytokine levels.[161]

As we could not elaborate a strong rationale that soluble mediators from either adaptive or innate immune responses have significant impact on initial angiogenesis emerging specifically after allo-HSCT, the transplanted HSCs themselves may connect allogeneic transplantation to target organ specific angiogenesis and subsequent immune cell infiltration. That angiogenesis may be connected with the bone marrow,[195] its microenvironment[196] and bone marrow (BM)-derived angiogenic soluble factors[197] was identified in cancer and other diseases. A rapid mobilization of BM-derived angiogenic soluble factors was shown in multiple myeloma and other hematological malignancies;[198-200] and increase of soluble adrenomedulin, sVCAM-1 and C-reactive protein was observed already 24 hours after BM mononuclear cell implantation.[201] Moreover, the endothelium may play an important role in regulating angiogenic mechanisms for blood vessel formation by itself. We showed that during early angiogenesis no BM-derived EPCs were detected, and recently, Patel et al.[202] published the existence of a vascular resident endothelial progenitor cell showing that the endothelium may regulate self-renewal and differentiation also in a BM-independent manner.

However, if soluble BM-dependent or BM-independent mediators are present in the periphery after allo-HSCT and could mediate angiogenesis in target organs remains to be elucidated experimentally. The main advantage of analysing soluble factors is the easy accessibility not only in GVHD mouse models, but also in GVHD patients. Small volumes of serum or plasma are needed for analysis and can be obtained also from asymptomatic patients with high bleeding and infection risk early after allo-HSCT, avoiding the ethically challenging performance of biopsies.

6.4 Pathway analysis of identified targets in initial angiogenesis during GVHD

To identify pathways and new targets during initial angiogenesis in GVHD, we performed microarray and proteome analyses in ECs during early GVHD (day+2). The most striking genes and proteins, being differentially expressed between allogeneic and syngeneic transplanted mice, were involved in metabolic and angiogenic pathways, the cytoskeleton, immune response, ATP-dependent pathways and RNA/DNA cell machinery (**Figure 4 and 5, Article II**). These changes in ECs had functional consequences, showed by significantly higher deformation of liver ECs from GVHD mice at d+2, measured by Real-Time deformability cytometry (**Figure 6, Article II**).

To observe connections between identified targets, I analyzed our microarray and proteome data with the Reactome Pathway Database,[203] revealing that the majority of identified targets obviously clustered in metabolic pathways. Indeed, there is growing evidence that the endothelial metabolism plays an essential role in angiogenesis, as angiogenic ECs enhance glycolysis which promotes tip cell migration, whereas FAO regulates stalk cell proliferation.[204-209] To gain a deeper understanding of the involved metabolic pathways, the identified metabolic genes were analyzed with the KEGG Pathway[210] and WikiPathways[211] databases. These target genes encode for enzymes that are involved in metabolic processes, which are responsible for 1) ATP energy production and *de novo* nucleotide biosynthesis for DNA replication representing the molecular basis for cell proliferation and migration (namely glycolysis, FAO and the pentose phosphate pathway (PPP)); and for 2) the availability and activity of proteins, e.g. receptor molecules, modified by N- and O-linked glycosylation (namely hexosamine biosynthesis pathway (HBP)). These metabolic pathways are connected and exhibit intersections. **Figure 19** shows the schematic overview of these pathways, including the identified target genes with their position and function in the particular pathway.

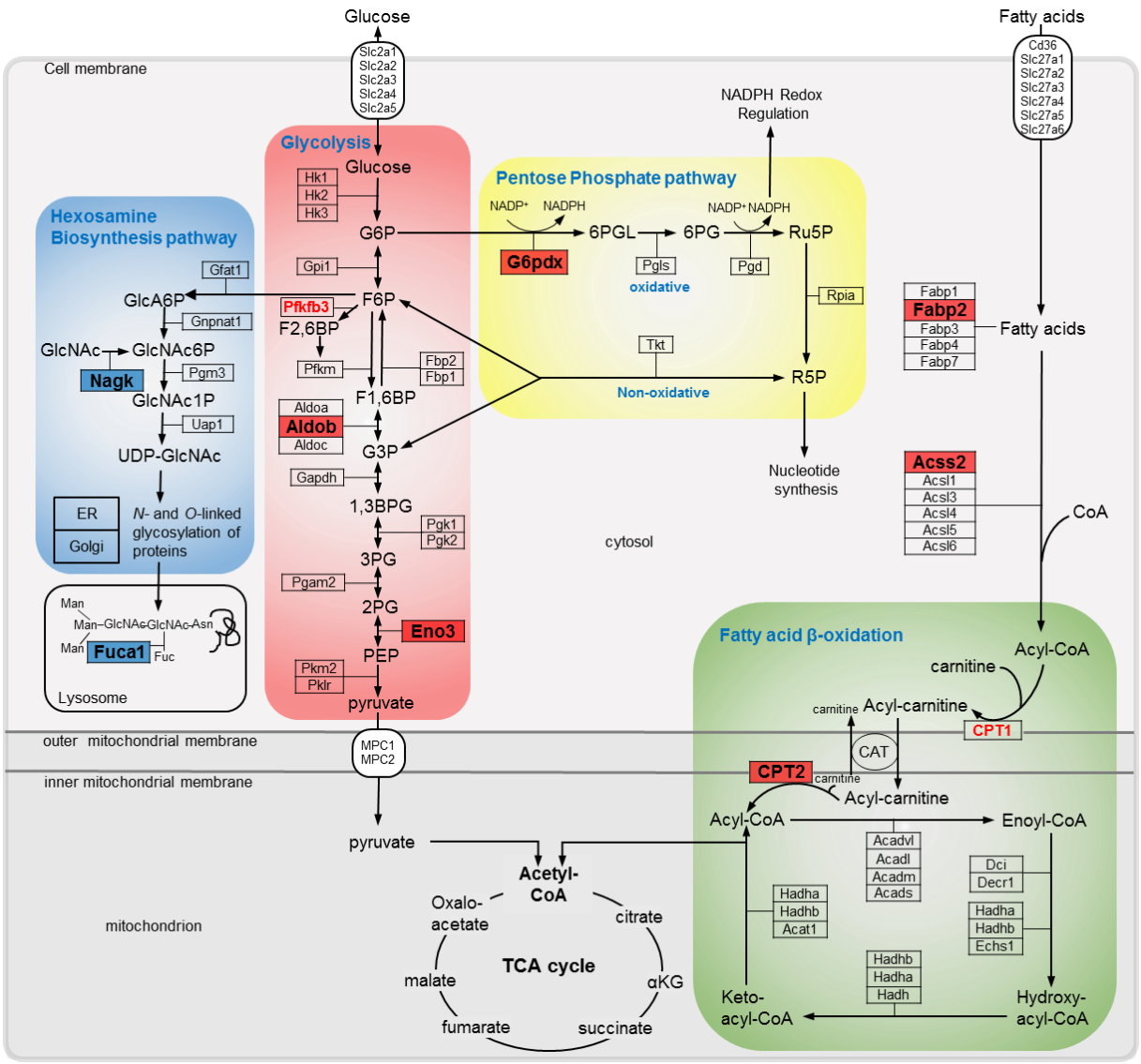

Figure 19: Identified up- and downregulated genes and proteins involved in metabolic pathways. (upregulated (red boxes): G6pdx, Alodb, Eno3, Fabp2, Acss2, CPT2; downregulated (blue boxes): Nagk, Fuca1). Schematic and simplified pathways, not all metabolites and enzymes are shown. Genes encoding for involved enzymes are framed. Scheme data relies on KEGG Pathway Database and WikiPathways. Pfkfb3 and CPT1 (red writing) are already described in EC metabolism and angiogenesis. **Hexosamine biosynthesis pathway:** Gfat1, glutamine fructose-6-phosphate aminotransferase. GlcA6P, glucosamine-6-phosphate. Gnpnat1, glucosamine-phosphate N-acetyltransferase 1. GlcNAc6P: N-acetyl-D-glucosamine-6-phosphate. GlcNAc, N-acetylglucosamin. Nagk, N-acetylglucosamine kinase. Pgm3, phosphoglucomutase 3. GlcNac1P, N-acetyl-D-glucosamine 1-phosphate. Uap1, UDP-N-acetylglucosamine pyrophosphorylase 1. UDP-GlcNAc, uridine diphosphate N-acetylglucosamine. ER, endoplasmic reticulum. Man, mannose. Fuc, fucose, Asn, asparagine. Fuca1, tissue alpha-L-fucosidase. **Glycolysis:** Hk, hexokinase. G6P, glucose-6-phosphate. Gpi1, glucose-6-phosphate isomerase. F6P, fructose-6-phosphate. Pfkfb3, 6-Phosphofructo-2-Kinase/Fructose-2,6-Biphosphatase 3. F2,6BP, fructose-2,6-bisphosphate. Pfkm, phosphofructokinase. Fbp, fructose-bisphosphatase 1. F1,6BP, fructose-1,6-bisphospate. Aldo, fructose-bisphosphate aldolase. G3P, glyceraldehyde-3-phosphate. Gapdh, glycerinaldehyd-3-phosphat-dehydrogenase. 1,3BPG, 1,3-bisphosphoglycerat. Pgk, phosphoglyceratkinase. 3PG, 3-phosphoglycerate. Pgam2, phosphoglycerate mutase 2. 2PG, 2-phosphoglycerate. Eno3, enolase 3. PEP, 2-phosphoenolpyruvate. Pkm2, pyruvate kinase M2. Pklr, pyruvate kinase, liver and RBC (red blood cells). **Pentose Phosphate Pathway:** G6pdx, glucose-6-phosphate dehydrogenase. NADP+/NADPH, nicotinamide adenine dinucleotide phosphate. 6PGL, 6-phosphonoglucono-delta-lactone. Pgls, 6-phosphogluconolactonase. 6PG, 6-phosphogluconate. Pgd, 6-phosphogluconate dehydrogenase. Ru5P, ribulose-5-phosphate. Rpia, ribose-5-phosphate isomerase a. R5P, ribose-5-phosphate. Tkt, transketolase. **Fatty acid β-oxidation:** Fabp, fatty-acid-binding protein. Acss2, Acyl-coenzyme A synthetase short-chain family member 2. Acsl, long-chain-fatty-acid-CoA ligase. CoA, coenzyme A. CPT, carnitine palmitoyltransferase. CAT: carnitine translocase. Acad, (very long (vl), long (l), medium (m), short (s) chain-specific) acyl-CoA dehydrogenase. Dci, enoyl-CoA delta isomerase 1. Decr1, 2,4-dienoyl-CoA reductase. Hadh, 3-hydroxyacyl-CoA dehydrogenase. Echs 1, enoyl-CoA hydratase. Acat1, sterol O-acyltransferase 1. **TCA (tricarboxylic acid) cycle:** αKG, alpha-ketoglutarate. Transporter: slc, solute carrier family. CD36, platelet glycoprotein 4. MPC, mitochondrial pyruvate carrier.

The genes *Aldob* and *Eno3* were found to be upregulated in ECs of allogeneic transplanted mice at d+2. They encode for the enzymes fructose-bisphosphate aldolase B, which catalyzes the reversible cleavage of fructose 1,6-bisphosphate (F1,6BP) into glyceraldehyde 3-phosphate (G3P), and enolase 3, which catalyzes the reversible conversion of 2-phosphoglycerate (2PG) into phosphoenolpyruvate (PEP) (**Figure 19**).[210,211] Both enzymes play essential roles in glycolysis and gene upregulation suggests an increase in glycolysis in angiogenic ECs of allogeneic transplanted mice. Although there is a direct access to oxygen in the blood, it was shown that ECs rely in their energy supply on anaerobic glycolysis generating up to 85 % of their ATP.[207] Even though the efficiency of glycolysis generating ATP molecules from glucose molecules is lower compared to oxidative glucose metabolism (2 vs. 34 ATP molecules per 1 molecule glucose), glycolysis is an advantageous mechanism for EC sprouting, as it allows activity also in avascular anoxic tissues; and it generates more ATP molecules in a shorter time than oxidative glucose metabolism. This fast energy supply enables ECs to quickly adopt a migratory phenotype and rapidly form new vessels.[209] Glycolytic enzymes were found to be concentrated in the lamellipodia and filopodia of tip cells, where they co-localized with actin filaments enabling a rapid change of the cytoskeleton and therefore migration.[212] Accordingly, we identified upregulated cytoskeletal genes and proteins in our gene and proteome analyses and showed a migratory phenotype of ECs from allogeneic transplanted mice (**Figure 4-6, Article II**). Upon induction of angiogenesis, e.g. by growth factors, quiescent ECs increase glycolysis and migrate and proliferate;[207] upon establishment of newly found vessels, ECs seem to downregulate glycolysis again.[209] It was shown in *in vitro* experiments, that non-proliferating, contact inhibited ECs (resembling quiescent ECs) exhibit a lower glycolytic activity than proliferating ECs;[204] and that laminar stress mimicking blood flow decreases glucose uptake and glycolysis.[213] Mechanistic insights revealed that targeting glycolysis by inactivating the *Pfkfb3* gene in ECs leads to impaired vessel sprouting, reduced EC motility and migration.[207] *Pfkfb3* encodes the enzyme 6-Phosphofructo-2-Kinase/Fructose-2,6-Biphosphatase (PFKFB3) converting fructose-6-phosphate (F6P) into fructose-2,6-bisphosphate (F2,6BP), a potent allosteric activator of 6-phosphofructokinase-1 (PFK-1), a rate-limiting enzyme of glycolysis (**Figure 19**). Overexpression of *Pfkfb3* on the other hand promoted a tip cell phenotype.[207] Interestingly, under- or overexpression of *Pfkfb3* and therefore increased or decreased glycolysis did not affect the expression of angiogenic sprout-governing genes, as e.g. *Vegfa*, *Vegfr2*, *Ang2*, *Dll4* or *Notch1*, implicating that glycolysis alone was sufficient to promote vessel sprouting.[207,209] This observation may also explain our findings, that metabolic genes were upregulated in proliferating ECs in allogeneic transplanted mice at d+2, whereas classical angiogenic genes remained unchanged or even decreased (**Appendix Table 9**).

The impact of glucose metabolism can be immense as intermediates from glycolysis are shifted in other metabolic side pathways. Glucose-6-phosphate (G6P) enters the oxidative branch of the PPP (**Figure 19**) and gets converted into 6-phosphonoglucono-delta-lactone (6PGL), catalyzed by the rate limiting oxidative PPP enzyme glucose-6-phosphate dehydrogenase (G6PDX).[210,211] In our proteome analysis data, we found G6PDX upregulated, implicating that the PPP is increased in ECs of allogeneic transplanted mice at d+2. The PPP produces ribose-5-phosphate (R5P) necessary for nucleotide synthesis and therefore for proliferative cell activity;[214] and nicotinamide adenine dinucleotide phosphate (NADPH) used for reductive lipid biosynthesis, NO production and conversion of oxidized glutathione to its reduced form (GSH), an effective antioxidant protecting ECs from oxidative stress.[208,209] Mechanistically, PPP was found to have an impact on angiogenesis, as inhibition of G6PDX and transketolase (TKT), an enzyme of the non-oxidative PPP branch, led to reduced EC migration and viability.[215]

Another glycolytic intermediate, F6P, can be shunted into the HBP (**Figure 19**) and converted over glucosamine-6-phosphate (GlcA6P), N-acetyl-D-glucosamine-6 and 1-phosphate (GlcNAc6P, GlcNAc1P) to uridine diphosphate N-acetylglucosamine (UDP-GlcNAc). The GlcNAc group of UDP-GlcNAc is needed for the O- and N-linked glycosylation of proteins in the endoplasmic reticulum or golgi apparatus. These posttranslational protein modifications determine protein function, localization, activity and availability and are essential e.g. for receptor signaling cascades.[216,217] In our microarray data, we found that the gene encoding for the N-acetylglucosamine kinase (NAGK) was downregulated in allogeneic ECs. NAGK converts GlcNac into GlcNAc6P and can therefore further promote the HBP. As proliferating ECs during early GVHD showed reduced gene levels of *Nagk*, it could be speculated that the HBP is also reduced, however this is highly hypothetically and data about the effects of HBP in angiogenesis is fragmentary and contextual.[209] There is evidence that overactive HPB promotes O-linked glycosylation of proteins involved in angiogenesis, which leads to decreased vessel sprouting and defects in EC migration.[218] N-glycosylation on the other hand was shown to enhance the functionality of Notch and VEGFR2[219] and increased protein glycosylation was involved in diabetes-induced dysfunction of ECs.[220] Additionally, we found downregulated gene expression of *Fuca1* encoding for the lysosomal enzyme α-L-fucosidase, which removes terminal L-fucose residues attached to GlcNAc in glycosylated proteins (**Figure 19**).[221] Various signaling molecules are fucosylated, e.g. EGFR, transforming growth factor-β1 receptors, E-cadherin and integrins, which regulate their function. Lack of FUCA1 activity causes accumulating fucosyl-glycoproteins which may impair signaling cascades.[222] Enhanced protein fucosylation was already associated to tumor development, e.g. in breast and colorectal cancer, implicating a role in pathological events.[223,224]

We also found allogeneic EC-specific upregulation of fatty-acid-binding protein 2 (*Fabp2*), acyl-coenzyme A synthetase short-chain family member 2 (*Acss2*) and carnitine palmitoyltransferase 2 (CPT2), which are involved in FAO (**Figure 19**), where fatty acids are broken down to generate energy through ATP production by the electron transport chain (ETC). Additionally, fatty-acid derived carbons are incorporated into precursors of nucleotides. Fatty acids enter the cells by fatty acid protein transporters and are distributed by the trafficking proteins FABP including FABP2. An acyl-Coenzyme A (CoA) group is added to fatty acids by the fatty acyl-CoA synthase enzyme complex including ACSS2 leading to long-chain acyl-CoA, which is further converted to acylcarnitine by CPT1. This allows the fatty acid moiety to cross the mitochondrial membrane as acylcarnitine is exchanged through carnitine via the carnitine translocase (CAT). At the inner mitochondrial membrane CPT2 converts acylcarnitine back to long-chain acyl-CoA, which enters the mitochondrial FAO pathway producing one molecule acetyl-CoA. Acetyl-CoA enters the tricarboxylic acid (TCA) cycle; and nicotinamide adenine dinucleotide (NADH) and flavin adenine dinucleotide (FADH2) produced by both FAO and the TCA cycle are used by the ETC chain to produce ATP.[225] Our data suggests that increased FAO is involved in angiogenesis, which was indeed demonstrated recently.[205,206] E.g. FABP4 was found to be increased upon VEGF activation and to be important for EC proliferation.[226] Endothelial loss of CPT1 resulted in impaired sprouting in *in vitro* and *in vivo* models, hyperpermeability of EC monolayers and increased endothelial leakiness.[205,206,227] Mechanistic studies revealed that inhibition of CPT1 and FAO resulted in the reduction of EC proliferation, but not of EC migration as filopodia numbers, vessel maturation and regression remained unchanged. ATP production was found to be important for a migratory phenotype, however fatty acids seem to be dispensable for ATP and NADPH production as CPT1 silencing (and therefore reduction of FAO) did not cause energy depletion or disturb redox homeostasis. However, the cellular pool of aspartate and glutamate, which contain fatty acid-derived carbons and represent essential precursors for nucleotide synthesis, was diminished. Therefore inhibition of FAO impaired de novo synthesis of deoxynucleotide triphosphates (dNTPs) required for DNA replication and thus proliferative cell activity (**Figure 20**).[205,206]

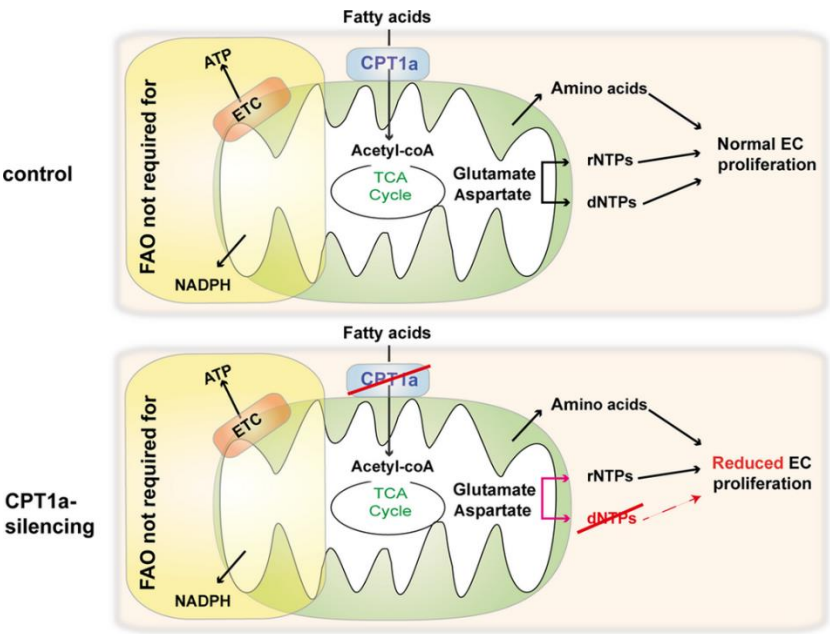

Figure 20: Mechanistic model describing the relation between FAO and nucleotide synthesis. CPT1a-silencing: decreased FAO depletes dNTP pools, rNTP and protein synthesis remained unaffected. rNTPs, ribonucleotide triphosphates. dNTPs, deoxynucleotide tri-phosphates. ETC, electron transport chain. ATP, adenosine triphosphate. CPT, carnitine palmitoyltransferase. EC, endo-thelial cell. NADPH, nicotinamide adenine dinucleotide phosphate. TCA, tricarboxylic acid. (from Vandekeere et al. 2015).[196]

In summary, we identified gene targets that are involved in metabolic pathways promoting a migratory tip cell phenotype (e.g. glycolysis) and a proliferative stalk cell phenotype (e.g. FAO). This combination probably occurs due to our EC isolation method, which includes all available ECs independent from their activation status (quiescent, migratory or proliferative). Our data provides a strong rationale that metabolic pathways and the identified genes are involved in promoting initial and pathological angiogenesis during acute GVHD and are valuable targets for further mechanistic and therapeutic analyses.

6.5 Therapeutic targeting of EC metabolism and angiogenesis after allo-HSCT

For a variety of malignant diseases of the hematopoietic system, allo-HSCT is the only curative treatment option and is therefore the last hope for many leukemia patients. However, the mortality after allo-HSCT is high: more than half of the patients die within the first two years because of GVHD or tumor relapse.[60] Current therapeutic approaches to prevent or treat acute GVHD aim at the suppression of alloreactive T cells. This has the significant disadvantage of creating a secondary immune deficiency with increased risk for tumour relapses and fatal infections.[62,63] Therefore, there is a large unmet medical need for the development of novel therapies for the prevention and treatment of GVHD. Our data and recent evidence suggest that the inhibition of GVHD-associated pathologic angiogenesis could be a novel therapeutic option during GVHD.[127,181] However, there is concern over the use of current anti-angiogenic strategies, as they provide only modest survival benefits in the order of weeks or months in most cancer patients, remaining immensely behind the expectations. Limitations of current anti-angiogenic therapies include intrinsic refractoriness, acquired resistance and targeting molecules and receptors that also show major importance in physiologic angiogenesis,[108,228]

e.g. *Vegfa* and *Vegfr1+2* (-/-) mice show embryonic lethality due to defects in vascular structure formation and in hematopoiesis.[229] Consequently, current anti-angiogenic strategies have limited efficacy and considerable toxicity.[108,228] Suitable targets that are differentially regulated during pathologic angiogenesis and physiologic angiogenesis are lacking. Therefore, there is a need to identify alternative therapeutic targets and novel anti-angiogenic drugs affecting a complete different mechanism or showing a higher specificity for pathologic angiogenesis.

Targeting EC metabolism might represent such an alternative approach. Cantelmo et al.[228] remarked, that "*this strategy is based on the postulate that EC metabolism is the engine onto which proangiogenic signals like VEGF and others converge and that 'cooling down the overheated metabolism' of ECs can paralyze angiogenic ECs and reduce pathological angiogenesis, regardless of how many angiogenic signals are still present upon neutralization of VEGF*." As described in chapter 6.4 metabolic processes are linked to increased proliferative activity and vessel sprouting; and inhibition of glycolysis by the PFKB3 inhibitor 3-(3-pyridinyl)-1-(4-pyridinyl)-2-propen-1-one (3PO)[204,230] as well as inhibition of FAO by etomoxir[205] showed beneficial antiangiogenic effects in several inflammatory models. FAO inhibitors as ranolazine or perhexiline are clinically available and showed good drug tolerability in humans.[231] 3PO also showed good tolerability as already a transient (short half-life of 30 minutes and rapid clearance of 3PO) and partial reduction by no more than 35 % of EC glycolysis led to impaired vessel sprouting by promoting quiescence and normalizing glycolysis rate to maintenance levels found in quiescent ECs. Additionally, proliferating ECs exhibit a higher dependence on glycolysis than other cells, which might reduce unwanted side effects.[204,207,232]

So far, our published data exclusively shows that metabolic changes in proliferating ECs may account for the initialization of acute GVHD. However, the rationale to further dissect metabolic mechanisms and develop preclinical data for treatment strategies, is not only strengthened by the above described implications in pathological angiogenesis, but also by the growing evidence, that both glycolysis and FAO are essential regulators of the T cell metabolism in alloreactive donor T cells inducing GVHD.[233] Nguyen et al. showed that glycolysis was required for optimal function of alloantigen-activated T cells and induction of GVHD. Inhibition of glycolysis by targeting mTORC1 or PFKFB3 ameliorated GVHD mortality and morbidity.[234] Many other analyses described the metabolic adaption of effector T cells toward aerobic glycolysis,[235-238] e.g. 7 days post-transplant alloreactive T cells upregulated the glucose transporter GLUT1 and demonstrated a 4-fold increase in lactate production over naive T cells,[239] consistent with an increased rate of glucose uptake imaged during GI GVHD.[240] However, alloreactive T cells also develop an increased reliance on oxidative metabolism. By day 7, T cells more than double their oxygen consumption compared to resting T cells.[239] Byersdorfer et al. showed that allogeneic T cells increased their reliance on FAO during GVHD. By day 7 post-transplant, alloreactive T cells increased fatty acid transport, drove up

expression of fat oxidation enzymes as CPT1+2, heightened rates of oxidation *ex vivo*, and had more FAO pathway intermediates than their naive counterparts.[241] Inhibition of FAO by etomoxir exclusively eliminated alloreactive T cells and decreased GVHD severity without affecting homeostatic T cells or immune reconstitution.[241] However, in this study they focused on analyzing immune cell subsets and did not elucidate if the inhibition of FAO may also have beneficial impact on angiogenesis, which would also account for reduced alloreactive T cell infiltration and reduced GVHD severity.

Also cancer cells are characterized by perturbations of their metabolic processes. The traditional point of view is that cancer cells predominately produce ATP by glycolysis, however recent studies showed that FAO may represent an alternative carbon source for anabolic processes appearing promising for therapeutic targeting.[242] FAO promotes leukemia stem cell survival and quiescence by supporting mitochondrial oxidative metabolism. Pharmacologic inhibition of FAO with etomoxir or ranolazine inhibited proliferation and sensitized human leukemia cells to apoptosis induction.[243] ST1326, a CPT1a inhibitor, effectively inhibited proliferation, survival, and chemoresistance in leukemia cell lines and primary cells obtained from patients with hematologic malignancies.[244] It was shown that chronic lymphocytic leukemia (CLL) cells expressed high levels of CPT1 and CPT2, exhibited mitochondrial dysfunction and altered lipid metabolism. Perhexiline, an anti-angina agent that inhibits CPT, killed CLL cells *in vitro* as well as *in vivo* using a CLL transgenic mouse model. Perhexiline significantly prolonged the overall animal survival by only 4 drug injections.[245] Additionally, the role of FAO was demonstrated in solid tumors: e.g. metastatic triple-negative breast cancer is dependent on FAO and CPT genes are critical for tumor progression and metastasis.[246]

Taken together, there is a strong rationale that targeting the identified genes being involved in EC metabolism during initial angiogenesis, may improve outcome of allo-HSCT as both GVHD and tumor relapse can be influenced; which deserves deeper mechanistic and functional studies.

6.6 Outlook

We identified angiogenesis as an initial mechanism preceding GVHD-characteristic infiltration of inflammatory leukocytes. Furthermore, we generated data identifying new candidate genes and proteins that are differentially regulated in endothelial cells during initial pathologic angiogenesis after allo-HSCT.

Aiming at a translational development of GVHD therapies targeting angiogenesis, our preclinical findings need to be correlated to the clinical setting. However, additional preclinical research is mandatory to assess mechanisms and identify optimal molecular targets for inhibition of pathologic angiogenesis during GVHD and tumor growth after allo-HSCT. These

aims could be achieved by 1) identifying BM- or endothelial-derived soluble factors in serum or plasma of GVHD mouse models and patients specifically arising after allo-HSCT by MS-based methods; 2) performing *in vitro* knockout/knockdown studies in mouse and human endothelial cells by deleting the identified genes using custom-made Clustered Regularly Interspaced Short Palindromic Repeats (CRISPR)/ CRISPR associated protein 9 (Cas9) vectors and analyze the effects on endothelial function; and 3) *in vivo* knockout/knockdown studies in GVHD mouse models by analyzing the influence of endothelium-specific target gene deletion on angiogenesis, GVHD, tumor growth and GVT activity.

The results from the planned experiments could help to gain a better understanding of the mechanisms leading to pathologic angiogenesis during inflammation and tumor growth, identify new therapeutic approaches for the inhibition of pathologic angiogenesis and deliver the preclinical data for the translational development of novel treatment strategies that inhibit pathologic angiogenesis after allo-HSCT.

7. References

1. Sureda A, Bader P, Cesaro S, et al. Indications for allo- and auto-SCT for haematological diseases, solid tumours and immune disorders: current practice in Europe, 2015. *Bone Marrow Transplant*. 2015;50(8):1037-1056.

2. Singh AK, McGuirk JP. Allogeneic Stem Cell Transplantation: A Historical and Scientific Overview. *Cancer Res*. 2016;76(22):6445-6451.

3. Jenq RR, van den Brink MR. Allogeneic haematopoietic stem cell transplantation: individualized stem cell and immune therapy of cancer. *Nat Rev Cancer*. 2010;10(3):213-221.

4. Passweg JR, Baldomero H, Bader P, et al. Hematopoietic SCT in Europe 2013: recent trends in the use of alternative donors showing more haploidentical donors but fewer cord blood transplants. *Bone Marrow Transplant*. 2015;50(4):476-482.

5. Gratwohl A, Pasquini MC, Aljurf M, et al. One million haemopoietic stem-cell transplants: a retrospective observational study. *Lancet Haematol*. 2015;2(3):e91-100.

6. Jacobson LO, Marks EK, Robson MJ, Gaston E, Zirkle RE. The Effect of Spleen Protection on Mortality Following X-Irradiation. *Journal of Laboratory and Clinical Medicine*. 1949;34(11):1538-1543.

7. Lorenz E, Uphoff D, Reid TR, Shelton E. Modification of Irradiation Injury in Mice and Guinea Pigs by Bone Marrow Injections. *Journal of the National Cancer Institute*. 1951;12(1):197-201.

8. Barnes DWH, Corp MJ, Loutit JF, Neal FE. Treatment of Murine Leukaemia with X-Rays and Homologous Bone Marrow - Preliminary Communication. *British Medical Journal*. 1956;2(Sep15):626-627.

9. Main JM, Prehn RT. Successful Skin Homografts after the Administration of High Dosage X-Radiation and Homologous Bone Marrow. *Journal of the National Cancer Institute*. 1955;15(4):1023-1029.

10. Thomas ED, Lochte HL, Lu WC, Ferrebee JW. Intravenous Infusion of Bone Marrow in Patients Receiving Radiation and Chemotherapy. *New England Journal of Medicine*. 1957;257(11):491-496.

11. Raju TN. The Nobel chronicles. 1990: Joseph Edward Murray (b 1919) and E Donnall Thomas (b 1920). *Lancet*. 2000;355:1282.

12. Bortin MM. A Compendium or Reported Human Bone Marrow Transplants. *Transplantation*. 1970;9(6):571-&.

13. Van Rood J, Van Leeuwen A. Leukocyte grouping. A method and its application. *Journal of Clinical Investigation*. 1963;42(9):1382.

14. Billingham RE, Brent L. Quantitative Studies on Tissue Transplantation Immunity .4. Induction of Tolerance in Newborn Mice and Studies on the Phenomenon of Runt Disease. *Philosophical Transactions of the Royal Society of London Series B-Biological Sciences*. 1959;242(694):439-477.

15. Van Bekkum O, De Vries H. Radiation Chimeras: Elsevier Science & Technology Books; 1967.

16. Lochte HL, Levy AS, Guenther DM, Thomas ED, Ferrebee JW. Prevention of delayed foreign marrow reaction in lethally irradiated mice by early administration of methotrexate. *Nature*. 1962;196:1110-1111.

17. Storb R, Epstein R, Rudolph R, Thomas E. Allogeneic canine bone marrow transplantation following cyclophosphamide. *Transplantation*. 1969;7(5):378-386.

18. Snell GD. The Nobel Lectures in Immunology. Lecture for the Nobel Prize for Physiology or Medicine, 1980: Studies in histocompatibility. *Scand J Immunol*. 1992;36(4):513-526.

19. Epstein RB, Storb R, Ragde H, Thomas ED. Cytotoxic typing antisera for marrow grafting in littermate dogs. *Transplantation*. 1968;6:45-58.

20. Gatti RA, Meuwissen HJ, Allen HD, Hong R, Good RA. Immunological reconstitution of sex-linked lymphopenic immunological deficiency. *Lancet*. 1968;2:1366-1369.

21. Thomas E, Buckner C, Rudolph R, et al. Allogeneic marrow grafting for hematologic malignancy using HL-A matched donor-recipient sibling pairs. *Blood*. 1971;38(3):267-287.

22. Thomas ED, Lochte Jr HL, Cannon JH, Sahler OD, Ferrebee JW. Supralethal whole body irradiation and isologous marrow transplantation in man. *Journal of Clinical Investigation*. 1959;38(10 Pt 1-2):1709.

23. Santos G, Owens Jr A. Allogeneic marrow transplants in cyclophosphamide treated mice. Transplantation proceedings; 1969:44.

24. Weiden PL, Flournoy N, Thomas ED, et al. Antileukemic effect of graft-versus-host disease in human recipients of allogeneic-marrow grafts. *New England Journal of Medicine*. 1979;300(19):1068-1073.

25. Bortin MM, Rimm AA, Saltzstein EC, Rodey GE. GRAFT VERSUS LEUKEMIA: III. Apparent Independent Antihost and Antileukemic Activity of Transplanted Immunocompetent Cells. *Transplantation*. 1973;16(3):182-188.

26. Thomas ED, Storb R, Clift RA, et al. Bone-marrow transplantation. *New England Journal of Medicine*. 1975;292(17):895-902.

27. Hansen JA, Clift RA, Thomas ED, Buckner CD, Storb R, Giblett ER. Transplantation of marrow from an unrelated donor to a patient with acute leukemia. *New England Journal of Medicine*. 1980;303(10):565-567.

28. Reisner Y, Kirkpatrick D, Dupont B, et al. Transplantation for acute leukaemia with HLA-A and B nonidentical parental marrow cells fractionated with soybean agglutinin and sheep red blood cells. *The Lancet*. 1981;318(8242):327-331.

29. Deeg HJ, Storb R, Weiden PL, et al. Cyclosporin A and methotrexate in canine marrow transplantation: engraftment, graft-versus-host disease, and induction of tolerance. *Transplantation*. 1982;34(1):30-35.

30. Powles R, Kay H, Clink H, et al. Mismatched family donors for bone-marrow transplantation as treatment for acute leukaemia. *The Lancet*. 1983;321(8325):612-615.

31. Kolb HJ. Donor leukocyte transfusions for treatment of recurrent chronic myelogenous leukemia in marrow transplant patients. *Blood*. 1990;76:2462-2465.

32. Gluckman E, Devergie A, Bourdeau-Esperou H, et al. Transplantation of umbilical cord blood in Fanconi's anemia. *Nouvelle revue francaise d'hematologie*. 1989;32(6):423-425.

33. Laporte J-P, Gorin N-C, Rubinstein P, et al. Cord-blood transplantation from an unrelated donor in an adult with chronic myelogenous leukemia. *New England Journal of Medicine*. 1996;335(3):167-170.

34. Fontaine P, Roy-Proulx G, Knafo L, Baron C, Roy D-C, Perreault C. Adoptive transfer of minor histocompatibility antigen-specific T lymphocytes eradicates leukemia cells without causing graft-versus-host disease. *Nature medicine*. 2001;7(7):789-794.

35. Ruggeri L, Capanni M, Urbani E, et al. Effectiveness of donor natural killer cell alloreactivity in mismatched hematopoietic transplants. *Science*. 2002;295(5562):2097-2100.

36. O'Donnell PV, Luznik L, Jones R, et al. Nonmyeloablative bone marrow transplantation from partially HLA-mismatched related donors using posttransplantation cyclophosphamide. *Biology of Blood and Marrow Transplantation*. 2002;8(7):377-386.

37. Fontenot JD, Gavin MA, Rudensky AY. Foxp3 programs the development and function of CD4+ CD25+ regulatory T cells. *Nature immunology*. 2003;4(4):330-336.

38. Yanez R, Lamana ML, García-Castro J, Colmenero I, Ramirez M, Bueren JA. Adipose Tissue-Derived Mesenchymal Stem Cells Have In Vivo Immunosuppressive Properties Applicable for the Control of the Graft-Versus-Host Disease. *Stem cells*. 2006;24(11):2582-2591.

39. Di Stasi A, Tey S-K, Dotti G, et al. Inducible apoptosis as a safety switch for adoptive cell therapy. *New England Journal of Medicine*. 2011;365(18):1673-1683.

40. Leen AM, Bollard CM, Mendizabal AM, et al. Multicenter study of banked third party virus-specific T-cells to treat severe viral infections after hematopoietic stem cell transplantation. *Blood*. 2013:blood-2013-2002-486324.

41. Grupp SA, Kalos M, Barrett D, et al. Chimeric antigen receptor–modified T cells for acute lymphoid leukemia. *New England Journal of Medicine*. 2013;368(16):1509-1518.

42. Kröger N, Zander, A. Allogene Stammzelltherapie-Grundlagen, Indikationen und Perspektiven. Bremen: UNI-MED Verl (UNI-MED Science); 3. Auflage; 2011.

43. EBMT Annual Report. 2015.

44. DeFranco A, Locksley RM, Robertson M. Immunity: The Immune Response in Infectious and Inflammatory Disease: OUP Oxford; 2007.

45. Abbas AK, Lichtman AHH, Pillai S. Cellular and Molecular Immunology E-Book: Elsevier Health Sciences; 2017.

46. Beck S, Trowsdale J. The human major histocompatability complex: lessons from the DNA sequence. *Annu Rev Genomics Hum Genet*. 2000;1:117-137.

47. Choo SY. The HLA System: Genetics, Immunology, Clinical Testing, and Clinical Implications. *Yonsei Medical Journal*. 2007;48(1):11-23.

48. Tsukada N, Kobata T, Aizawa Y, Yagita H, Okumura K. Graft-versus-leukemia effect and graft-versus-host disease can be differentiated by cytotoxic mechanisms in a murine model of allogeneic bone marrow transplantation. *Blood*. 1999;93(8):2738-2747.

49. Tiercy M, Nicoloso G, Passweg J, et al. The probability of identifying a 10/10 HLA allele-matched unrelated donor is highly predictable. *Bone Marrow Transplantation*. 2007;40(6):515-522.

50. Ottinger HD, Ferencik S, Beelen DW, et al. Hematopoietic stem cell transplantation: contrasting the outcome of transplantations from HLA-identical siblings, partially HLA-mismatched related donors, and HLA-matched unrelated donors. *Blood*. 2003;102(3):1131-1137.

51. Passweg JR, Baldomero H, Gratwohl A, et al. The EBMT activity survey: 1990-2010. *Bone Marrow Transplantation*. 2012;47(7):906-923.

52. Aversa F. Hematopoietic stem cell transplantation from alternative donors for high-risk acute leukemia: the haploidentical option. *Curr Stem Cell Res Ther*. 2007;2:105-112.

53. Beatty PG, Clift RA, Mickelson EM, et al. Marrow Transplantation from Related Donors Other Than Hla-Identical Siblings. *New England Journal of Medicine*. 1985;313(13):765-771.

54. Pasquini M, Wang Z, Schneider L. CIBMTR summary slides. *CIBMTR Newsletter*. 2007;13:2-9.

55. Slavin S, Nagler A, Naparstek E, et al. Nonmyeloablative stem cell transplantation and cell therapy as an alternative to conventional bone marrow transplantation with lethal cytoreduction for the treatment of malignant and nonmalignant hematologic diseases. *Blood*. 1998;91(3):756-763.

56. Tang X, Alatrash G, Ning J, et al. Increasing chimerism after allogeneic stem cell transplantation is associated with longer survival time. *Biol Blood Marrow Transplant*. 2014;20(8):1139-1144.

57. Auletta JJ, Lazarus HM. Immune restoration following hematopoietic stem cell transplantation: an evolving target. *Bone Marrow Transplant*. 2005;35(9):835-857.

58. Ogonek J, Kralj Juric M, Ghimire S, et al. Immune Reconstitution after Allogeneic Hematopoietic Stem Cell Transplantation. *Front Immunol*. 2016;7:507.

59. Servais S, Beguin Y, Delens L, et al. Novel approaches for preventing acute graft-versus-host disease after allogeneic hematopoietic stem cell transplantation. *Expert Opinion on Investigational Drugs*. 2016;25(8):957-972.

60. Li M, Sun K, Welniak LA, Murphy WJ. Immunomodulation and pharmacological strategies in the treatment of graft-versus-host disease. *Expert Opin Pharmacother*. 2008;9:2305-2316.

61. Storb R, Gluckman E, Thomas ED, et al. Treatment of established human graft-versus-host disease by antithymocyte globulin. *Blood*. 1974;44(1):56-75.

62. Marmont AM, Horowitz MM, Gale RP, et al. T-cell depletion of HLA-identical transplants in leukemia. *Blood*. 1991;78(8):2120-2130.

63. Miller HK, Braun TM, Stillwell T, et al. Infectious Risk after Allogeneic Hematopoietic Cell Transplantation Complicated by Acute Graft-versus-Host Disease. *Biology of Blood and Marrow Transplantation*;23(3):522-528.

64. Young J-AH. Infectious complications of acute and chronic GVHD. *Best Practice & Research Clinical Haematology*. 2008;21(2):343-356.

65. Mattsson J, Ringden O, Storb R. Graft failure after allogeneic hematopoietic cell transplantation. *Biology of Blood and Marrow Transplantation*. 2008;14(1):165-170.

66. Bearman SI, Appelbaum FR, Buckner CD, et al. Regimen-Related Toxicity in Patients Undergoing Bone-Marrow Transplantation. *Journal of Clinical Oncology*. 1988;6(10):1562-1568.

67. Einsele H, Bertz H, Beyer J, et al. Infectious complications after allogeneic stem cell transplantation: epidemiology and interventional therapy strategies - Guidelines of the Infectious Diseases Working Party (AGIHO) of the German Society of Hematology and Oncology (DGHO). *Annals of Hematology*. 2003;82:S175-S185.

68. Chatzidimitriou D, Gavriilaki E, Sakellari I, Diza E. Hematopoietic cell transplantation and emerging viral infections. *J Med Virol*. 2010;82(3):528-538.

69. Rimkus C. Acute Complications of Stem Cell Transplant. *Seminars in Oncology Nursing*;25(2):129-138.

70. Ferrara JL, Levine JE, Reddy P, Holler E. Graft-versus-host disease. *Lancet*. 2009;373(9674):1550-1561.

71. Flomenberg N, Baxter-Lowe LA, Confer D, et al. Impact of HLA class I and class II high-resolution matching on outcomes of unrelated donor bone marrow transplantation: HLA-C mismatching is associated with a strong adverse effect on transplantation outcome. *Blood*. 2004;104(7):1923-1930.

72. Schroeder MA, DiPersio JF. Mouse models of graft-versus-host disease: advances and limitations. *Dis Model Mech*. 2011;4(3):318-333.

73. Horowitz MM. Graft-versus-leukemia reactions after bone marrow transplantation. *Blood*. 1990;75:555-562.

74. Bortin MM, Truitt RL, Rimm AA, Bach FH. Graft-Versus-Leukemia Reactivity Induced by Alloimmunization without Augmentation of Graft Versus Host Reactivity. *Nature*. 1979;281(5731):490-491.

75. Truitt RL, Johnson BD. Principles of graft-vs.-leukemia reactivity. *Biol Blood Marrow Transplant*. 1995;1(2):61-68.

76. Storb R, Gyurkocza B, Storer BE, et al. Graft-Versus-Host Disease and Graft-Versus-Tumor Effects After Allogeneic Hematopoietic Cell Transplantation. *Journal of Clinical Oncology*. 2013;31(12):1530-1538.

77. Johnson BD, Hanke CA, Truitt RL. The graft-versus-leukemia effect of post-transplant donor leukocyte infusion. *Leukemia & Lymphoma*. 1996;23(1-2):1-9.

78. Higano CS, Brixey M, Bryant EM, et al. Durable complete remission of acute nonlymphocytic leukemia associated with discontinuation of immunosuppression following relapse after allogeneic bone marrow transplantation. *Transplantation*. 1990;50(1):175-177.

79. Storb R, Gyurkocza B, Storer BE, et al. Graft-versus-host disease and graft-versus-tumor effects after allogeneic hematopoietic cell transplantation. *J Clin Oncol*. 2013;31(12):1530-1538.

80. Ball LM, Egeler RM. Acute GvHD: pathogenesis and classification. *Bone Marrow Transplant*. 2008;41 Suppl 2:S58-64.

81. Ratanatharathorn V, Nash RA, Przepiorka D, et al. Phase III study comparing methotrexate and tacrolimus (prograf, FK506) with methotrexate and cyclosporine for graft-versus-host disease prophylaxis after HLA-identical sibling bone marrow transplantation. *Blood*. 1998;92(7):2303-2314.

82. Loiseau P, Busson M, Balere M-L, et al. HLA Association with Hematopoietic Stem Cell Transplantation Outcome: The Number of Mismatches at HLA-A, -B, -C, -DRB1, or -DQB1 Is Strongly Associated with Overall Survival. *Biology of Blood and Marrow Transplantation*. 2007;13(8):965-974.

83. Blazar BR, Murphy WJ, Abedi M. Advances in graft-versus-host disease biology and therapy. *Nat Rev Immunol*. 2012;12(6):443-458.

84. Vogelsang GB, Lee L, Bensen-Kennedy DM. Pathogenesis and treatment of graft-versus-host disease after bone marrow transplant. *Annu Rev Med*. 2003;54:29-52.

85. Socie G, Blazar BR. Acute graft-versus-host disease: from the bench to the bedside. *Blood*. 2009;114(20):4327-4336.

86. Zeiser R, Socie G, Blazar BR. Pathogenesis of acute graft-versus-host disease: from intestinal microbiota alterations to donor T cell activation. *Br J Haematol*. 2016;175(2):191-207.

87. Martin PJ, Schoch G, Fisher L, et al. A retrospective analysis of therapy for acute graft-versus-host disease: initial treatment. *Blood*. 1990;76(8):1464-1472.

88. Krenger W, Hollander GA. The role of the thymus in allogeneic hematopoietic stem cell transplantation. *Swiss Med Wkly*. 2010;140:w13051.

89. Krenger W, Hollander GA. The thymus in GVHD pathophysiology. *Best Pract Res Clin Haematol*. 2008;21(2):119-128.

90. Szyska M, Na I-K. Bone Marrow GvHD after Allogeneic Hematopoietic Stem Cell Transplantation. *Frontiers in Immunology*. 2016;7:118.

91. Cahn J-Y, Klein JP, Lee SJ, et al. Prospective evaluation of 2 acute graft-versus-host (GVHD) grading systems: a joint Société Française de Greffe de Moëlle et Thérapie Cellulaire (SFGM-TC), Dana Farber Cancer Institute (DFCI), and International Bone Marrow Transplant Registry (IBMTR) prospective study. *Blood*. 2005;106(4):1495-1500.

92. Baron F, Labopin M, Niederwieser D, et al. Impact of graft-versus-host disease after reduced-intensity conditioning allogeneic stem cell transplantation for acute myeloid leukemia: a report from the Acute Leukemia Working Party of the European group for blood and marrow transplantation. *Leukemia*. 2012;26(12):2462-2468.

93. Baron F. Graft-versus-tumor effects after allogeneic hematopoietic cell transplantation with nonmyeloablative conditioning. *J Clin Oncol*. 2005;23:1993-2003.

94. Storb R, Antin JH, Cutler C. Should Methotrexate plus Calcineurin Inhibitors Be Considered Standard of Care for Prophylaxis of acute Graft-versus-Host Disease? *Biology of Blood and Marrow Transplantation*. 2010;16(1, Supplement):S18-S27.

95. Ruutu T, Gratwohl A, de Witte T, et al. Prophylaxis and treatment of GVHD: EBMT-ELN working group recommendations for a standardized practice. *Bone Marrow Transplantation*. 2014;49(2):168-173.

96. Storb R, Deeg HJ, Pepe M, et al. Methotrexate and cyclosporine versus cyclosporine alone for prophylaxis of graft-versus-host disease in patients given HLA-identical marrow grafts for leukemia: long-term follow-up of a controlled trial. *Blood*. 1989;73(6):1729-1734.

97. Woo M, Przepiorka D, Ippoliti C, et al. Toxicities of tacrolimus and cyclosporin A after allogeneic blood stem cell transplantation. *Bone Marrow Transplant*. 1997;20(12):1095-1098.

98. Martin PJ, Rizzo JD, Wingard JR, et al. First- and second-line systemic treatment of acute graft-versus-host disease: recommendations of the American Society of Blood and Marrow Transplantation. *Biol Blood Marrow Transplant*. 2012;18(8):1150-1163.

99. MacMillan ML, Weisdorf DJ, Wagner JE, et al. Response of 443 patients to steroids as primary therapy for acute graft-versus-host disease: comparison of grading systems. *Biol Blood Marrow Transplant*. 2002;8(7):387-394.

100. Hill GR, Crawford JM, Cooke KR, Brinson YS, Pan L, Ferrara JL. Total body irradiation and acute graft-versus-host disease: the role of gastrointestinal damage and inflammatory cytokines. *Blood*. 1997;90(8):3204-3213.

101. van Leeuwen L, Guiffre A, Atkinson K, Rainer SP, Sewell WA. A two-phase pathogenesis of graft-versus-host disease in mice. *Bone Marrow Transplant*. 2002;29(2):151-158.

102. Reddy P, Ferrara JLM. Mouse models of graft-versus-host disease. StemBook. Cambridge (MA); 2008.

103. Folkman J. Angiogenesis in cancer, vascular, rheumatoid and other disease. *Nat Med*. 1995;1(1):27-31.

104. Tas SW, Maracle CX, Balogh E, Szekanecz Z. Targeting of proangiogenic signalling pathways in chronic inflammation. *Nat Rev Rheumatol*. 2016;12(2):111-122.

105. Simons M. Angiogenesis: where do we stand now? *Circulation*. 2005;111(12):1556-1566.

106. Carmeliet P, Collen D. Molecular basis of angiogenesis. Role of VEGF and VE-cadherin. *Ann N Y Acad Sci*. 2000;902:249-262; discussion 262-244.

107. Szade A, Grochot-Przeczek A, Florczyk U, Jozkowicz A, Dulak J. Cellular and molecular mechanisms of inflammation-induced angiogenesis. *IUBMB Life*. 2015;67(3):145-159.

108. Welti J, Loges S, Dimmeler S, Carmeliet P. Recent molecular discoveries in angiogenesis and antiangiogenic therapies in cancer. *J Clin Invest*. 2013;123(8):3190-3200.

109. Otsuka F, Finn AV, Yazdani SK, Nakano M, Kolodgie FD, Virmani R. The importance of the endothelium in atherothrombosis and coronary stenting. *Nat Rev Cardiol*. 2012;9(8):439-453.

110. Armulik A, Genove G, Betsholtz C. Pericytes: developmental, physiological, and pathological perspectives, problems, and promises. *Dev Cell*. 2011;21(2):193-215.

111. Bou-Gharios G, Ponticos M, Rajkumar V, Abraham D. Extra-cellular matrix in vascular networks. *Cell Prolif*. 2004;37(3):207-220.

112. Hood JD, Cheresh DA. Role of integrins in cell invasion and migration. *Nat Rev Cancer*. 2002;2(2):91-100.

113. Carmeliet P, Jain RK. Molecular mechanisms and clinical applications of angiogenesis. *Nature*. 2011;473(7347):298-307.

114. Murakami M. Signaling required for blood vessel maintenance: molecular basis and pathological manifestations. *Int J Vasc Med*. 2012;2012:293641.

115. Adams RH, Alitalo K. Molecular regulation of angiogenesis and lymphangiogenesis. *Nat Rev Mol Cell Biol*. 2007;8(6):464-478.

116. Carmeliet P, De Smet F, Loges S, Mazzone M. Branching morphogenesis and antiangiogenesis candidates: tip cells lead the way. *Nat Rev Clin Oncol*. 2009;6(6):315-326.

117. Bryant DM, Datta A, Rodriguez-Fraticelli AE, Peranen J, Martin-Belmonte F, Mostov KE. A molecular network for de novo generation of the apical surface and lumen. *Nat Cell Biol*. 2010;12(11):1035-1045.

118. Nejsum LN, Nelson WJ. A molecular mechanism directly linking E-cadherin adhesion to initiation of epithelial cell surface polarity. *J Cell Biol*. 2007;178(2):323-335.

119. Jain RK. Molecular regulation of vessel maturation. *Nat Med*. 2003;9(6):685-693.

120. Montero-Balaguer M, Swirsding K, Orsenigo F, Cotelli F, Mione M, Dejana E. Stable vascular connections and remodeling require full expression of VE-cadherin in zebrafish embryos. *PLoS One*. 2009;4(6):e5772.

121. Szekanecz Z, Koch AE. Mechanisms of Disease: angiogenesis in inflammatory diseases. *Nat Clin Pract Rheumatol*. 2007;3(11):635-643.

122. Costa C, Incio J, Soares R. Angiogenesis and chronic inflammation: cause or consequence? *Angiogenesis*. 2007;10(3):149-166.

123. Subimerb C, Pinlaor S, Lulitanond V, et al. Circulating CD14(+) CD16(+) monocyte levels predict tissue invasive character of cholangiocarcinoma. *Clin Exp Immunol*. 2010;161(3):471-479.

124. Pober JS, Sessa WC. Evolving functions of endothelial cells in inflammation. *Nat Rev Immunol*. 2007;7(10):803-815.

125. Pober JS, Cotran RS. The role of endothelial cells in inflammation. *Transplantation*. 1990;50(4):537-544.

126. Ley K, Laudanna C, Cybulsky MI, Nourshargh S. Getting to the site of inflammation: the leukocyte adhesion cascade updated. *Nat Rev Immunol*. 2007;7(9):678-689.

127. Penack O, Henke E, Suh D, et al. Inhibition of neovascularization to simultaneously ameliorate graft-vs-host disease and decrease tumor growth. *J Natl Cancer Inst*. 2010;102(12):894-908.

128. Folkman J. Tumor angiogenesis: therapeutic implications. *N Engl J Med*. 1971;285(21):1182-1186.

129. Sidky YA, Auerbach R. Lymphocyte-induced angiogenesis: a quantitative and sensitive assay of the graft-vs.-host reaction. *J Exp Med*. 1975;141(5):1084-1100.

130. Tichelli A, Gratwohl A. Vascular endothelium as 'novel' target of graft-versus-host disease. *Best Pract Res Clin Haematol*. 2008;21(2):139-148.

131. Sviland L, Sale GE, Myerson D. Endothelial changes in cutaneous graft-versus-host disease: a comparison between HLA matched and mismatched recipients of bone marrow transplantation. *Bone Marrow Transplant*. 1991;7(1):35-38.

132. Dumler JS, Beschorner WE, Farmer ER, Di Gennaro KA, Saral R, Santos GW. Endothelial-cell injury in cutaneous acute graft-versus-host disease. *Am J Pathol*. 1989;135(6):1097-1103.

133. Matsuda Y, Hara J, Osugi Y, et al. Serum levels of soluble adhesion molecules in stem cell transplantation-related complications. *Bone Marrow Transplant*. 2001;27(9):977-982.

134. Salat C, Holler E, Kolb HJ, Pihusch R, Reinhardt B, Hiller E. Endothelial cell markers in bone marrow transplant recipients with and without acute graft-versus-host disease. *Bone Marrow Transplant*. 1997;19(9):909-914.

135. Biedermann BC, Tsakiris DA, Gregor M, Pober JS, Gratwohl A. Combining altered levels of effector transcripts in circulating T cells with a marker of endothelial injury is specific for active graft-versus-host disease. *Bone Marrow Transplant*. 2003;32(11):1077-1084.

136. Rachakonda SP, Penack O, Dietrich S, et al. Single-Nucleotide Polymorphisms Within the Thrombomodulin Gene (THBD) Predict Mortality in Patients With Graft-Versus-Host Disease. *J Clin Oncol*. 2014;32(30):3421-3427.

137. Dietrich S, Falk CS, Benner A, et al. Endothelial vulnerability and endothelial damage are associated with risk of graft-versus-host disease and response to steroid treatment. *Biol Blood Marrow Transplant*. 2013;19(1):22-27.

138. Andrulis M, Dietrich S, Longerich T, et al. Loss of endothelial thrombomodulin predicts response to steroid therapy and survival in acute intestinal graft-versus-host disease. *Haematologica*. 2012;97(11):1674-1677.

139. Pihusch V, Rank A, Steber R, et al. Endothelial cell-derived microparticles in allogeneic hematopoietic stem cell recipients. *Transplantation*. 2006;81(10):1405-1409.

140. Uderzo C, Bonanomi S, Busca A, et al. Risk factors and severe outcome in thrombotic microangiopathy after allogeneic hematopoietic stem cell transplantation. *Transplantation*. 2006;82(5):638-644.

141. McDonald GB, Hinds MS, Fisher LD, et al. Veno-occlusive disease of the liver and multiorgan failure after bone marrow transplantation: a cohort study of 355 patients. *Ann Intern Med*. 1993;118(4):255-267.

142. Carreras E, Bertz H, Arcese W, et al. Incidence and outcome of hepatic veno-occlusive disease after blood or marrow transplantation: a prospective cohort study of the European Group for Blood and Marrow Transplantation. European Group for Blood and Marrow Transplantation Chronic Leukemia Working Party. *Blood*. 1998;92(10):3599-3604.

143. Majhail NS, Parks K, Defor TE, Weisdorf DJ. Diffuse alveolar hemorrhage and infection-associated alveolar hemorrhage following hematopoietic stem cell transplantation:

related and high-risk clinical syndromes. *Biol Blood Marrow Transplant*. 2006;12(10):1038-1046.

144. Wojno KJ, Vogelsang GB, Beschorner WE, Santos GW. Pulmonary hemorrhage as a cause of death in allogeneic bone marrow recipients with severe acute graft-versus-host disease. *Transplantation*. 1994;57(1):88-92.

145. Spitzer TR. Engraftment syndrome following hematopoietic stem cell transplantation. *Bone Marrow Transplant*. 2001;27(9):893-898.

146. Gorak E, Geller N, Srinivasan R, et al. Engraftment syndrome after nonmyeloablative allogeneic hematopoietic stem cell transplantation: incidence and effects on survival. *Biol Blood Marrow Transplant*. 2005;11(7):542-550.

147. Nurnberger W, Willers R, Burdach S, Gobel U. Risk factors for capillary leakage syndrome after bone marrow transplantation. *Ann Hematol*. 1997;74(5):221-224.

148. Gyger M, Rosenberg A, Shamy A, et al. Vascular leak syndrome and serositis as an unusual manifestation of chronic graft-versus-host disease in nonmyeloablative transplants. *Bone Marrow Transplant*. 2005;35(2):201-203.

149. Biedermann BC, Sahner S, Gregor M, et al. Endothelial injury mediated by cytotoxic T lymphocytes and loss of microvessels in chronic graft versus host disease. *Lancet*. 2002;359(9323):2078-2083.

150. Tichelli A, Bucher C, Rovó A, et al. Premature cardiovascular disease after allogeneic hematopoietic stem-cell transplantation. *Blood*. 2007;110(9):3463-3471.

151. Leonhardt F, Grundmann S, Behe M, et al. Inflammatory neovascularization during graft-versus-host disease is regulated by alphav integrin and miR-100. *Blood*. 2013;121(17):3307-3318.

152. Penack O, Socie G, van den Brink MR. The importance of neovascularization and its inhibition for allogeneic hematopoietic stem cell transplantation. *Blood*. 2011;117(16):4181-4189.

153. Medinger M, Tichelli A, Bucher C, et al. GVHD after allogeneic haematopoietic SCT for AML: angiogenesis, vascular endothelial growth factor and VEGF receptor expression in the BM. *Bone Marrow Transplant*. 2013;48(5):715-721.

154. Stolfi JL, Pai CC, Murphy WJ. Preclinical modeling of hematopoietic stem cell transplantation - advantages and limitations. *FEBS J*. 2016;283(9):1595-1606.

155. Seok J, Warren HS, Cuenca AG, et al. Genomic responses in mouse models poorly mimic human inflammatory diseases. *Proc Natl Acad Sci U S A*. 2013;110(9):3507-3512.

156. Takao K, Miyakawa T. Genomic responses in mouse models greatly mimic human inflammatory diseases. *Proc Natl Acad Sci U S A*. 2015;112(4):1167-1172.

157. van der Worp HB, Howells DW, Sena ES, et al. Can animal models of disease reliably inform human studies? *PLoS Med*. 2010;7(3):e1000245.

158. Panoskaltsis-Mortari A, Taylor PA, Rubin JS, et al. Keratinocyte growth factor facilitates alloengraftment and ameliorates graft-versus-host disease in mice by a mechanism independent of repair of conditioning-induced tissue injury. *Blood*. 2000;96(13):4350-4356.

159. Blazar BR, Weisdorf DJ, Defor T, et al. Phase 1/2 randomized, placebo-control trial of palifermin to prevent graft-versus-host disease (GVHD) after allogeneic hematopoietic stem cell transplantation (HSCT). *Blood*. 2006;108(9):3216-3222.

160. Levine JE, Blazar BR, DeFor T, Ferrara JL, Weisdorf DJ. Long-term follow-up of a phase I/II randomized, placebo-controlled trial of palifermin to prevent graft-versus-host disease (GVHD) after related donor allogeneic hematopoietic cell transplantation (HCT). *Biol Blood Marrow Transplant*. 2008;14(9):1017-1021.

161. Xun CQ, Thompson JS, Jennings CD, Brown SA, Widmer MB. Effect of total body irradiation, busulfan-cyclophosphamide, or cyclophosphamide conditioning on inflammatory cytokine release and development of acute and chronic graft-versus-host disease in H-2-incompatible transplanted SCID mice. *Blood*. 1994;83(8):2360-2367.

162. Antin JH, Weisdorf D, Neuberg D, et al. Interleukin-1 blockade does not prevent acute graft-versus-host disease: results of a randomized, double-blind, placebo-controlled trial of

interleukin-1 receptor antagonist in allogeneic bone marrow transplantation. *Blood*. 2002;100(10):3479-3482.

163. Gyurkocza B, Sandmaier BM. Conditioning regimens for hematopoietic cell transplantation: one size does not fit all. *Blood*. 2014;124(3):344-353.

164. Ferrara JL. Pathogenesis of acute graft-versus-host disease: cytokines and cellular effectors. *J Hematother Stem Cell Res*. 2000;9(3):299-306.

165. Medzhitov R. Origin and physiological roles of inflammation. *Nature*. 2008;454(7203):428-435.

166. Ordemann R, Hutchinson R, Friedman J, et al. Enhanced allostimulatory activity of host antigen-presenting cells in old mice intensifies acute graft-versus-host disease. *J Clin Invest*. 2002;109(9):1249-1256.

167. Gupta V, Eapen M, Brazauskas R, et al. Impact of age on outcomes after bone marrow transplantation for acquired aplastic anemia using HLA-matched sibling donors. *Haematologica*. 2010;95(12):2119-2125.

168. Boraschi D, Aguado MT, Dutel C, et al. The gracefully aging immune system. *Sci Transl Med*. 2013;5(185):185ps188.

169. Lynch HE, Goldberg GL, Chidgey A, Van den Brink MR, Boyd R, Sempowski GD. Thymic involution and immune reconstitution. *Trends Immunol*. 2009;30(7):366-373.

170. Gleimer M, Li Y, Chang L, et al. Baseline body mass index among children and adults undergoing allogeneic hematopoietic cell transplantation: clinical characteristics and outcomes. *Bone Marrow Transplant*. 2015;50(3):402-410.

171. Nelson MH, Paulos CM. Novel immunotherapies for hematological malignancies. *Immunological reviews*. 2015;263(1):90-105.

172. Bachireddy P, Burkhardt UE, Rajasagi M, Wu CJ. Haematological malignancies: at the forefront of immunotherapeutic innovation. *Nat Rev Cancer*. 2015;15(4):201-215.

173. Lichtman MA. Battling the hematological malignancies: the 200 years' war. *Oncologist*. 2008;13(2):126-138.

174. Jenq RR, Ubeda C, Taur Y, et al. Regulation of intestinal inflammation by microbiota following allogeneic bone marrow transplantation. *J Exp Med*. 2012;209(5):903-911.

175. Beura LK, Hamilton SE, Bi K, et al. Normalizing the environment recapitulates adult human immune traits in laboratory mice. *Nature*. 2016;532(7600):512-516.

176. Luft T, Dietrich S, Falk C, et al. Steroid-refractory GVHD: T-cell attack within a vulnerable endothelial system. *Blood*. 2011;118(6):1685-1692.

177. Luft T, Benner A, Jodele S, et al. It Is Easix to Predict Non-Relapse Mortality (NRM) of Allogeneic Stem Cell Transplantation (alloSCT). *Blood*. 2016;128(22).

178. Kim DH, Sohn SK, Jeon SB, et al. Prognostic significance of platelet recovery pattern after allogeneic HLA-identical sibling transplantation and its association with severe acute GVHD. *Bone Marrow Transplant*. 2006;37(1):101-108.

179. Ichiba T, Teshima T, Kuick R, et al. Early changes in gene expression profiles of hepatic GVHD uncovered by oligonucleotide microarrays. *Blood*. 2003;102(2):763-771.

180. Sugerman PB, Faber SB, Willis LM, et al. Kinetics of gene expression in murine cutaneous graft-versus-host disease. *Am J Pathol*. 2004;164(6):2189-2202.

181. Riesner K, Shi Y, Jacobi A, et al. Initiation of acute graft-versus-host disease by angiogenesis. *Blood*. 2017.

182. Antin JH, Ferrara JL. Cytokine dysregulation and acute graft-versus-host disease. *Blood*. 1992;80(12):2964-2968.

183. Ferrara JL. Cytokine dysregulation as a mechanism of graft versus host disease. *Curr Opin Immunol*. 1993;5(5):794-799.

184. Deeg HJ. Cytokines in graft-versus-host disease and the graft-versus-leukemia reaction. *Int J Hematol*. 2001;74(1):26-32.

185. Huang XJ, Wan J, Lu DP. Serum TNFalpha levels in patients with acute graft-versus-host disease after bone marrow transplantation. *Leukemia*. 2001;15(7):1089-1091.

186. Min CK, Lee WY, Min DJ, et al. The kinetics of circulating cytokines including IL-6, TNF-alpha, IL-8 and IL-10 following allogeneic hematopoietic stem cell transplantation. *Bone Marrow Transplant*. 2001;28(10):935-940.

187. Schots R, Kaufman L, Van Riet I, et al. Proinflammatory cytokines and their role in the development of major transplant-related complications in the early phase after allogeneic bone marrow transplantation. *Leukemia*. 2003;17(6):1150-1156.

188. Visentainer JE, Lieber SR, Persoli LB, et al. Serum cytokine levels and acute graft-versus-host disease after HLA-identical hematopoietic stem cell transplantation. *Exp Hematol*. 2003;31(11):1044-1050.

189. Fowler DH, Foley J, Whit-Shan Hou J, et al. Clinical "cytokine storm" as revealed by monocyte intracellular flow cytometry: correlation of tumor necrosis factor alpha with severe gut graft-versus-host disease. *Clin Gastroenterol Hepatol*. 2004;2(3):237-245.

190. Imamura M, Hashino S, Kobayashi H, et al. Serum cytokine levels in bone marrow transplantation: synergistic interaction of interleukin-6, interferon-gamma, and tumor necrosis factor-alpha in graft-versus-host disease. *Bone Marrow Transplant*. 1994;13(6):745-751.

191. Imamura M, Tanaka J, Hashino S, et al. Cytokines involved in graft-versus-host disease. *Hokkaido Igaku Zasshi*. 1994;69(6):1348-1353.

192. Toren A, Barak V, Novick D, Nagler A. Soluble interferon-gamma receptor and interferon-gamma in patients undergoing allogeneic bone marrow transplantation for hematological malignancies. *Cytokines Cell Mol Ther*. 1997;3(3):153-158.

193. Nakamura H, Komatsu K, Ayaki M, et al. Serum levels of soluble IL-2 receptor, IL-12, IL-18, and IFN-gamma in patients with acute graft-versus-host disease after allogeneic bone marrow transplantation. *J Allergy Clin Immunol*. 2000;106(1 Pt 2):S45-50.

194. Holler E, Kolb HJ, Mittermuller J, et al. Modulation of acute graft-versus-host-disease after allogeneic bone marrow transplantation by tumor necrosis factor alpha (TNF alpha) release in the course of pretransplant conditioning: role of conditioning regimens and prophylactic application of a monoclonal antibody neutralizing human TNF alpha (MAK 195F). *Blood*. 1995;86(3):890-899.

195. Fang D, Hu S, Liu Y, Quan VH, Seuntjens J, Tran SD. Identification of the active components in Bone Marrow Soup: a mitigator against irradiation-injury to salivary glands. *Sci Rep*. 2015;5:16017.

196. Schipani E, Wu C, Rankin EB, Giaccia AJ. Regulation of Bone Marrow Angiogenesis by Osteoblasts during Bone Development and Homeostasis. *Front Endocrinol (Lausanne)*. 2013;4:85.

197. Yancopoulos GD, Davis S, Gale NW, Rudge JS, Wiegand SJ, Holash J. Vascular-specific growth factors and blood vessel formation. *Nature*. 2000;407(6801):242-248.

198. Pour L, Svachova H, Adam Z, et al. Levels of angiogenic factors in patients with multiple myeloma correlate with treatment response. *Ann Hematol*. 2010;89(4):385-389.

199. Gabrilove JL. Angiogenic growth factors: autocrine and paracrine regulation of survival in hematologic malignancies. *Oncologist*. 2001;6 Suppl 5:4-7.

200. De Raeve H, Van Marck E, Van Camp B, Vanderkerken K. Angiogenesis and the role of bone marrow endothelial cells in haematological malignancies. *Histol Histopathol*. 2004;19(3):935-950.

201. Tachi Y, Fukui D, Wada Y, et al. Changes in angiogenesis-related factors in serum following autologous bone marrow cell implantation for severe limb ischemia. *Expert Opin Biol Ther*. 2008;8(6):705-712.

202. Patel J, Seppanen EJ, Rodero MP, et al. Functional Definition of Progenitors Versus Mature Endothelial Cells Reveals Key SoxF-Dependent Differentiation Process. *Circulation*. 2016.

203. Reactome. A curated Pathway database. http://www.reactome.org/. April 2017.

204. Schoors S, De Bock K, Cantelmo AR, et al. Partial and transient reduction of glycolysis by PFKFB3 blockade reduces pathological angiogenesis. *Cell Metab*. 2014;19(1):37-48.

205. Schoors S, Bruning U, Missiaen R, et al. Fatty acid carbon is essential for dNTP synthesis in endothelial cells. *Nature*. 2015;520(7546):192-197.

206. Schoors S, Bruning U, Missiaen R, et al. Corrigendum: Fatty acid carbon is essential for dNTP synthesis in endothelial cells. *Nature*. 2015;526(7571):144.

207. De Bock K, Georgiadou M, Schoors S, et al. Role of PFKFB3-driven glycolysis in vessel sprouting. *Cell*. 2013;154(3):651-663.

208. Cantelmo AR, Brajic A, Carmeliet P. Endothelial Metabolism Driving Angiogenesis: Emerging Concepts and Principles. *Cancer J*. 2015;21(4):244-249.

209. Vandekeere S, Dewerchin M, Carmeliet P. Angiogenesis Revisited: An Overlooked Role of Endothelial Cell Metabolism in Vessel Sprouting. *Microcirculation*. 2015;22(7):509-517.

210. KEGG: Kyoto Encyclopedia of Genes and Genomes. http://www.genome.jp/kegg/. April 2017.

211. WIKIPATHWAYS. http://www.wikipathways.org/index.php/WikiPathways. April 2017.

212. Real-Hohn A, Zancan P, Da Silva D, et al. Filamentous actin and its associated binding proteins are the stimulatory site for 6-phosphofructo-1-kinase association within the membrane of human erythrocytes. *Biochimie*. 2010;92(5):538-544.

213. Doddaballapur A, Michalik KM, Manavski Y, et al. Laminar shear stress inhibits endothelial cell metabolism via KLF2-mediated repression of PFKFB3. *Arterioscler Thromb Vasc Biol*. 2015;35(1):137-145.

214. Riganti C, Gazzano E, Polimeni M, Aldieri E, Ghigo D. The pentose phosphate pathway: an antioxidant defense and a crossroad in tumor cell fate. *Free Radic Biol Med*. 2012;53(3):421-436.

215. Vizan P, Sanchez-Tena S, Alcarraz-Vizan G, et al. Characterization of the metabolic changes underlying growth factor angiogenic activation: identification of new potential therapeutic targets. *Carcinogenesis*. 2009;30(6):946-952.

216. Luo B, Soesanto Y, McClain DA. Protein modification by O-linked GlcNAc reduces angiogenesis by inhibiting Akt activity in endothelial cells. *Arterioscler Thromb Vasc Biol*. 2008;28(4):651-657.

217. Laczy B, Hill BG, Wang K, et al. Protein O-GlcNAcylation: a new signaling paradigm for the cardiovascular system. *American Journal of Physiology - Heart and Circulatory Physiology*. 2009;296(1):H13-H28.

218. Merchan JR, Kovacs K, Railsback JW, et al. Antiangiogenic activity of 2-deoxy-D-glucose. *PLoS One*. 2010;5(10):e13699.

219. Croci DO, Cerliani JP, Dalotto-Moreno T, et al. Glycosylation-dependent lectin-receptor interactions preserve angiogenesis in anti-VEGF refractory tumors. *Cell*. 2014;156(4):744-758.

220. Du XL, Edelstein D, Rossetti L, et al. Hyperglycemia-induced mitochondrial superoxide overproduction activates the hexosamine pathway and induces plasminogen activator inhibitor-1 expression by increasing Sp1 glycosylation. *Proc Natl Acad Sci U S A*. 2000;97(22):12222-12226.

221. Darby JK, Johnsen J, Nakashima P, et al. Pvu II RFLP at the human chromosome 1 alpha-L-fucosidase gene locus (FUCA1). *Nucleic Acids Res*. 1986;14(23):9543.

222. Ezawa I, Sawai Y, Kawase T, et al. Novel p53 target gene FUCA1 encodes a fucosidase and regulates growth and survival of cancer cells. *Cancer Science*. 2016;107(6):734-745.

223. Kyselova Z, Mechref Y, Kang P, et al. Breast cancer diagnosis and prognosis through quantitative measurements of serum glycan profiles. *Clin Chem*. 2008;54(7):1166-1175.

224. Muinelo-Romay L, Vazquez-Martin C, Villar-Portela S, Cuevas E, Gil-Martin E, Fernandez-Briera A. Expression and enzyme activity of alpha(1,6)fucosyltransferase in human colorectal cancer. *Int J Cancer*. 2008;123(3):641-646.

225. Houten SM, Wanders RJA. A general introduction to the biochemistry of mitochondrial fatty acid β-oxidation. *Journal of Inherited Metabolic Disease*. 2010;33(5):469-477.

226. Elmasri H, Karaaslan C, Teper Y, et al. Fatty acid binding protein 4 is a target of VEGF and a regulator of cell proliferation in endothelial cells. *Faseb j*. 2009;23(11):3865-3873.

227. Patella F, Schug ZT, Persi E, et al. Proteomics-based metabolic modeling reveals that fatty acid oxidation (FAO) controls endothelial cell (EC) permeability. *Mol Cell Proteomics*. 2015;14(3):621-634.

228. Cantelmo AR, Pircher A, Kalucka J, Carmeliet P. Vessel pruning or healing: endothelial metabolism as a novel target? *Expert Opin Ther Targets*. 2017;21(3):239-247.

229. Hiratsuka S, Kataoka Y, Nakao K, et al. Vascular endothelial growth factor A (VEGF-A) is involved in guidance of VEGF receptor-positive cells to the anterior portion of early embryos. *Mol Cell Biol*. 2005;25(1):355-363.

230. Xu Y, An X, Guo X, et al. Endothelial PFKFB3 plays a critical role in angiogenesis. *Arterioscler Thromb Vasc Biol*. 2014;34(6):1231-1239.

231. Carracedo A, Cantley LC, Pandolfi PP. Cancer metabolism: fatty acid oxidation in the limelight. *Nat Rev Cancer*. 2013;13(4):227-232.

232. Schoors S, Cantelmo AR, Georgiadou M, et al. Incomplete and transitory decrease of glycolysis: a new paradigm for anti-angiogenic therapy? *Cell Cycle*. 2014;13(1):16-22.

233. Chiaranunt P, Ferrara JL, Byersdorfer CA. Rethinking the paradigm: How comparative studies on fatty acid oxidation inform our understanding of T cell metabolism. *Mol Immunol*. 2015;68(2 Pt C):564-574.

234. Nguyen HD, Chatterjee S, Haarberg KM, et al. Metabolic reprogramming of alloantigen-activated T cells after hematopoietic cell transplantation. *J Clin Invest*. 2016;126(4):1337-1352.

235. Gerriets VA, Rathmell JC. Metabolic pathways in T cell fate and function. *Trends Immunol*. 2012;33(4):168-173.

236. MacIver NJ, Michalek RD, Rathmell JC. Metabolic regulation of T lymphocytes. *Annu Rev Immunol*. 2013;31:259-283.

237. Pearce EL, Poffenberger MC, Chang CH, Jones RG. Fueling immunity: insights into metabolism and lymphocyte function. *Science*. 2013;342(6155):1242454.

238. O'Sullivan D, Pearce EL. Targeting T cell metabolism for therapy. *Trends Immunol*. 2015;36(2):71-80.

239. Gatza E, Wahl DR, Opipari AW, et al. Manipulating the bioenergetics of alloreactive T cells causes their selective apoptosis and arrests graft-versus-host disease. *Sci Transl Med*. 2011;3(67):67ra68.

240. Stelljes M, Hermann S, Albring J, et al. Clinical molecular imaging in intestinal graft-versus-host disease: mapping of disease activity, prediction, and monitoring of treatment efficiency by positron emission tomography. *Blood*. 2008;111(5):2909-2918.

241. Byersdorfer CA, Tkachev V, Opipari AW, et al. Effector T cells require fatty acid metabolism during murine graft-versus-host disease. *Blood*. 2013;122(18):3230-3237.

242. Samudio I, Konopleva M. Targeting leukemia's "fatty tooth". *Blood*. 2015;126(16):1874-1875.

243. Samudio I, Harmancey R, Fiegl M, et al. Pharmacologic inhibition of fatty acid oxidation sensitizes human leukemia cells to apoptosis induction. *J Clin Invest*. 2010;120(1):142-156.

244. Ricciardi MR, Mirabilii S, Allegretti M, et al. Targeting the leukemia cell metabolism by the CPT1a inhibition: functional preclinical effects in leukemias. *Blood*. 2015;126(16):1925-1929.

245. Liu PP, Liu J, Jiang WQ, et al. Elimination of chronic lymphocytic leukemia cells in stromal microenvironment by targeting CPT with an antiangina drug perhexiline. *Oncogene*. 2016;35(43):5663-5673.

246. Park JH, Vithayathil S, Kumar S, et al. Fatty Acid Oxidation-Driven Src Links Mitochondrial Energy Reprogramming and Oncogenic Properties in Triple-Negative Breast Cancer. *Cell Rep*. 2016;14(9):2154-2165.

8. Appendix

8.1 Appendix Figures and Tables

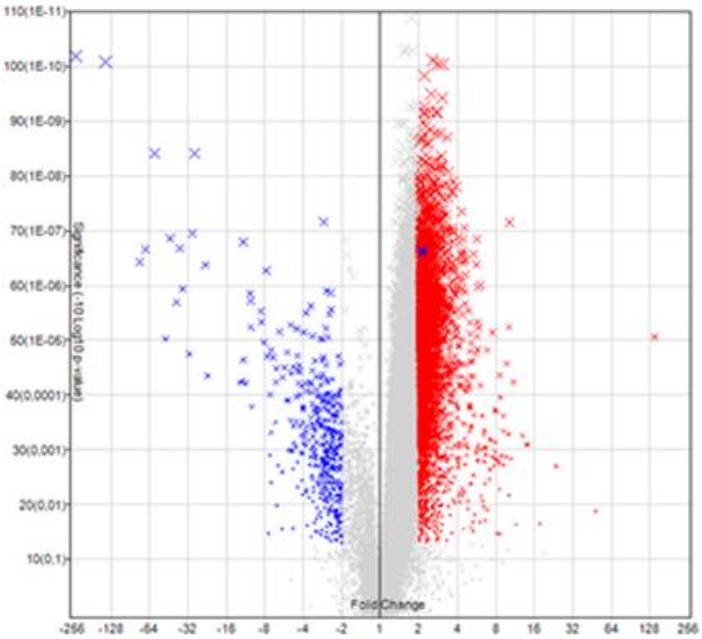

Appendix Figure 18: Volcano Plot of microarray analysis of liver ECs. d+2 vs. d+15 after allo-HSCT. (Algorithm Options: One-Way Between-Subject ANOVA (unpaired), Default Filter Criteria: Fold Change (linear) < -2 or Fold Change (linear) > 2, ANOVA p-value (Condition pair) < 0.05).

Appendix Table 8: Fold change of selected genes concerning inflammatory EC activation. From microarray analysis of colon ECs at d+2 after allo-HSCT in allogeneic versus syngeneic transplanted mice.

	Gene	Fold change (linear)	ANOVA p-value	FDR p-value
Adhesion molecules	*Icam-1*	-2.83	0.01	0.346
	Vcam-1	-1.83	0.069	0.529
	E-selectin	-1.23	0.259	0.719
Type II endothelial activation	*Il1r1*	-1.21	0.309	0.751
	Tirap	1.05	0.862	0.969
	Myd88	-1.35	0.045	0.479
	Traf6	1.1	0.628	0.895
	Irak1	1.03	0.988	0.998
	Irak4	1,12	0.046	0.482
	Tnfr1	-1.19	0.041	0.463
	Tradd	1.01	0.765	0.942
	Traf2	-1.24	0.311	0.751
	Nfκb	-1.06	0.292	0.740

Appendix Table 9: Fold change of selected genes concerning classical angiogenic pathways. From microarray analysis of colon ECs at d+2 after allo-HSCT in allogeneic versus syngeneic transplanted mice.

	Gene	Fold change (linear)	ANOVA p-value	FDR p-value
Classical Angiogenic Pathways	*Hif1a*	-1.45	0.0165	0.381
	Vegfa	-1.3	0.002	0.266
	Vegfr2	-1.52	0.211	0.682
	Ang1	1.08	0.213	0.683
	Ang2	-1.13	0.213	0.979
	Ffg2	-1.1	0.100	0.574
	Fgfr1	1.07	0.927	0.985
	Dll4	1.15	0.763	0.942
	Notch1	-1.32	0.188	0.665
	Nrp1	-1.09	0.562	0.870
	Cdc42	1.08	0.142	0.625
	Rac1	-1.3	0.108	0.584

8.2 List of figures

8.3 List of tables

Figures and Tables of the manuscripts and corresponding supplemental materials are self-contained and are not included in the present list.

8.4 Curriculum vitae

„Der Lebenslauf ist in der Online-Version aus Gründen des Datenschutzes nicht enthalten.“

8.5 List of publications

Original research articles

Mengwasser J, Babes L, Cordes S, Mertlitz S, **Riesner K**, Shi Y, McGearey A, Kalupa M, Reinheckel T, Penack O. Cathepsin E Deficiency Ameliorates Graft-versus-Host Disease and Modifies Dendritic Cell Motility. *Front Immunol.* 2017 Mar 1;8:203. **Impact factor: 5,695**

Riesner K, Shi Y, Jacobi A, Kraeter M, Kalupa M, McGearey A, Mertlitz S, Cordes S, Schrezenmeier JF, Mengwasser J, Westphal S, Perez-Hernandez D, Schmitt C, Dittmar G, Guck J, Penack O. Initiation of acute graft-versus-host disease by angiogenesis. *Blood.* 2017 Apr 6;129(14):2021-2032. **Impact factor: 11,847**

Mertlitz S, Shi Y, Kalupa M, Grötzinger C, Mengwasser J, **Riesner K**, Cordes S, Elezkurtaj S, Penack O. Lymphangiogenesis is a feature of acute GVHD, and VEGFR-3 inhibition protects against experimental GVHD. *Blood.* 2017 Mar 30;129(13):1865-1875. **Impact factor: 11,847**

Nogai A, Shi Y, Pérez-Hernandez D, Cordes S, Mengwasser J, Mertlitz S, **Riesner K**, Kalupa M, Erdmann JH, Ziebig R, Dittmar G, Penack O. Organ siderosis and hemophagocytosis during acute graft-versus-host disease. *Haematologica.* 2016 Aug;101(8):e344-6. **Impact factor: 6,671**

Riesner K, Kalupa M, Shi Y, Elezkurtaj S, Penack O. A preclinical acute GVHD mouse model based on chemotherapy conditioning and MHC-matched transplantation. *Bone Marrow Transplant*. 2016 Mar;51(3):410-7. **Impact factor: 3,570**

Lehnen NC, von Mässenhausen A, Kalthoff H, Zhou H, Glowka T, Schütte U, Höller T, **Riesner K**, Boehm D, Merkelbach-Bruse S, Kirfel J, Perner S,Gütgemann I. Fibroblast growth factor receptor 1 gene amplification in pancreatic ductal adenocarcinoma. *Histopathology.* 2013 Aug;63(2):157-66. **Impact factor: 3,453**

Leonhardt F, Grundmann S, Behe M, Bluhm F, Dumont RA, Braun F, Fani M, **Riesner K**, Prinz G, Hechinger AK, Gerlach UV, Dierbach H, Penack O, Schmitt-Gräff A, Finke J, Weber WA, Zeiser R. Inflammatory neovascularization during graft-versus-host disease is regulated by αv integrin and miR-100. *Blood.* 2013 Apr 25;121(17):3307-18. **Impact factor: 9,775**

Schildhaus HU, Heukamp LC, Merkelbach-Bruse S, **Riesner K**, et al. Definition of a fluorescence in-situ hybridization score identifies high- and low-level FGFR1 amplification types in squamous cell lung cancer. *Mod Pathol.* 2012 Nov;25(11):1473-80. **Impact factor: 5,253**

Körner C, **Riesner K**, Krämer B, Eisenhardt M, Glässner A, Wolter F, Berg T, Müller T, Sauerbruch T, Nattermann J, Spengler U, Nischalke HD. TRAIL receptor I (DR4) polymorphisms C626G and A683C are associated with an increased risk for hepatocellular carcinoma (HCC) in HCV-infected patients. *BMC Cancer.* 2012 Mar 8;12:85. **Impact factor: 3,333**

Körner C, Tolksdorf F, **Riesner K**, Krämer B, Schulte D, Nattermann J, Rockstroh JK, Spengler U. Hepatitis C coinfection enhances sensitization of CD4(+) T-cells towards Fas-induced apoptosis in viraemic and HAART-controlled HIV-1-positive patients. *Antivir Ther.* 2011;16(7):1047-55. **Impact factor: 3,161**

Abstracts

Riesner K, Kalupa M, Cordes S, et al. Close To Clinics: Acute Gvhd In a Novel Chemotherapy Based Minor Mismatch Transplantation Model. *Blood*. 2013;122(21):2.

Oral presentations

EBMT 2014: **Riesner K**, Shi Yu, Mengwasser J, Cordes S, Penack O. Neovascularization precedes leukocyte infiltration and target organ damage during acute GVHD. *Bone Marrow Transplant* 49: S6-S88; doi:10.1038/bmt.2014.43; PH-O040 (S22)

DGHO 2014: **Riesner K**, Cordes S, Mengwasser J, Shi Y, Westphal S, Penack O. Neovascularization precedes leukocyte infiltration and target organ damage during acute GVHD and experimental colitis. *Oncology Research and Treatment*. 10/2014;37,Supplement 5:110.

EBMT 2016: Mengwasser J, Shi Y, Cordes S, **Riesner K**, Mertlitz S, McGearey A, Kalupa M, Penack O. The role of Cathepsin E in GVHD

DGHO 2016: **Riesner K**, Shi Y, Jacobi A, Kraeter M, Kalupa M, McGearey A, Mertlitz S, Cordes S, Schrezenmeier JF, Mengwasser J, Westphal S, Perez-Hernandez D, Schmitt C, Dittmar G, Guck J, Penack O. Angiogenesis in acute GVHD

Poster presentations

EBMT 2014: Shi Y, Pérez-Hernandez D, **Riesner K**, Cordes S, Mengwasser J, Dittmar G, Penack O. Proteomic Peptide Profiling in the liver during acute GVHD

EBMT 2016: Nogai A, Shi Y, Cordes S, **Riesner K**, Mertlitz S, Mengwasser J, Pérez-Hernandez D, Erdmann JH, Ziebig R, Dittmar G, Penack O. Organsiderosis and Hemophagocytosis during acute GVHD

ASH 2016: **Riesner K**, Shi Y, Jacobi A, Kraeter M, Kalupa M, McGearey A, Mertlitz S, Cordes S, Schrezenmeier JF, Mengwasser J, Westphal S, Perez-Hernandez D, Schmitt C, Dittmar G, Guck J, Penack O. Initiation of Acute Graft-Versus-Host Disease By Angiogenesis

8.6 Selbständigkeitserklärung

Hiermit erkläre ich, dass ich diese Arbeit selbständig verfasst habe und keine anderen als die angegebenen Quellen und Hilfsmittel in Anspruch genommen habe. Ich versichere, dass diese Arbeit in dieser oder anderer Form keiner anderen Prüfungsbehörde vorgelegt wurde.

Berlin, den 02.05.2017 Katarina Riesner